Evidence for a Novel Multipotent Mammary Progenitor with Pregnancy-Specific Activity

Citation

Kaanta, Alice. 2012. Evidence for a Novel Multipotent Mammary Progenitor with Pregnancy-Specific Activity. Doctoral dissertation, Harvard University.

Permanent link

http://nrs.harvard.edu/urn-3:HUL.InstRepos:10087379

Terms of Use

Share Your Story

Dr. Joan Brugge   Alice S. Kaanta

Evidence for a novel multipotent mammary progenitor with pregnancy-specific activity

Abstract

The mouse mammary gland has emerged as a model system for studying processes involved in the development of epithelial tissues. Current evidence suggests the existence of a differentiation hierarchy in the mammary gland, consisting of a stem cell capable of reconstituting the tissue, progenitors with the capacity to produce specific functional cell types, and differentiated cells with limited or no repopulation potential. Although markers for mammary stem cells and progenitors have been identified, these populations have not been isolated to purity and our understanding of how they function in different stages of mammary development remains incomplete.

Many adult stem cells are mitotically quiescent and can therefore retain a DNA or histone label significantly longer than differentiated cells. In an attempt to identify mammary stem cells/progenitors by histone label retention, I crossed a mouse carrying the tetracycline-inducible histone 2b/eGFP (H2BGFP) gene with tetracycline transactivator strains expected to induce H2BGFP in the mammary gland. H2BGFP expression was induced in the mammary gland until puberty and then chased for 6-8 weeks; H2BGFP$^+$ label retaining cells were isolated and assayed. Transplantation experiments comparing MMTVrtTA/H2BGFP MECs isolated after induction to MMTVrtTA/H2BGFP MECs retaining label post-chase failed to prove that label retention enriches for stem cells/progenitors in the MMTVrtTA/H2BGFP system. During the course of these experiments, I unexpectedly discovered that MMTVrtTA induced H2BGFP expression

exclusively in the $CD24^+/CD29^+$ and $CD24^+/CD29^{lo}$ populations, which contain stem cells and progenitors, respectively.

Interestingly, I also discovered that H2BGFP+/CD24+/CD29lo MECs developed limited mammary outgrowths *in vivo* and that pregnancy increased the repopulation ability of these cells by 5-10-fold. H2BGFP+/CD24+/CD29lo outgrowths contained all mammary lineages and produced milk, but were unable to self-renew in serial transplant assays. Furthermore, $H2BGFP^+/CD24^+/CD29^{lo}$ and $H2BGFP^-/CD24^+/CD29^{lo}$ MECs had distinct gene expression profiles, with H2BGFP+/CD24+/CD29lo MECs expressing lower levels of transcripts involved in mammary development and differentiation.

These data provide evidence for the existence of a multipotent, pregnancy-activated mammary progenitor and suggests that different progenitor populations are responsible for mammary expansion during puberty and pregnancy. Future studies may identify FACS markers for purification of pregnancy-activated progenitors and further elucidate the role of different mammary cell types during pregnancy.

Table of Contents

List of Figures

Chapter 1 – Introduction

Chapter 3 – Histone Label Retention in the Mouse Mammary Gland

Chapter 4 – Evidence for a Pregnancy-Activated Multipotent Mammary Progenitor

Appendix A. Testing Candidate Cell Surface Markers for Independent Isolation of the H2BGFP+/CD24+/CD29lo Population by FACS

Abbreviations

AREG	amphiregulin
BLG	beta-lactoglobulin
BrdU	Bromodeoxyuridine
Cav1	Caveolin 1
CK5	Cytokeratin 5
CK8	Cytokeratin 8
CK14	Cytokeratin 14
CMV	Cytomegalo Virus
ER	Estrogen receptor
Esr1	Estrogen receptor 1
FACS	Fluorescence-activated cell sorting
FGFR2	Fibroblast growth factor receptor 2
GR	Glucocotorticoid receptor
H2BGFP	Histone 2b/eGFP fusion (can refer to gene or protein)
LRC	Label retaining cell
MEC	Mammary epithelial cell
MMTV	Mouse Mammary Tumor Virus
MRU	Mammary Repopulating Unit
Muc1	Mucin 1
NOD-SCID	Non-Obese Diabetic Severe Combined Immune Deficieny
PI-MEC	Parity-Induced Mammary Epithelial Cell
PR	Progesterone Receptor
PRLR	Prolactin Receptor
Robo1	Roundabout homolog 1
rtTA	Reverse Tetracycline Transactivator
Sca-1	Stem cell antigen 1
tTA	Tetracycline Transactivator
WAP	Whey Acidic Protein
Wnt5a	Wingless-type MMTV integration site family, member 5A

Acknowledgements

It has been a privilege to be co-mentored by Ben Neel and Joan Brugge. In their unique ways, they have inspired, taught and led myself among many, through the wilderness of science. It takes brains to do science, but serious guts to raise scientists. Thank you.

Much affection and appreciation goes my labmates, past and present. Thank for all the conversations and the baked goods that kept me sane. Special thanks goes to Amy Bui, who never failed to make me smile, no matter how many mice or hours there were left in a day. Science is hard, but without exceptional people around you to help you out with those daily slings and arrows, it would be impossible to do it at all.

I would like to thank my Dissertation Advisory Committee, Amy Wagers and Myles Brown, for their advice over these many years. I also extend my thanks to my defense committee, Charlotte Kuperwasser, Kornelia Polyak and Peter Sicinski.

I will always be grateful to Momo Bentires-Alj, Ina Rhee and Arnaud Mailleux, who helped me figure things out at the start(s) and to Liz Reczek, who was there at my first mouse (and my first mouse bite, which was, alas, not my last). You have passed along more lab karma than I can ever repay, though I will try.

Thanks are in order to my friends, who have listened to me alternately squee and sulk for these many years of grad school. Especial thanks go to Jessica Fry, who always manages to make matters look sane again. I also have to thank the membership of CW Taekwondo, who have been there on those days when I just had to kick something.

I owe special thanks to my parents, Ming-Ju Tsay and Wen-Yang Tsay, who gave me both the will and the way to purse my dreams, and to my sister Tiffany, who gets to be a "real doctor" quite soon now. And I thank my in-laws, Carter and Nancy Kaanta, who might not quite know what I'm doing, but have always supported my doing it, even when it meant their son had to clean the house, which is a lot of the time.

Now and always, I thank Brad, for being there for me and with me. I'm going to really enjoy us being "The Doctors Kaanta".

"The most exciting phrase to hear in science, the one that heralds new discoveries, is not 'Eureka!' but 'That's funny ...'"

   --Isaac Asimov

"While I'm still confused and uncertain, it's on a much higher plane, d'you see, and at least I know I'm bewildered about the really fundamental and important facts of the universe."

   -- Terry Pratchett

Chapter 1 Introduction

Overview of Mammary Development in the Mouse

The mammary gland is an impressively dynamic epithelial tissue. During the lifetime of a female mammal, the mammary gland undergoes three distinct modes of growth: the pubertal ductal elongation and branching which establishes the mammary architecture, the cyclic expansion and regression of the estrus/menstrual cycle, and the dramatic pregnancy-associated proliferation and alveolar differentiation that is critical for lactation [6]. These processes are governed by different signals and hormones, and could involve the activity of different cell types at each stage [7, 8].

The adult mammary gland is a branched network of bilayer ducts. Each duct is composed of an inner luminal layer and an outer myoepithelial layer (Figure 1-1, top) [1]. Luminal cells are cuboidal in shape and are often identified by expression of cytokeratin 8 (CK8) and cytokeratin 18 (CK18) [9]. The myoepithelium comprises a continuous layer of long, thin cells, which express cytokeratin 14 (CK14), p63 and smooth muscle actin (SMA). Contractile force from the myoepithelial layer is required for the movement of milk from alveoli, through the ducts and towards the nipple during lacation [10]. Spaced at intervals in the myoepithelial layer are basal cells, small rounded cells that express CK14 and the transcription factor p63 [11]. By flow cytometric analysis, p63^{+} cells are found in mammary epithelial cell (MEC) sub-populations with stem cell activity [7, 12, 13].

The mouse mammary gland is first detectable as an epithelial placode during embryogenesis at E11. This placode develops into a small bud between E13-E15 and eventually becomes a small branched structure with short ducts by E18 [14]. At the onset of puberty (approximately three weeks of age, for the female mouse) estrogen signaling initiates the development of the mammary gland [15]. A club-shaped, multi-layer structure known as the terminal end bud (TEB) develops at the tip of each mammary duct (Figure 1-1, bottom).
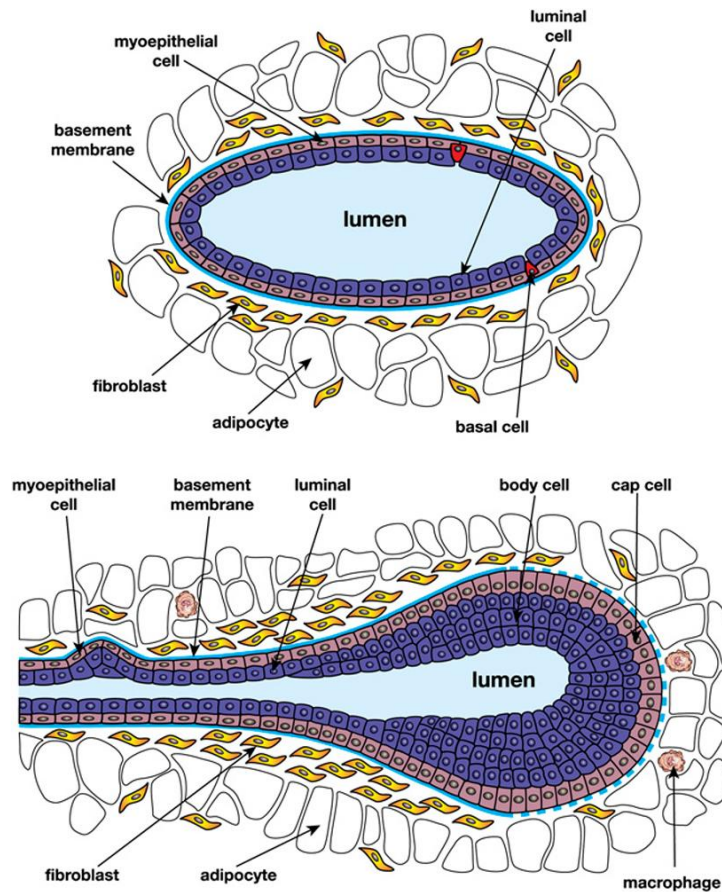
Figure 1-1. Schematic of the Mouse Mammary Gland. Cross section of a mouse mammary duct (top). Longitudinal section of a terminal end bud (bottom). From Visvader et al. [1]

TEBs are the major site of mammary proliferation during puberty and comprise an outer layer of cap cells and an inner mass of body cells. CK14 expression begins at the neck of the TEB where the outer cap cells cease proliferation and differentiate into myoepithelial cells. . Most TEB body cells express CK8, with a small number of CK14$^+$ and p63$^+$ cells interspersed throughout. Cap cells are p63+, but have a cuboidal shape and are larger than most basal cells[16]. Within TEBs, rapid proliferation combined with Bcl-2/Bim-mediated apoptosis results in a hollow bilayer ductal structure [17]. Throughout puberty, TEBs bifurcate at intervals, generating new branches of the mammary duct. Once the mammary network has reaches the outer perimeter of the mammary fat pad, ductal elongation ceases and TEBs regress, forming distal end tips.
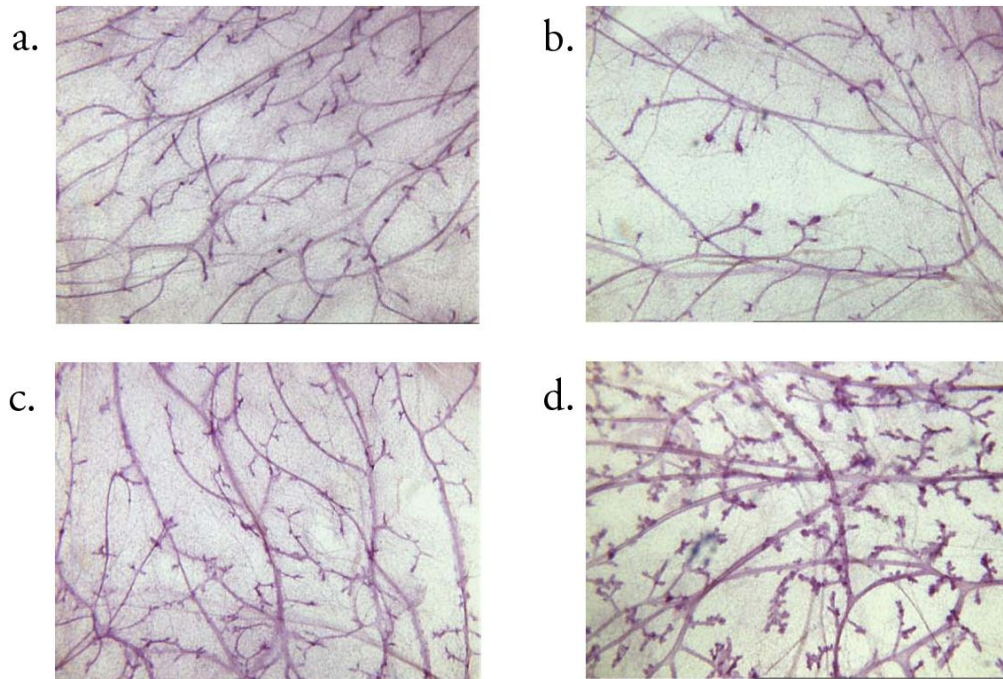
Figure 1-2. Whole Mounts of the Mouse Mammary Gland during the Estrous Cycle. Mammary gland whole mounts during a) proestrus b) estrus c) metestrus d) diestrus. From Joshi et al. [2]

Upon reaching sexual maturity, the female mouse begins four- to six- day estrous cycles, during which the mammary gland undergoes a cyclical process of expansion and regression (Figure 1-2). Whereas pubertal mammary expansion is primarily a process of ductal elongation, with some branching to generate new ducts, the estrous cycle produces small side branches, presumably as a prelude to alveologenesis during pregnancy. The four stages of the estrus cycle, proestrus, estrus, metestrus and diestrus are characterized by different levels of estrogen and progesterone [18]. During proestrus, estrogen levels rise and progesterone levels fall, in preparation for ovulation. At estrus, estrogen levels have reached their peak, progesterone levels are at their nadir, and the female mouse ovulates. Estrus is followed by metestrus, during which estrogen levels fall and progesterone levels rise. It is during diestrus, the longest phase of the estrous cycle, that the appearance of pre-alveolar structures and side branches in the mammary gland is most prominent; later in diestrus,

4
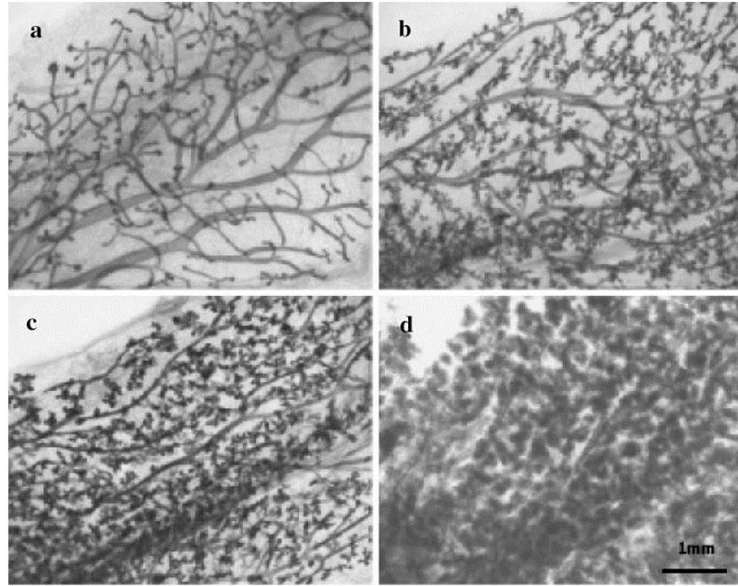
Figure 1-3. Whole Mounts of the Mammary Gland during Pregnancy. Mammary gland whole mounts from a) virgin gland b) early pregnancy c) mid- to late pregnancy d) lactation. From Brisken et al. [3]

many of these side branches and alveolar growths undergo apoptosis, restoring the

mammary gland to its original state for the next cycle [6, 18].

If the female is fertilized during estrus, rising progesterone levels during early

pregnancy initiate the development of small side branches throughout the mammary gland

[19] (Figure 1-3). Instead of undergoing apoptosis, as occurs in estrus, these side branches

become the structural scaffold for developing alveoli [3]. Prolactin signaling induces the

growth of rounded structures, known as alveolar buds, at the distal ends of these side

branches. During mid-pregnancy, alveolar buds divide into numerous individual alveoli,

forming alveolar clusters, which expand rapidly, filling the mammary fat pad [20]. Unlike

pubertal proliferation, which produces a contiguous myoepithelium on the outside of the

luminal cell layer, alveologenesis results in an expanded, but non-continuous, myoepithelial

layer, such that luminal cells are in direct contact with the extracellular matrix [21]. At

approximately day 18 of pregnancy, secretory cells within the alveoli begin to produce milk.

Females give birth around day 20 of pregnancy, after a drop in progesterone levels and the

5

beginning of milk secretion into the alveoli [20, 22]. Females with normal mammary glands will lactate as long as the physical stimulus of nursing is present. Within 24 hours of weaning, the mammary epithelium begins to undergo involution, an apoptotic clearing of alveoli from the mammary ductal structure. The mammary gland is restored to its pre-pregnancy state and will respond to the estrous cycle and pregnancy as it did previously [20].

Mammary Stem Cells and Progenitors

The functional definition of an adult stem cell is one that is capable of giving rise to the original tissue *in vivo* throughout repeated transplants [23]. These functional criteria of mutipotent differentiation and self-renewal have been observed in the normal function of the adult mammary gland. The ability of the mammary gland to undergo repeated rounds of proliferation and remodeling in response to pregnancy has long been cited as evidence for the existence of mammary stem cells. As early as 1959, transplantation studies of normal mammary glands have suggested that a single cell can give rise to a complete mammary gland [24]. In 1998, Smith et al. transplanted fragments of mammary glands infected with the Mouse Mammary Tumor Virus (MMTV) and, by analyzing the retroviral insertion site patterns of the newly grown glands, demonstrated that these mammary glands arose from a single cell [25]. While isolation of the mammary stem cell proved elusive, repeated attempts were made to characterize prospective mammary stem cells and progenitors by use of morphological analysis, stem cell markers from other tissue types (such as Sca-1), dye efflux assays, and cell lines with stem-like properties [26-29].

In 2006, two groups concurrently reported the isolation of a population containing mouse mammary stem cells. Using CD29 (β1 integrin) or CD49f (α6 integrin) in combination with CD24 (heat stable antigen), the Visvader and Eaves laboratories reported isolation of cell populations capable of forming a fully functional and serially transplantable
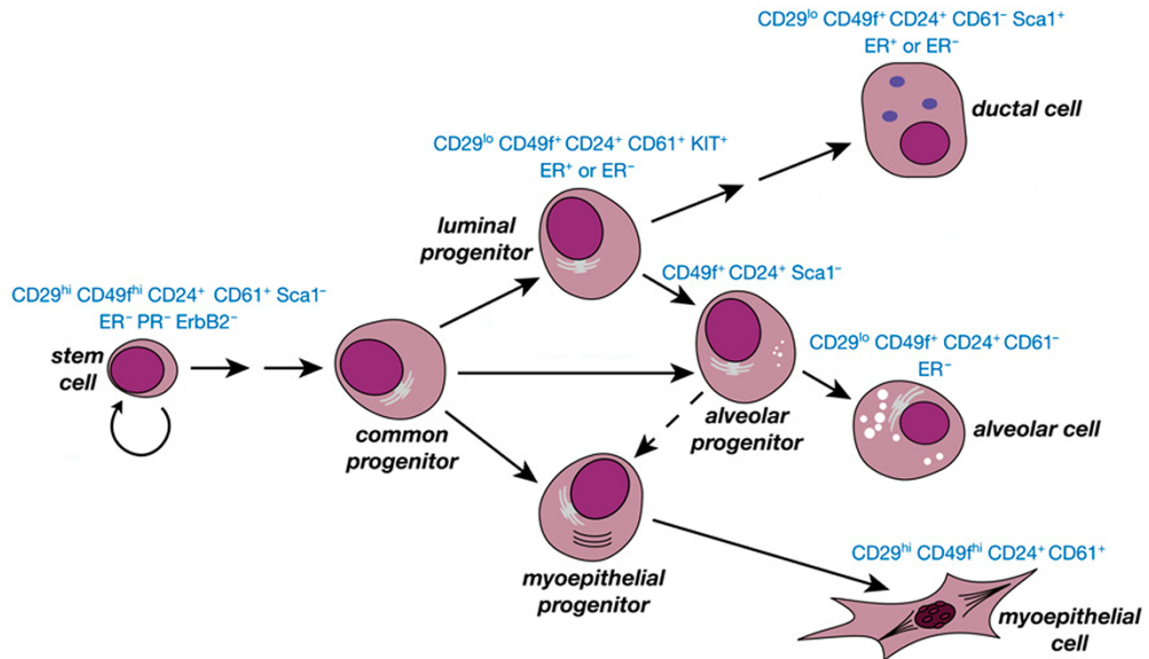
Figure 1-4. Mammary Epithelial Stem Cell Hierarchy. Known markers for mammary epithelial stemcells, progenitors and differentiated cells. From Visvader et al. [1]

mammary gland. Although single cells from both the $CD24^+/CD29^+$ and $CD24^+/CD49f^+$ populations could perform all mammary stem cell functions *in vivo*, neither set of markers purified mammary stem cells to homogeneity; the stem cell frequencies in the $CD24^+/CD29^+$ and $CD24^+/CD49f^+$ populations were calculated to be 1/64 and 1/100, respectively. The $CD24^+/CD29^+$ and $CD24^+/CD49f^+$ populations demonstrated multipotent growth ability *in vitro*, as well as *in vivo*, forming colonies of varying sizes and morphologies in 2D growth assays, and developing multi-layered acini with occasional branched structures on reconstituted basement membrane (Matrigel™). These stem cell-containing populations were found to express high levels of myoepithelial/basal markers, such as CK14, SMA and p63. The expression levels of CD29 and CD49f corresponded strongly, suggesting that the α6/β1 complex is highly expressed in mammary stem cells. Notably, mammary stem cell populations were negative for steroid hormone receptors ER and PR [12, 13].

In addition to labeling mammary stem cells, CD24, CD29 and CD49f have been used to isolate and characterize candidate mammary progenitors through *in vitro* assays. Progenitors are defined by the ability to give rise to at least one differentiated lineage and by the lack of self-renewal, which uniquely defines stem cells. Shackleton et al. reported that only $CD24^+/CD29^+$ and $CD24^+/CD29^{lo}$ cells could form colonies when grown in 2D colony assays on irradiated NIH3T3 feeder cells, and that $CD24^+/CD29^{lo}$-derived colonies were significantly fewer and smaller than those from $CD24^+/CD29^+$ cells. $CD24^+/CD29^{lo}$ and $CD24^+/CD49f^{lo}$ cells, when grown on Matrigel to form 3D colonies, gave rise to single-layer acini of cuboidal cells. Both the $CD24^+/CD29^{lo}$ and $CD24^+/CD49f^{lo}$ populations were initially reported as having no *in vivo* growth ability [12, 13].

These groundbreaking studies were followed by the discovery of additional markers for the purification and characterization of an increasing number of mammary epithelial cell types. The $CD24^+/CD29^{lo}$ population, which is believed to contain luminal progenitors, has been subdivided by expression of CD61 (β3 integrin) into a population of differentiated MECs ($CD24^+/CD29^{lo}/CD61^-$) and mammary progenitors ($CD24^+/CD29^{lo}/CD61^+$), based on *in vitro* colony forming ability. Most $CD24^+/CD29^{lo}/CD61^+$ progenitors were found to be ER negative [30]. Mammary epithelial cells also show different *in vitro* activity based on CD49b (α2 integrin) expression; $CD24^+/CD49b^+$ MECs were able to form colonies *in vitro* while $CD24^+/CD49b^{lo}$ MECs did not [31]. Expression of CD14 and c-Kit has been used to identify prospective alveolar progenitors. The $CD24^+/CD29^{lo}/CD14^+/c\text{-}Kit^-$ population expands during pregnancy and can give rise to lactogenic colonies *in vitro* [32, 33]. Stem cell antigen-1 (Sca-1), which has been used as a marker for hematopoietic stem cells, was originally believed to label mammary stem cells and/or progenitors[27]. However, later

studies proved the reverse, demonstrating that mammary stem cells were Sca-1$^-$ and that Sca-1$^+$ MECs were unable to repopulate the mammary gland *in vivo* [12, 34] (Figure 1-4).

Whereas a mammary epithelial stem cell can be defined by its ability to establish a fully functional mammary tree *in vivo*, the identification and characterization of mammary progenitors requires more complex analyses and assays. Lineage-restricted progenitors that differentiated into myoepithelial and luminal MECs have been identified, principally as a result of *in vitro* assays [12, 13, 30, 31]. Although it was initially reported that CD24$^+$/CD29^{lo} and CD24$^+$/CD49f^{lo} MECs were unable to form outgrowths *in vivo,* recent reports have demonstrated that these MECs can form small, branched mammary structures, when co-injected with Matrigel into mammary fat pads. Transplantation of CD24$^+$/CD29$^+$ cells, by contrast were unaffected by Matrigel[35, 36]. This evidence for Matrigel-dependent outgrowths suggest that the CD24$^+$/CD29^{lo} and CD24$^+$/CD49f^{lo} populations contains multipotent progenitors that develop *in vivo* if provided with the additional stimuli present in Matrigel preparations. Other groups have taken broader *in vivo* approaches, by transplanting mixed populations and extrapolating, based on the different mammary glandular structures grown, that the mammary gland contains unidentified progenitors which can give rise to mammary glands of different sizes and morphological characteristics [34, 37].

Details about the *in vivo* activity of mammary stem cells and progenitors have been revealed by real-time tracking of MEC populations and lineage tracing. Van Keymeulen et al. recently conducted extensive lineage tracing studies using transgenic mice that inducibly express fluorescent proteins driven by promoters for known mammary lineage markers, such as CK14, CK8 and CK18. This study revealed that all mammary lineages derive from stem cells that express CK14 during embryogenesis. Adult mammary epithelial cells were derived from lineage-restricted progenitors, including CK14-expressing myoepithelial progenitors

and CK8-expressing luminal progenitors, which were $CD24^+/CD29^+$ and $CD24^+/CD29^{lo}$, respectively. Cells expressing CK5, which were also in the $CD24^+/CD29^+$ compartment, gave rise to myoepithelial cells specifically during pregnancy, while CK18-expressing cells were either committed progenitors or terminally differentiated MECs. Unexpectedly, myoepithelial progenitors, which could give rise only to myoepithelial cells when in their native context, could be induced to adopt a multipotent progenitor phenotype when co-transplanted with luminal cells. This suggested that paracrine signaling can change the *in vivo* cell fate of a mammary progenitor. This study demonstrated that lineage tracing in solid tissues can provide details of *in vivo* progenitor activity that might not be obtainable through repopulation studies [38].

Mammary Stem Cells and Progenitors in Pregnancy

An early pregnancy is known to reduce the risk of breast cancer, a phenomenon that is believed to arise from a reduction in the proliferative potential of mammary stem cells and progenitors, making them less susceptible to oncogenic transformation [39]. Therefore, the mechanisms of mammary expansion during pregnancy and the identity of the cell types directly activated by pregnancy signaling is a matter of both medical and scientific interest [4].

In the mouse mammary gland, a plausible candidate for the mammary cell type directly activated by pregnancy is the same mammary stem cell that establishes the ductal architecture during puberty. In this model, a single type of stem cell produces different structures (duct vs. alveoli) in response to the different signaling pathways that are active in each phase of mammary development. Basal cells, which are contained within the $CD24^+/CD29^+$ mammary stem cell populationare seeded along the mammary ducts at regular intervals that suggest the spacing of alveoli[12, 13]. During pregnancy, the

CD24$^+$/CD29$^+$ compartment expands temporarily, peaking by day 12.5, at an 11-fold

increase over what is found in virgin glands, and returning to its original fraction of the

MEC population after involution. However, the CD24$^+$/CD29$^+$ population in pregnant

mice also loses 60% of its repopulation ability, which suggests that the size of stem and non-

stem populations within this compartment are increased [40]. In a real-time tracking study,

the CD29/β1 integrin promoter was used to drive expression of luciferase in order to track

the dynamics of mammary stem cells *in vivo*. β1 integrin-luciferase expression labeled the

entire CD24$^+$/CD29$^+$ compartment, which expands dramatically during pregnancy,

increasing as a proportion of total MECs until the first week of lactation [41]. Additionally,

the CD24$^+$/CD49f$^+$ stem cell population expands during the diestrus phase of the estrus

cycle; it is during diestrus that side branches, which are thought to be either precursors to or

stunted versions of alveoli, appear throughout the mammary tree [2]. However, these

studies are limited by the markers used and it is remains possible that the expansion of these

populations during the estrous cycle and pregnancy reflects increased numbers of non-stem

MECs.

An alternative hypothesis is that different mammary stem cell/progenitor

populations are responsible for the different modes of proliferation in puberty and

pregnancy. In this model, progenitors capable of giving rise to alveoli exist throughout the

mammary gland but remain dormant until pregnancy. The existence of pregnancy-specific

progenitors has been suggested by a transplantation study of MECs from pregnancy

mammary glands. Limiting dilution transplants of MECs from pregnant mice gave rise to

ductal-limited, lobule-limited, or bi-lineage outgrowths *in vivo* [37]. Further evidence for a

pregnancy-specific progenitor has been provided by a lineage tracing study, in which MECs

that are active during lactation were labeled using a lactation-specific transgene and a floxed

LacZ allele (WAP-cre/floxed Rosa26-LacZ). Most labeled lactating cells underwent

apoptosis during involution, but some MECs survived to produce LacZ-expressing alveoli in

subsequent pregnancies [42]. These "parity induced MECs" (PI-MECs) were found to exist

in pre-pubertal glands and were initially reported to have no *in vivo* repopulation ability,

suggesting that pregnancy-activated progenitors are part of the normal mammary epithelium

[43]. A later study found that PI-MECs contain mammary stem cells with *in vivo*

repopulation ability, as well as alveolar progenitors. However, the percentage of stem cells

was comparatively small, and therefore this finding does not invalidate the evidence for

alveolar-specific progenitors [44]. Additional support for the existence of a progenitor

population with pregnancy-specific function is provided by work demonstrating that the

mammary glands of mice expressing a defective form of cyclin D1 have reduced numbers of

$CD24^+/CD49f^{lo}$ MECs. When transplanted, cyclin D1-impaired $CD24^+/CD49f^{lo}$ MECs

give rise to diminished mammary outgrowths with lobular defects, whereas $CD24^+/CD49f^{lo}$

MECs expressing wild-type cyclin D1 produce larger outgrowths with extensive alveolar

development during pregnancy [35]. These data support the hypothesis that mammary stem

cells are responsible for the development of the mammary gland during puberty, but a

different population of MEC progenitors is responsible for mammary proliferation during

pregnancy.

The Mouse Mammary Tumor Virus (MMTV) Promoter

Mouse Mammary Tumor Virus (MMTV) provided one of the earliest mouse models

of cancer. The first description of a mouse mammary tumor, which might have been caused

by MMTV, dates back to 1854 [45]. In subsequent decades, an apparently inherited mouse

mammary cancer, which could sometimes be "transplanted", became established as an

important mouse model of cancer. In 1933, researchers at Jackson Labs identified the cause
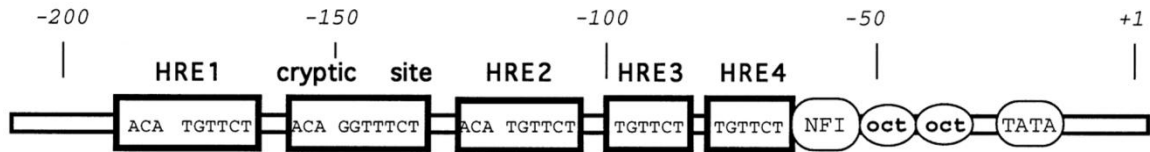
Figure 1-5. MMTV Promoter Structure. The MMTV promoter contains at least four hormone responsiveelements (HREs) which bind to progesterone receptor and glucocorticoid receptor. From Beato et al. [5]

of this mammary cancer as a milk-borne "extrachromosomal factor" that eventually was classified as a retrovirus [45]. Unlike the Rous Sarcoma Virus, MMTV did not cause cancer by expression of an oncogene carried within its own genome, but by insertion of the provirus near to and activation of critical proto-oncogenes including Wnt1, Notch and FGF3 [46-48].

The MMTV long terminal repeat (MMTV-LTR), often termed the MMTV promoter, was cloned in 1981, enabling structural analysis of its 1.3 kb sequence [49]. The MMTV promoter has binding sites for NF1 (nuclear factor 1) and Oct-1, as well as numerous hormone responsive elements, which bind to glucocorticoid receptor (GR) and progesterone receptor (PR) [50-53]. (Figure 1-5) These hormone responsive elements were found to be the mechanism behind the activity of the MMTV promoter *in vivo* [5, 54]. Glucocorticoids and progesterone can bind to and directly activate the MMTV promoter, but MMTV activity is also heavily dependent on nucleosome position [55-58].

The MMTV promoter is frequently used to express transgenes in the mouse mammary gland. Although other mammary-specific promoters exist, their timing and activity can reduce their utility. The beta-lactoglobulin (BLG) promoter drives gene expression at very low levels until pregnancy and the whey-acidic protein (WAP) promoter is active during late pregnancy and lactation, also with minimal activity before pregnancy [59, 60]. By contrast, the MMTV promoter is expressed early in mammary development and

does not require pregnancy or lactation for full activation, lowering the technical barriers for its use [60-62].

Since the development of the MMTV-myc mouse in 1984, dozens of mouse models of breast cancer have utilized the MMTV promoter, both directly and indirectly [63]. Although these models have provided valuable insights into mammary neoplasia, tumor invasion and metastasis, their dependence on the incompletely characterized activity of a viral promoter should be considered when interpreting these data. MMTV-driven transgenes are usually inserted randomly rather than being knocked in at a specific location. Consequently, expression patterns can vary between different MMTV-driven clones, depending on the insertion site or genetic background [60, 64]. The MMTV promoter also is active in non-mammary tissues, including the salivary gland, seminal vesicles and B-cells [61, 65]. Expression in the lymphoid system is a particular handicap and has resulted in transgenic mice that die of lymphoma before they can develop mammary tumors from an MMTV-driven oncogene [66, 67].

Nevertheless, mice expressing MMTV-driven transgenes have provided some information about MMTV promoter activity during mammary development. Although the MMTV promoter is active in the mammary gland before and during puberty [60], studies of MMTV-driven tumor models have found that multiple pregnancies result in decreased latency and increased size and metastatic potential of tumors, suggesting that promoter activity is upregulated during pregnancy and lactation [68-70]. Some studies have suggested that MMTV is active in all MECs, but this is unlikely for several reasons [65]. Given that the MMTV promoter is responsive to steroid hormone receptors and MECs vary widely in hormone receptor status, it is unlikely that the MMTV promoter is expressed equally across all MECs [51, 56]. MMTV activity also depends on nucleosome position, and therefore is

likely to be sensitive to the chromatin state in any given cell [71]. Further study is required to fully elucidate the dynamics of MMTV promoter activity in the transgenic mammary gland.

Identification of Prospective Stem Cells by Label Retention

Prospective adult stem cells and stem cell niches have been identified through a variety of methods, including dye exclusion, drug resistance, expression of known stem cell markers, *in vitro* proliferation, and label retention. These assays rely on the hypothetical properties of adult stem cells, and are used mainly in tissue systems where the stem cell hierarchy is unknown or incomplete, or where no definitive *in vivo* reconstitution assays exist.

Pulse-chase studies of various tissues have identified cell populations that are able to maintain a DNA-based label significantly longer than the bulk of the tissue. Label retention is hypothesized to be a property of adult stem cells with two possible explanations. One is that stem cells divide infrequently, preventing the dilution of label through successive mitoses. The alternative explanation is that when a stem cell undergoes asymmetric division, producing a stem cell and a more differentiated cell, the older template DNA is retained by the stem cell, allowing for maintenance of a strong signal through many divisions. This theory, known as the parental strand or immortal strand hypothesis, suggests an unknown but fundamental difference in the mechanisms of DNA segregation in stem cells. In both of these models, label retention is hypothesized to be a mechanism for maintaining genome integrity [72-74] (Figure 1-6).

Label retention studies have been conducted to identify the stem cells and stem cell niches in various organ systems, most notably in the small intestine and the epidermis [75-77]. In the small intestine experiments, mice were irradiated to clear the small intestinal

epithelium and to activate stem cell proliferation, then given extensive treatments of radiolabeled thymidine or BrdU (bromodeoxyuridine), and sacrificed at intervals to identify and locate the label retaining cells (LRCs). LRCs were found near the bottom of the small intestinal crypts, at specific locations. Further studies demonstrated that these cells were also actively cycling, which provided the first evidence of parental strand retention in an *in vivo* mammalian system [72]. Different intestinal cells recently have been identified as stem cell candidates based on separate criteria, including expression of potential stem cell markers such as Lgr5 and telomerase, and *in vitro* proliferation assays, raising questions over the role of LRCs in the small intestinal stem cell hierarchy [78-80]. In the mammalian epidermis, DNA label retention identified the hair follicle bulge as the repository of LRCs and a potential stem cell niche [81, 82]; epidermal LRCs had a higher proliferative potential than non-LRCs in *ex vivo* cultures and proliferated in response to damage [83, 84]. The epidermal bulge was verified as a stem cell niche when Tumbar et al. isolated fluorescently-tagged epidermal LRCs and demonstrated their stem cell activity *in vivo* [85].

In the mammary gland, label retention studies have been applied to the task of identifying mammary gland stem cells and tracing stem cell activity throughout mammary development. However, the dynamics of the mammary gland, which cycles slowly in comparison to the rapid turnover of the small intestine and epidermis, has resulted in the development of different pulse-chase methods. To stimulate label dilution, some groups transplanted labeled MECs, triggering a fresh round of mammary proliferation in the recipient fat pad. In other studies, pregnancy was induced as a method of label dilution [29, 86-88].

In these studies, mammary LRCs were located in the terminal end buds and along the mammary ducts at regular intervals [29]. A more detailed study found LRCs made up
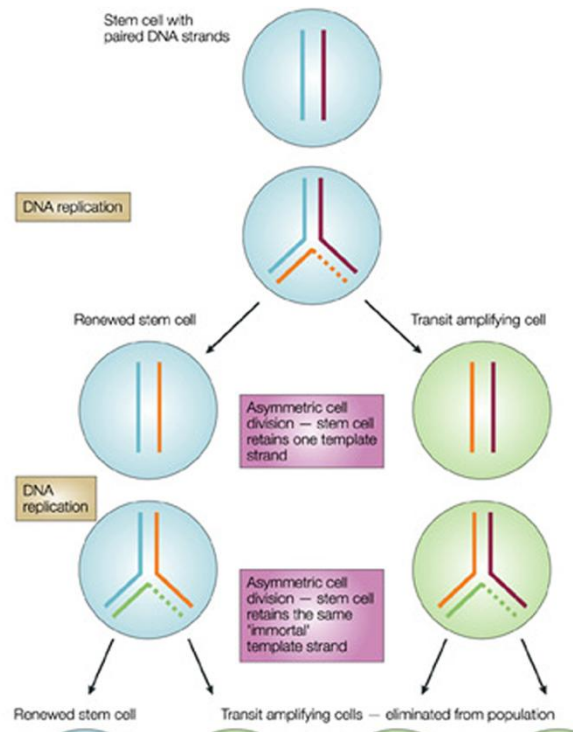
Figure 1-6. The Parental Strand Hypothesis. During an asymetric stem cell division, the older "parental" DNA strands are segregated into the daughter cell which remains a stem cell. A division which produces two stem cells would result in the unsegregated distribution of parental DNA. Immortal/Parental strand segregation is hypothesized to be the mechanism behind label retention in some somatic stem cells. From Smalley and Ashworth [4]

4% of the luminal cells, 20% of the myoepithelial cells and 28% of the basal cell populations [88]. To examine the kinetics of mammary LRCs, Smith and colleagues administered a second DNA label to mammary glands that had already undergone an initial pulse-chase protocol. Mammary cells already retaining the first label were found to incorporate the second DNA label, indicating that they were actively undergoing mitosis; this study raised the possibility of parental strand retention in the mammary epithelium [86]. In contrast to the mammary stem cells isolated by Shackleton et al. and Stingl et al., 40% of mammary LRCs were found to express ER and PR [12, 13, 89]. Mammary LRCs were also found to be actively cycling during pregnancy, suggesting a role for them during alveologenesis [88, 90]. Welm et al. found that MECs exhibiting other hypothesized stem cell characteristics, such as Sca-1 expression and dye efflux, were found to be enriched for mammary LRCs [27];

however, later studies found that dye efflux does not correlate with stem cell activity, and that Sca-1 in fact labeled differentiated mammary cells [12, 13] .

These studies have raised interesting questions about the mechanisms of mammary proliferation and development. The continued cycling of label-retaining cells suggests that parental strand segregation is in operation in mammary epithelial cells. LRC expression of hormone receptors and Sca-1, as well as their activity during pregnancy suggest that LRCs might not be stem cells, but progenitors or stem cells with a pregnancy-specific function [12]. Further study of mammary LRCs is required to elucidate their function in the mammary gland.

The critical weakness of label retention as a method of identifying somatic stem cells is that use of a DNA-based label such as BrdU or tritiated thymidine precludes the isolation of live LRCs for transplantation assays. This limitation has been resolved with the development of a transgenic mouse carrying histone 2b/eGFP fusion (H2BGFP) under the control of a tetracycline responsive regulatory element. When crossed with a strain expressing the tetracycline transactivator, H2BGFP can be turned on and off by administering or withholding tetracycline or doxycycline, resulting in fluorescently labeled cells that can be isolated by FACS [85]. Functional homology between DNA label retention assays and histone label retention assays is probable but not conclusively confirmed. There is conflicting evidence over whether new and old histones distribute evenly or segregate preferentially between daughter strands during DNA synthesis, so no conclusions can be drawn about a "parental histone" hypothesis on current evidence [91-93]. There is also evidence that H2B proteins are continuously synthesized and exchanged without the stimulus of DNA replication, a phenomenon that could alter the kinetics of H2BGFP label retention [94]. However, when the H2BGFP label retention system was used to study skin

development, histone LRCs were found in the epidermal bulge, precisely as DNA LRCs had been. Histone-retaining bulge cells are able to regrow the original epidermis in transplant and proliferate in response to wounding. These histone LRCs were also found to express low levels of proliferation-associated transcripts, suggesting that the mechanism for histone label retention is infrequent mitosis [85, 95].

Subsequently, the transgenic H2BGFP system has been used to identify prospective adult stem cells in the kidney papilla and the ovarian coelomic epithelium [96, 97]. Interestingly, H2BGFP label retention in the hematopoietic system was found to correlate with higher repopulation potential and stem cell markers; this result was unexpected because a previous study had reported that hematopoietic stem cells did not retain a BrdU label [98, 99]. These data demonstrate that H2BGFP label retention is a powerful tool in the isolation of stem cells and identification of stem cell niches.

Contributions of this Thesis

The goal of my studies was to identify and assess prospective mammary epithelial stem cell and progenitor populations, building upon previous knowledge by examining known and potentially novel members of the mammary stem cell hierarchy. I have provided evidence for the existence of a novel pregnancy-activated multipotent mammary progenitor.

Chapter 2 describes the testing of four different transgenic models of inducible H2BGFP expression to identify label-retaining cells in the mouse mammary gland. The MMTVrtTA line[65] proved to be most amenable for labeling MECs with H2BGFP. However, I found that in the MMTVrtTA/H2BGFP model, label retention does not enrich for cells with mammary repopulating ability. However, these studies revealed the existence of an H2BGFP-labeled subpopulation of the CD24$^+$/CD29^{lo} compartment that has *in vivo* repopulation ability.

Chapter 3 evaluates the stem cell and progenitor activity of mammary epithelial subpopulations identified by MMTVrtTA/H2BGFP expression. I found that the H2BGFP$^+$/CD24$^+$/CD29^{lo} population contains multipotent progenitors with the ability to form mammary glandular structures *in vivo*. The repopulation ability of H2BGFP$^+$/CD24$^+$/CD29^{lo} cells increases five- to ten-fold when the transplant recipient is made pregnant, providing evidence that these progenitors are preferentially activated by pregnancy. Expression analysis supports the conclusion that H2BGFP$^+$/CD24$^+$/CD29^{lo} cells are distinct from H2BGFP$^-$/CD24$^+$/CD29^{lo} cells. H2BGFP$^+$/CD24$^+$/CD29^{lo} cells express lower levels of transcripts for genes involved in mammary and differentiation and development than H2BGFP$^-$/CD24$^+$/CD29^{lo} cells, contributing to the evidence that H2BGFP$^+$/CD24$^+$/CD29^{lo} contains mammary progenitors.

The Appendix describes the analysis and testing of candidate cell surface markers for isolation of the H2BGFP$^+$/CD24$^+$/CD29^{lo} population. CD14 is identified as a potential marker for pregnancy-activated progenitors.

This thesis expands on previous work on the mammary stem cell hierarchy by providing evidence for a pregnancy-specific progenitor *in vivo*. This work supports the hypothesis that mammary cells responsible for pregnancy-induced expansion are different from the stem cells and progenitors that establish the mammary gland architecture during puberty.

Chapter 2 Materials & Methods

Mice. CMVrtTA (#003273) [100] and MMTVtTA (#002618) [101] transgenic strains were purchased from Jackson labs. Rosa26rtTA mice were donate by R. Jaenisch [102]. MMTVrtTA mice were donated by L. Chodosh [65]. H2BGFP mice in the CD-1 background were provided by E. Fuchs [85]. H2BGFP was backcrossed onto the FVB strain for a minimum of 5 generations prior to crossing with MMTVrtTA and CMVrtTA mice. To induce transgene expression, breeders and experimental mice were maintained on 2 mg/ml doxycycline (Research Products International 50213285). Mouse colonies were maintained according to federal, state and institutional regulations.

Genotyping. Tail biopsies were obtained from transgenic mice and dissolved in 0.5 ml tail lysis buffer (10 mM Tris + 100 mM NaCL + 10 mM EDTA + 0.5% SDS + 1 mg/ml Proteinase K) at 60ºC for >4 hours. After proteinase K treatment, 250 µl 6 M NaCL was added and each sample, inverted 2-3 times and incubated on ice for 10 minutes. Samples were clarified at 10,000 rpm in a microcentrifuge for 10 minutes. Supernatant was added to 650 µl of isopropanol and inverted 2-3 times. Samples were centrifuged at the highest speed in a microcentrifuge for 10 minutes. Supernatant was decanted, precipitates were air-dried and dissolved in 100 µl ddH$_2$O. For H2BGFP mice: GFP-F: 5'-GCAAGGGCGAGGAGCTGTTCACC-3', GFP-R: 5'-GGCGAGCTGCACGCTGCCGTCCTC-3', expected band size 500 bp. For all tTA/rtTA strains: tTA-F: 5'- CgCTgTggggCATTTTACTTTAg -3', tTA-R: 5'-CATgTCCAgATCgAAATCgTC-3', expected band size 450. Control genotyping PCR: TCRD-F: 5'- CAAATgTTgCTTgTCTggTg -3, TCRD-R: 5'- gTCAgTCgAgTgCACAgTTT -3', expected band size 200 bp. All genotyping PCRs were run as follows: 95ºC 5 min, 95 ºC 45 sec, 58 ºC 45 sec, 72 ºC 60 sec, repeat from second 95 ºC step 25X, 72 ºC 5 min, 4 ºC final. PCR products were run on a 2% agarose gel.

Mammary gland harvesting and preparation. Mice were sacrificed and harvested for mammary glands. Lymph nodes were removed from inguinal gland #4. Mammary tissue was manually minced, placed in culture medium (DMEM/F12 + 500 ng/ml hydrocortisone + 10 ng/ml EGF + 10μg/ml insulin + 20 ng/ml cholera toxin + 1% Pen/Strep) [12] with 600 U/ml collagenase and 200 U/ml hyaluronidase and shaken at 37°C for 1-1.5 hrs. Digested tissue was pelleted and resuspended in a mixture of .25% Trypsin-EDTA (Gibco #15050-065), 5 mg/ml dispase (Roche 04942078001) and .1 mg/ml DNAse (Sigma # D5319) for 5-7 minutes. Trypsin digestion was quenched with DMEM/F12+10% FBS. Cells were pelleted and resuspended in Tris-buffered .64% NH_3Cl for 3 minutes on ice, and filtered sequentially through 100um and 40um filters.

Flow Cytometry. Single cell suspensions were blocked in FACS buffer (PBS + 2 mM EDTA + 0.1% BSA) containing 1:25 normal rat serum (eBioscience 24-5555) and 1:25 anti-mouse FC receptor block (eBioscience 16-0161) for 10 minutes, stained in FACS buffer containing directly conjugated antibodies for 20 minutes. Cells were resuspended in FACS buffer (containing 1μg/ml DAPI for viability analysis) and analyzed on a BD Aria II or FACS Canto II using BD Aria software. Antibodies used for flow cytometry included CD24•PE (eBioscience 12-0242), CD29•APC (Biolegend 102215), CD49f •Biotin (eBioscience 13-0495), CD31•PeCy7 (eBioscience 25-0311), CD45•PeCy7 (eBioscience 25-0451), Ter119•PeCy7 (eBioscience 25-5921) and Streptavidin APC-eFluor 780 (eBioscience 47-4317-82). All populations were double-sorted with doublet discrimination to ensure purity, and were recounted by hemocytometer post-sort to obtain an accurate cell count. Antibodies used for flow cytometry studies described in the Appendix included AlCam•PE (eBioscience 12-1661-81), amphiregulin (R&D BAF989), CD14 (eBioscience 13-0141-80), CD24 (eBioscience 13-0242-80), CD44 (eBioscience 13-0441-81), CD49b (eBioscience 13-

5971-80), CD49f (eBioscience 13-0495), CD55 (eBioscience 12-0559-71), CD61

(eBioscience 13-0611-80), CD86 (eBioscience 13-0862-80), CD138/Syndecan•PE (R&D

FAB2966P), CD164 (R&D BAF3118), c-Kit (eBioscience 13-1171-81), CXCL16 (R&D

BAF503), E-cadherin (eBioscience 13-3249-80), EpCAM (eBioscience 13-5791-80),

FGFR2•PE (R&D FAB684A), IL1R1•PE (R&D FAB7712P), IL33 (R&D BAF3626),

Jag1•PE (Ebioscience 12-3391-80), Muc1 (AbCam ab13970), Osteoactivin (R&D BAF2330),

PRLR (R&D BAF1445), and Sca-1 (eBioscience), Secondary antibodies included

Streptavidin APC-eFluor 780 (eBioscience 47-4317-82), Anti-rabbit Alexa750 (Invitrogen A-

21039)

Mammary fat pad clearing and transplantation. Sorted cells were counted and

resuspended in growth factor-reduced Matrigel (BD Biosciences 354230) for injection.

Three week-old female mice between 10-12g were obtained from Charles River

Laboratories. Mice were anesthetized with 4mg/10g body weight Avertin (Sigma #T48402);

abdomens were shaved and cleaned with 70% ethanol and Betadine. An inverted Y-shaped

incision was made along the thoracic-inguinal region and mammary glands were exposed.

The nipple and mammary artery connecting the #4 and #5 glands were cauterized.

Endogenous epithelium was removed from the inguinal (#4) mammary glands of 3 week-old

female mice; removed epithelium was fixed and stained with carmine alum to verify

complete clearing. Cells were injected into the cleared fat pad pads in 10 µl volumes, using a

Hamilton syringe. Incisions were then closed with wound clips. Mice were administered

with two doses of 0.5 mg/kg body weight Buprenorphine (Webster Vetinary #07-867-1196)

in the 24 hours after surgery. Mammary fat pads were harvested 6 weeks after injection,

unless pregnancy induction required an earlier harvest date. Harvested tissues were either

whole mounted and scored for mammary outgrowths or dissociated for re-analysis and/or serial transplants. [103]

Pregnancy induction. Adult males were housed with post-transplant females 3-4 weeks after surgery. Plugs were checked daily to verify the timing of pregnancies. Females were sacrificed and mammary glands were harvested between day 14-20 of the pregnancy.

Whole Mounts. Mice were sacrificed and #4 mammary glands were dissected, spread onto slides, air-dried for 5 minues and fixed in Methyl Carnoy (1:3:6 glacial acetic acid, chloroform, methanol) for 4-24 hrs. Tissues were treated with successive washes of 100%, 75%, 50% and 25% EtOH, distilled water, and then stained overnight in carmine alum staining solution (2 g/l carmine + 5 g/l aluminum potassium sulfate). Mammary glands were dehydrated in washes of 70% and 100% EtOH, washed twice in xylenes and then mounted in Permount (Fisher SP15-100) and coverslipped. Whole mounts were scored and imaged using a dissecting microscope [103]. All mammary outgrowths observed by carmine alum staining were confirmed by tissue sectioning and immunostaining.

Statistical Analysis of Transplant Data. MRU frequencies were calculated using single-hit Poisson statistical methods [104]. Poisson9 software developed by the Iscov lab was used for these analyses. (http://www.uhnresearch.ca/labs/iscove/homebrew.html)

RNA Isolation and Microarray Analysis. RNA was harvested from sorted cells using the Qiagen RNeasy Micro Kit (Qiagen 74004), amplified using the NuGen RNA amplification system, and analyzed for differences in gene expression on the Illumina Mouse platform.

qPCR. For qPCR confirmation of the microarray experiments, RNA was harvested from sorted cells using the Qiagen RNeasy Micro Kit and amplified using the NuGen RNA amplification system, and labeled using the SYBR Green Master Mix (Applied Biosystems 4309155). qPCR reactions were run on an Applied Biosystems 7900HT. qPCR primers

were: Esr1-F 5'- tgggcgacattcttctcaa-3', Esr1-R 5'-tggaccagaggtacatccatt-3', PRLR-F 5'-ggttatagcatgatgacctgcat-3', PRLR-R 5'- cagttcttcagacttgcccttc -3', AREG-F 5'-gcgaatgcagatacatcgag-3', AREG-R 5'- ccacaccgttcaccaaagta-3', FGFR2-F 5'-gagcgctgccattcaagt-3', FGFR2-R 5'-ttgctgttgttactgctgttcc-3', Muc1-F 5'-ctgttcaccaccaccatgac-3', Muc1-R 5'-cttggaagggcaagaaaacc-3', Wnt5a-F 5'- acgcttcgcttgaattcct -3', Wnt5a-R 5'-cccgggcttaatattccaa-3', Il1R1-F 5'-cgaaccgtgaacaacacaaa-3', Il1R1-R 5'- aatctccagcgacagcagag-3', Cav1-F 5'- acgacgacgtggtcaagatt-3', Cav1-R 5'-cacagtgaaggtggtgaagc-3', Robo1-F 5'-ccacccaccagacaggag-3', Robo1-R 5'-gtatgaggtggggaaattgg-3', Ly6a-F 5'- cccctaccctgatggagtct-3', Ly6a-R 5'- tgttctttactttccttgtttgagaa-3'

3D Matrigel assays. Matrigel™ (BD Biosciences 354230) was pipetted into the wells of an 8-well chamber slide and allowed to polymerize for 15 minutes at 37°C. Sorted MECs were plated at 1,000 cells/well in growth media (DMEM/F12 + 500 ng/ml hydrocortisone + 10 ng/ml EGF + 10 µg/ml insulin + 20 ng/ml cholera toxin + 1% Pen/Strep + 1% FCS) for 1 week, and differentiation media (DMEM/F12 + 5 µg/ml insulin + 500 ng/ml hydrocortisone + 5 µg/ml prolactin + 1% FCS) [12].

Immunostaining. For whole tissue sections, mammary glands were either fixed in Methyl Carnoy, or, if stained previously with carmine alum, unmounted by washing in xylenes. Tissues were paraffin-embedded and sectioned. Slides were deparaffinized in xylenes, and rehydrated in decreasing concentrations of EtOH, followed by 20 minutes boiling in 10 mM sodium citrate for antigen retrieval. For frozen sections, freshly dissected tissues were mounted in OCT (Sakura 4583), flash-frozen in liquid nitrogen and sectioned.

For cytospins and colony assays, slides and coverslips were fixed in 4% PFA and rinsed with PBS for staining. 3D matrigel cultures were fixed and stained as described by

Debnath et al[105]. Primary antibody staining was performed at 4ºC overnight; secondary

antibody staining was performed at room temperature for 1 hr.

Primary antibodies used for immunostaining included cytokeratin 8/TROMA-1

(Developmental Studies Hybridoma Bank TROMA-I-c), cytokeratin 18 (Covance SIG-

3466), cytokeratin 14 (Lifespan Biosciences LS-C22637), p63 (Biolegend 619001), β1 integrin

(BD Biosciences 550531), estrogen receptor (Santa Cruz SC-542), progesterone receptor

(DAKO A0098), glucocorticoid receptor (Santa Cruz SC-1004), milk (Nordic

Immunological Laboratories RAM/MSP), and amphiregulin (Santa Cruz sc-25436). All

secondary antibodies were Alexa Fluor-conjugatedantibodies from Invitrogen.

Chapter 3 Histone Label Retention in the Mouse Mammary Gland

Introduction

Adult stem cells have been observed to retain a DNA-based label for extended periods of time. This has been hypothesized to be either the result of relative mitotic quiescence, or due to stem cell retention of the older "parental" DNA strand. Label retention has been utilized to identify adult stem cells/progenitors and locate stem cell niches in several tissue systems [72, 77]. In the mammary gland, label retaining cells (LRCs) have been found preferentially in the myoepithelial/basal compartment, which is hypothesized to contain mammary stem cells [88]. Although their activity in mammary development is still unclear, mammary LRCs have been observed to be actively undergoing mitosis, which suggests parental strand retention, and might play a role in alveologenesis [86, 90].

The major limitation of the DNA label retention system is that it precludes isolation of live LRCs for functional characterization. These DNA-based labels also damage DNA and can stimulate repair pathways and/or cell division [106]. To enable isolation of live LRCs by fluorescence-activated cell sorting (FACS), Tumbar et al. developed a transgenic mouse carrying the tetracycline-inducible histone 2B/eGFP fusion (H2BGFP), which can be regulated in a tissue- or cell-specific manner by crossing to another strain expressing the tetracycline transactivator driven by a specific promoter [85]. This technique has been effective in isolating prospective adult stem cells in the epidermis, the ovarian coelomic epithelium, the kidney papilla and the hematopoietic system [85, 96, 97, 99].

To identify and isolate prospective stem cells and progenitors through label retention in the mammary gland, I crossed H2BGFP transgenic mice with four different inducible lines, one that expresses the tetracycline transactivator, MMTVtTA [101, 107] and
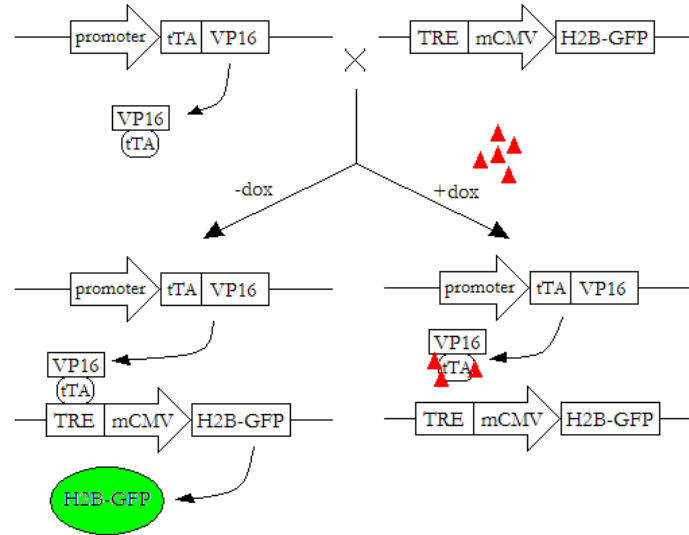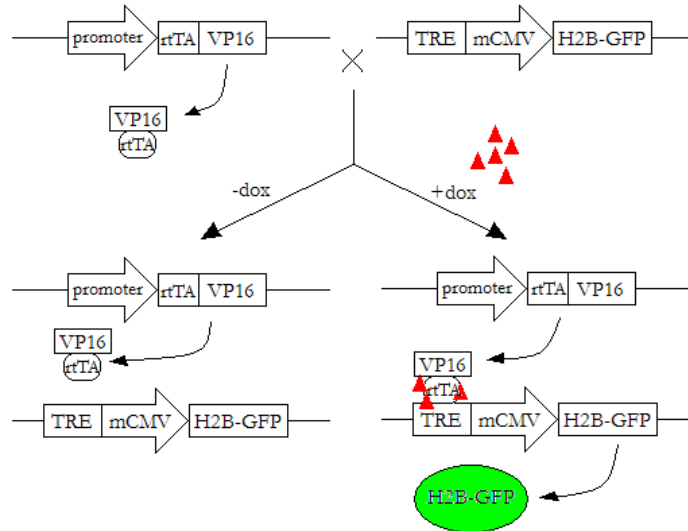
Figure 3- 1. H2BGFP induction under control of tetracycline transactivator vs. reverse tetracycline transactivator. Administration of doxycycline turns off transgene expression in tTA systems (left) and turns on transgene expression in rtTA systems (right).

4 weeks induction　　　　　　　　　*4 weeks induction + chase*
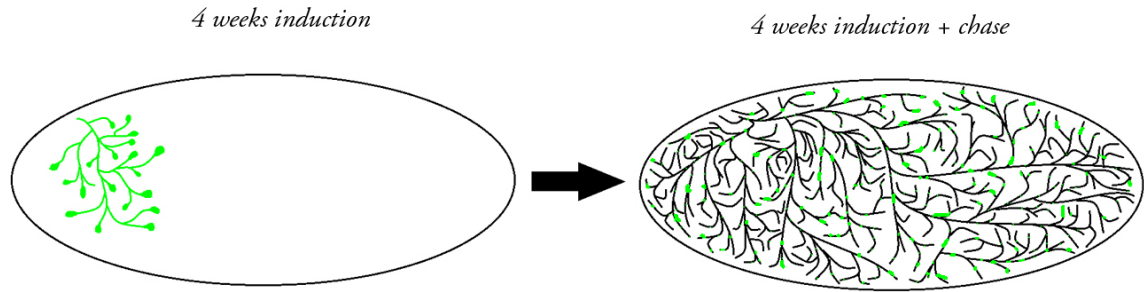
Figure 3- 2. H2BGFP label retention in the mammary gland. H2BGFP expression is induced in the mammary gland until four weeks after birth (left) and turned off for 6-8 weeks. At the end of puberty, H2BGFP LRCs remain in the adult mammary gland (right).

and three that express the reverse tetracycline transactivator, CMVrtTA [100], Rosa26rtTA [102], MMTVrtTA [65] (Figure 3-1). (Tetracycline transactivator is inhibited by tetracycline/doxycycline treatment, and reverse tetracycline transactivator is activated by these drugs.) These strains were selected for their probable expression in mammary epithelial cells. Double transgenic mice were assessed for H2BGFP induction by immunostaining and flow cytometry. Transgene expression was induced until four weeks after birth, and then turned off for six to eight weeks, allowing the high level of mammary proliferation during puberty to act as a "chase" period (Figure 2-2). Label retaining cells were isolated from the mammary gland by FACS and were analyzed for stem cell characteristics and activity. This chapter describes the results of these crosses and the characterization of H2BGFP label-retaining cells in the mammary gland.

Results

CMVrtTA does not induce H2BGFP expression in the mammary gland

The cytomegalovirus (CMV) promoter is known for its high activity in many tissue types and is therefore commonly used to express target genes in both *in vitro* and *in vivo* studies [108]. Kistner et al. developed a transgenic mouse expressing the reverse tetracycline

transactivator under control of the CMV promoter. This transgene is reported to induce

tetracycline-responsive genes in the pancreas, kidney, stomach, muscle, thymus, heart and

tongue; no previous studies of this mouse tested for CMVrtTA activity in the mammary

gland [100].

I crossed the CMVrtTA strain to the H2BGFP transgenic mouse. Because this

transgene expresses the reverse tetracycline transactivator, which is activated by tetracycline

or doxycycline treatment, I maximized H2BGFP induction by treating experimental breeders

and pups with doxycycline throughout breeding, pregnancy, lactation, and after weaning,

until sacrifice. At four weeks post-birth, female double transgenic mice were sacrificed. A

selection of tissues was harvested and cut for frozen sections for direct assessment of

endogenous H2BGFP expression. As controls, tissues were analyzed from doxycycline-

treated H2BGFP single transgenic mice and double transgenic mice that had not received

any drug.

H2BGFP expression was assessed by monitoring direct fluorescence of frozen tissue

sections with DAPI and phalloidin counterstaining. Mosaic H2BGFP expression was

observed in the thymus, stomach, pancreas, kidney and muscle, but not in the lung, liver,

spleen and mammary gland (Figure 3-3). No H2BGFP expression was detected in the

tissues of untreated mice or single transgenic mice (data not shown). The pattern of

H2BGFP detection in the thymus, stomach, pancreas, kidney and muscle was consistent

with previous reports, indicating that the absence of H2BGFP detection in the lung, liver,

spleen and mammary gland were not due to technical issues in my analysis.

To ask whether H2BGFP was expressed at levels below the threshold of

microscopic visualization, mammary glands were harvested from CMVrtTA/H2BGFP mice,
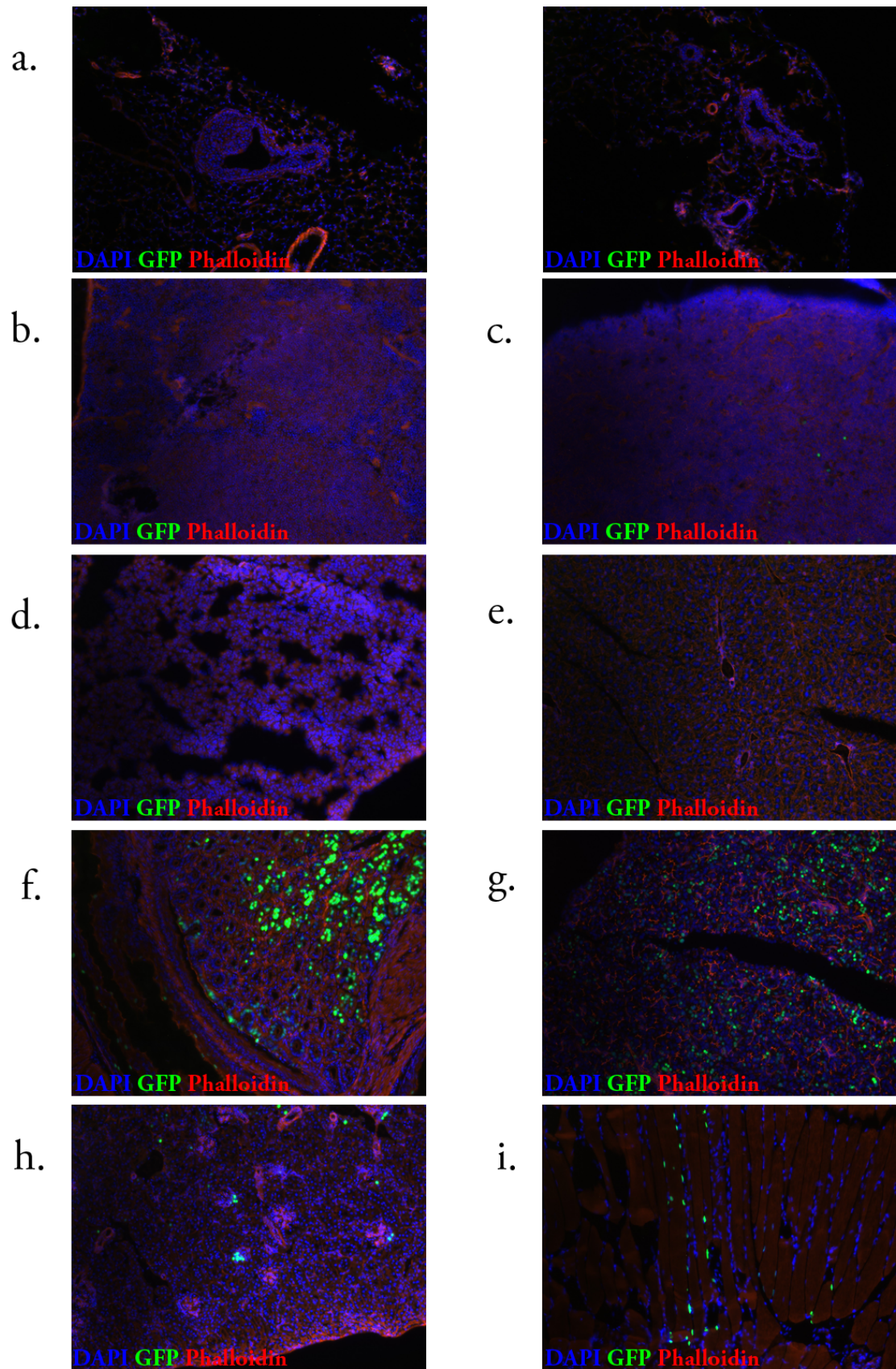
Figure 3- 3. CMVrtTA/H2BGFP expression in various tissues. H2BGFP expression at 4 weeksin a) mammary gland b) spleen c) thymus d) lung e) liver f) stomach g) pancreas h) kidney i) muscle
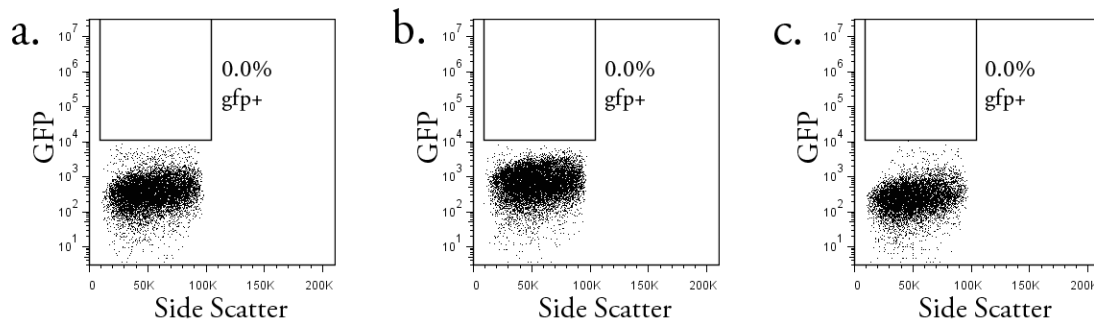
Figure 3- 4. CMVrtTA/H2BGFP expression in the mammary gland. Mammary glands were harvested, dissociated and analyzed by flow cytometry from four week old transgenic females which were a) H2BGFP single transgenic b) CMVrtTA/H2BGFP, no doxycycline treatment c) CMVrtTA

mammary glands from induced double transgenic four week-old females were dissociated

into a single cell suspension and analyzed by flow cytometry. There was no evidence of

H2BGFP expression in CMVrtTA/H2BGFP mice when compared with either single

transgenic mice or double transgenic mice that had received no doxycycline treatment

(Figure 3-4). I therefore discontinued use of the CMVrtTA mouse model.

MMTVtTA expression and label retention in the mammary gland

The MMTV promoter is frequently used to direct transgene expression in the

mammary gland. To create an inducible system for transgene expression in the mammary

gland, Furth et al. developed the MMTVtTA mouse, which expresses the tetracycline

transactivator under control of the MMTV promoter. This transgenic mouse was found to

have tetracycline transactivator activity in the seminal vesicle, salivary gland, epidermis and

mammary gland [107]. Later studies demonstrated that MMTVtTA also is expressed in

lymphoid cells [66].

To express H2BGFP inducibly in the mammary gland for label retention studies, I

crossed the MMTVtTA transgenic strain with H2BGFP mice. Because this system

expresses the tetracycline transactivator, which is deactivated by tetracycline or doxycycline
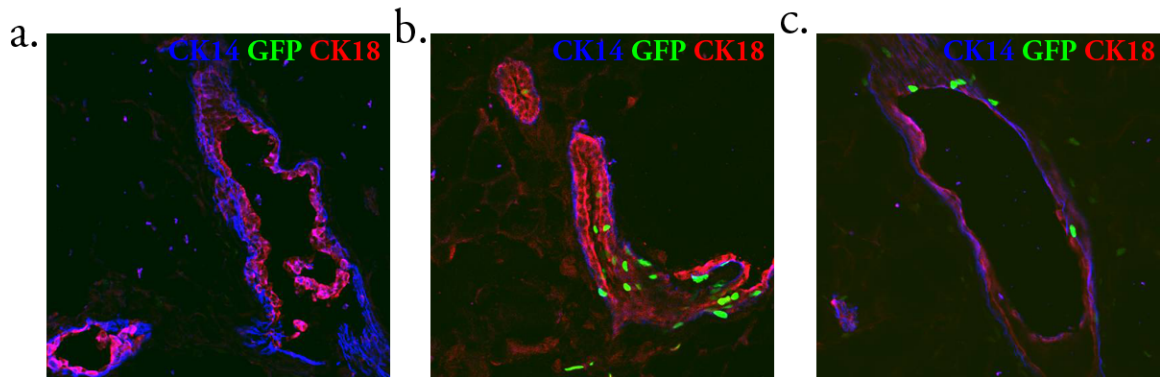
Figure 3- 5 MMTVtTA/H2BGFP Expression and Label Retention in the Mammary Gland - Immunofluorescence. Mammary glands were harvested and stained from female mice a) H2BGFP single transgenic b) MMTVtTA/H2BGFP, four weeks induction c) MMTVtTA/H2BGFP, 4 weeks induction

treatment, mice were kept off of doxycycline until the start of the chase period for the label retention experiment. Tissues were assessed by immunofluorescence and flow cytometry for H2BGFP expression at four weeks after birth, to measure transgene induction, and after 6 weeks of doxycycline treatment, to measure label retention. By flow cytometry, MMTVtTA/H2BGFP induction was detected in $5.8\pm2.1\%$ of MECs, which was reduced to $0.8\pm0.2\%$ after six weeks of doxycycline treatment (Figure 3-6). By immunofluorescence, no correlation was observed between CK14 or CK8 expression and H2BGFP induction or label retention (Figure 3-5). H2BGFP induction and label retention also were observed in hematopoietic tissues at levels higher than those found in the mammary gland.

Although initial experiments with the MMTVtTA mouse were promising, I ultimately discarded this model of H2BGFP induction because the relatively high level of H2BGFP expression in the lymphoid system compared to the mammary gland made the MMTVtTA system unsuitable for further use. Although the flow cytometry assays are gated to exclude hematopoietic lineages, label retention assays necessarily isolate very small populations and are therefore particularly sensitive to contamination. Additionally, in parallel crosses of other tetracycline transactivator strains with H2BGFP, I found that crosses between H2BGFP and the MMTVrtTA or the Rosa26rtTA strains resulted in
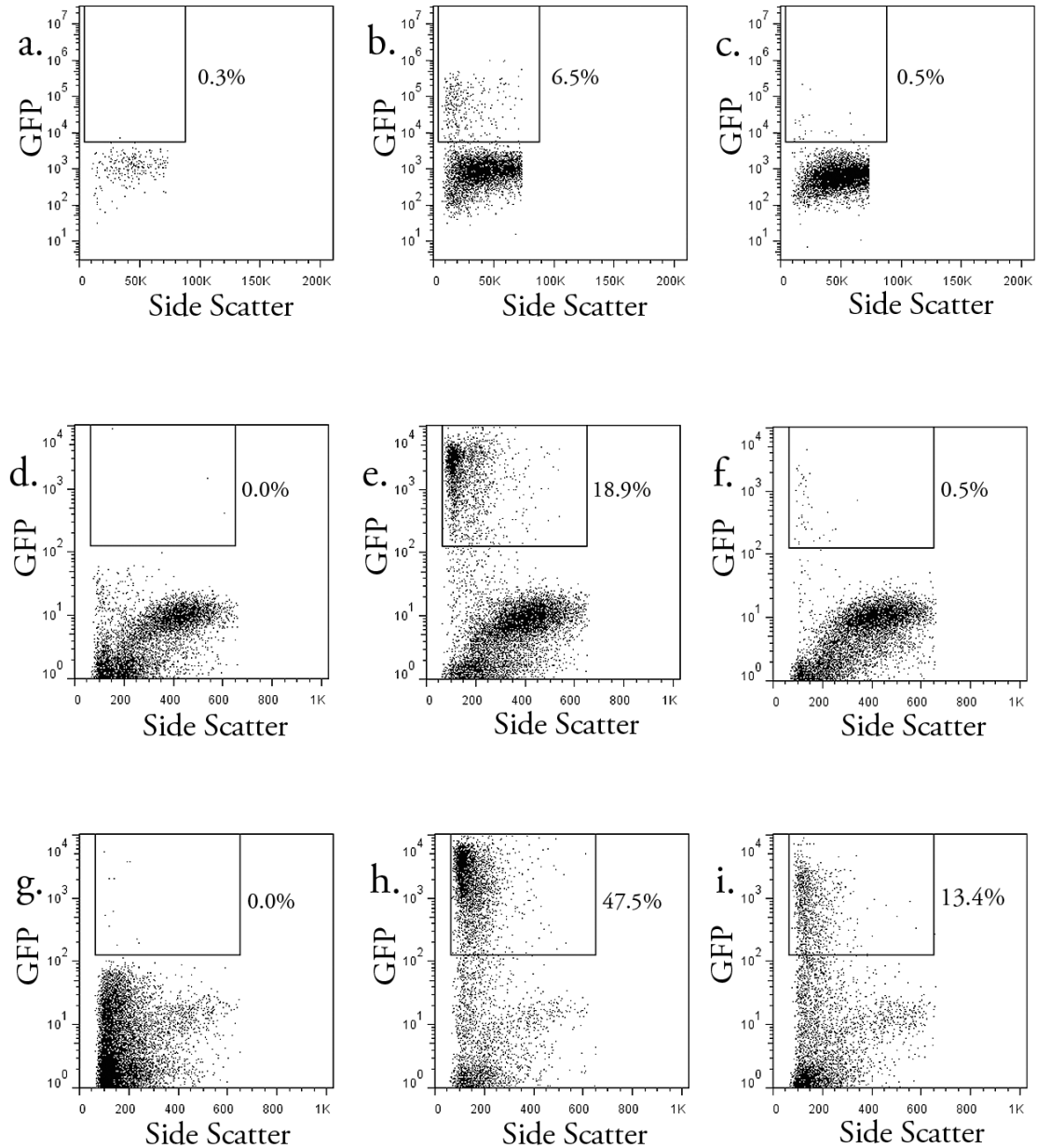
Figure 3- 6. MMTVtTA/H2BGFP Induction and Label Retention – Flow Cytometry. Representative plots for flow cytometric analysis of MMTVtTA/H2BGFP model.. a) Mammary gland, H2BGFP single transgenic b) Mammary gland, MMTVtTA/H2BGFP, 4 weeks induction c) Mammary gland, MMTVtTA/H2BGFP, 4 weeks induction + 6 weeks chase d) Bone marrow, H2BGFP single transgenic e) Bone marrow, MMTVtTA/H2BGFP, 4 weeks induction f) Bone marrow, MMTVtTA/H2BGFP, 4 weeks induction,+ 6 weeks chase g) Spleen, H2BGFP single transgenic h) Spleen, MMTVtTA/H2BGFP, 4 weeks induction i) Spleen, MMTVtTA/H2BGFP, 4 weeks induction + 6 weeks chase

significantly higher levels of transgene induction in the mammary gland, making those two models better suited for my experiments than MMTVtTA.

Rosa26rtTA/H2BGFP expression and label retention in the mammary gland

The Rosa26 reverse tetracycline transactivator (Rosa26rtTA) mouse was developed to allow inducible expression of transgenes in multiple tissues at different stages of development [102]. To ask whether Rosa26rtTA could induce H2BGFP expression in the mammary gland, I crossed the Rosa26rtTA mouse with the H2BGFP strain.

To determine which tissues expressed H2BGFP under the control of Rosa26rtTA, I harvested tissues from four week-old female mice that had undergone constant doxycycline treatment. H2BGFP fluorescence was directly visualized in frozen sections with a DAPI and phalloidin counterstain (Figure 3-7). H2BGFP expression was observed in the mammary gland, lung, liver, muscle, small intestine, pancreas, kidney, spleen, ovary and fallopian tubes. This expression pattern is in accordance with findings reported previously for the Rosa26rtTA transgenic mouse[102, 109].

Mammary glands from four week-old female double transgenics undergoing doxycycline treatment were harvested and analyzed by flow cytometry and immunofluorescence. By flow cytometry, H2BGFP expression was detected in $8.6\pm1.2\%$ of MECs. In the $CD24^+/CD29^+$ compartment, which contains mammary stem cells, $13\pm9.3\%$ of MECs were $H2BGFP^+$ and in the $CD24^+/CD29^{lo}$ progenitor compartment, $4\pm2.5\%$ of MECs were $H2BGFP^+$ (Figure 3-8). Given that $10\pm3.7\%$ of $H2GFP^+$ MECs were found to be $CD24^+/CD29^+$ and $17\pm7.4\%$ of H2BGFP+ MECs were $CD24^+/CD29^{lo}$, I concluded that most $H2BGFP^+$ MECs were differentiated and that there is no special correlation between H2BGFP expression and mammary stem cell/progenitor populations. (Averages and standard deviations were derived from experimental n = 4). Tissue sections from four-
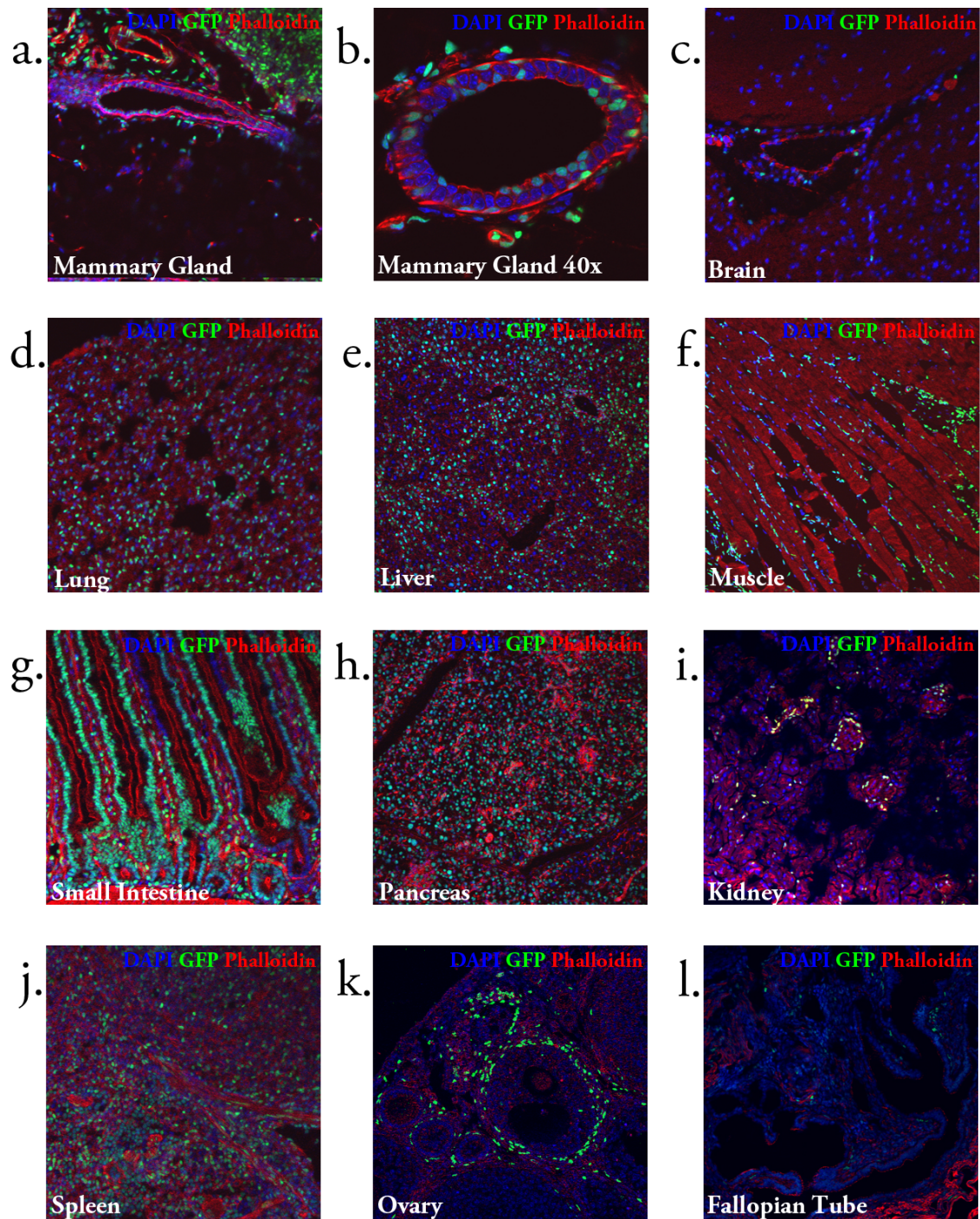
Figure 3- 7. Rosa26rtTA/H2BGFP Induction – Immunofluorescence. Tissues were harvested from 4 week old double transgenic females treated with constant doxycycline. Direct visualization of frozen sections from a) Mammary gland b) Mammary gland 40x c) Brain d) Lung e) Liver f) Muscle g) Small intestine h) Pancreas i) Kidney j) Spleen k) Ovary l) Fallopian tube

38
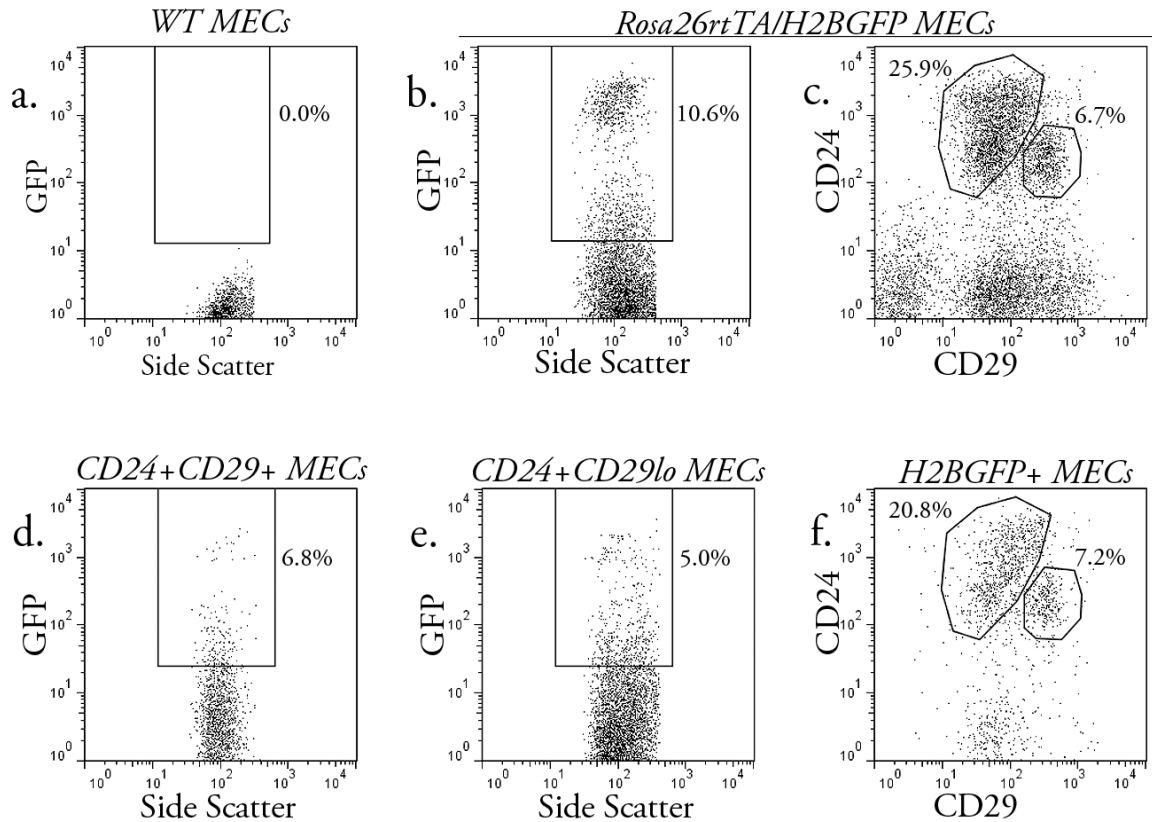
Figure 3- 8. Rosa26rtTA/H2BGFP Induction – Flow Cytometry. Mammary glands were harvested from Rosa26rtTA/ H2BGFP doxycycline-treated females at 4 weeks. Flow cytometric analysis was performed on a) Wild-type MECs b) Rosa26rtTA/H2BGFP MECs, H2BGFP expression c) Rosa26rtTA/H2BGFP MECs, CD24/CD29 expression d) Rosa26rtTA/H2BGFP MECs, CD24+/CD29+ gate, H2BGFP expression e) Rosa26rtTA/H2BGFP MECs, CD24+/CD29lo gate, H2BGFP expression f) Rosa26rtTA/H2BGFP MECs, H2BGFP+ gate, CD24/CD29 expression

week old induced Rosa26rtTA/H2BGFP female mice were immunostained for the

mammary lineage markers CK18 and CK14 (Figure 23-9). By immunofluorescence, no

correlation was observed between H2BGFP expression and known mammary lineages.

Although this level of H2BGFP induction was lower than what was originally hoped

for at the start of a label retention experiment, it remained possible that label-retaining cells

derived from a small percentage of total MECs could still yield a novel population with

potentially interesting stem cell/progenitor properties. Therefore, Rosa26rtTA/H2BGFP

transgenic mice were removed from doxycycline treatment at four weeks post-birth for a six
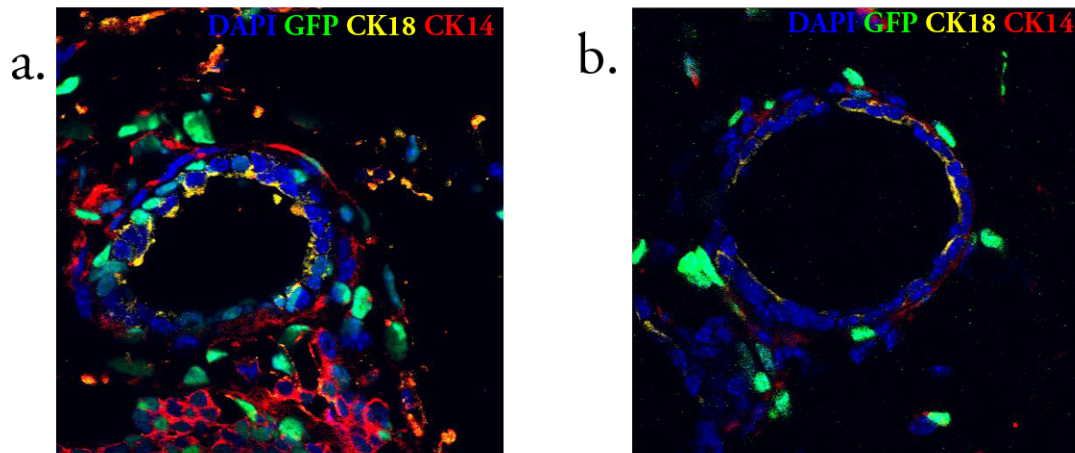
Figure 3- 9. Rosa26rtTA/H2BGFP Induction and Label Retention - Immunofluorescence. Immunofluorescent staining of Rosa26rtTA/H2BGFP mammary glands after a) 4 weeks induction, left b) 4 weeks induction + 6 weeks chase, right. Blue = DAPI, Green = GFP, Yellow = CK18, Red = CK14

to eight week "chase" period, after which mammary glands were harvested and analyzed by flow cytometry and immunofluorescence. After the chase period, 2.9±0.9% of all MECs remained H2BGFP$^+$. Within the CD24$^+$/CD29$^+$ population, 2.7±1.6% of MECs were 2BGFP$^+$, while only 0.6±0.4% of CD24$^+$/CD29^{lo} MECs retained H2BGFP label (Figure 3-10). (Averages and standard deviations were derived from experimental n = 5)   H2BGFP$^+$ cells declined in both number and intensity over the chase period, suggesting label dilution through successive mitoses. No correlation was observed between LRCs and markers of mammary stem cells/progenitors (Figures 3-9, 3-10). However, given the limited number of verified markers of mammary stem cells and progenitors, the possibility remained that mammary LRCs could represent a previously undefined functional mammary epithelial population. To test this hypothesis, mammary LRCs were isolated by FACS and tested by transplantation.

NOD-SCID mice exhibit a mammary transplant growth defect
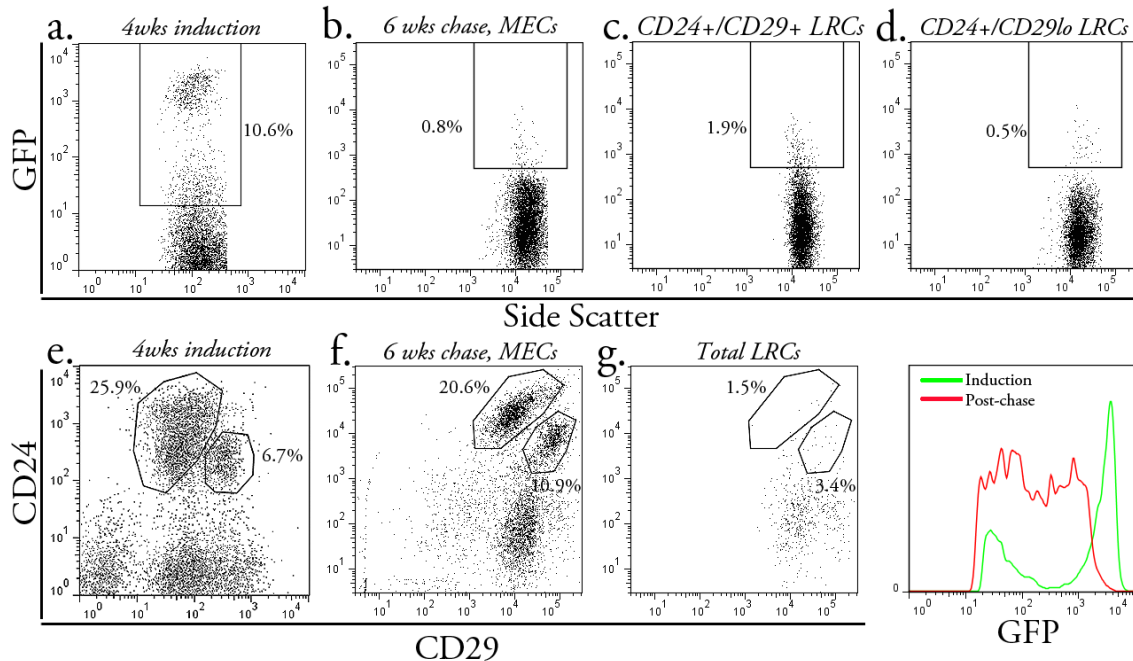
Figure 3- 10. Rosa26rtTA/H2BGFP Label Retention – Flow Cytometry. **Doxycycline was removed from Rosa26rtTA/H2BGFP females four weeks post birth. After 6 weeks of chase, mammary glands were harvested and analyzed for label retention. a) Total MECs from 4 weeks Rosa26rtTA/H2BGFP induction b) Total MECs after 6 weeks of chase, total LRCs c) LRCs within the CD24+/CD29+ population d) LRCs within the CD24+/CD29lo population e) Total MECs from 4 weeks Rosa26rtTA/H2BGFP induction f) Total MECsafter 6-8 weeks chase g) CD24/CD29 expression of LRCs h) Comparison of intensity of H2BGFP+ cells before (green) and after (red) label retention**

The cleared mammary fat pad transplant is the standard *in vivo* assay for testing the stem cell function of MECs. At three weeks of age, the mouse mammary gland has not yet fully penetrated the mammary fat pad. The pubertal mammary epithelium can be surgically removed, and other cells or tissue pieces can be grown in the remaining fat pad without interference from endogenous mammary tissue. Injected cells are sometimes mixed with reconstituted basement membrane (Matrigel™), which polymerizes at body temperature and can therefore physically stabilize the cells in the mammary gland. In control experiments, single cell suspensions of mammary glands were gated for viability and against hematopoietic and endothelial lineages, and sorted for MEC populations with known repopulation activity. I injected these MECs into the cleared fat pads of syngeneic mice (Figure 3-11). In parallel, I transplanted cells from the experimental populations. This approach allowed me to control

41

Injected cells	# cells	# glands	MRU frequency (C.I.)	n
a) Control clearings	0	0/17		3
Cleared, uninjected glands				
b) Mammary Epithelial Cells	10^1	1/25	1/2,600 (1,900-3,500)	3
DAPI⁻/Lin⁻	10^2	14/78		4
	10^3	40/72		4
	10^4	40/49		7
c) MRU markers	10^1	11/37	1/85 (55-130)	3
CD24⁺/CD29⁺	10^2	15/28		3
	10^3	24/24		3
d) Non-MRU	10^2	0/5		1
CD24⁻	10^3	0/32		5
	10^4	0/33		6

Figure 3- 11. Cleared Fat Pad Transplants of Control Populations. Mammary epithelial cells were sorted and transplanted at limiting dilutions into the cleared mammary fat pads of syngeneic mice. Mammary fat pads were harvested after 6 weeks. Transplants were conducted as follows a) Control clearings, no MEC injection b) Unfractionated mammary epithelial cells, gated against other lineages c) MECs gated from the CD24+/CD29+ stem cell compartment d) Differentiated MECs

for technical variability between individual experiments. The calculated mammary repopulation frequency was determined to be 1/2,600, with a 95% confidence interval of 1/1,900 to 1/3,500, for total MECs. The repopulation frequency for the CD24$^+$/CD29$^+$ stem cell population was 1/85, with a 95% confidence interval of 1/55 to 1/130. These data fall within the range of previously published mammary repopulation data for both total MECs (1/1,400 - 1/4,900) and CD24$^+$/CD29$^+$ cells [12, 13].

To assess the repopulation ability of label-retaining cells from the Rosa26rtTA/H2BGFP crosses, LRCs were isolated by flow cytometry after the chase period. Because the H2BGFP transgenic line and the Rosa26rtTA mice were on different genetic backgrounds, these mixed background MECs were transplanted into NOD-SCID mice. To assay the comparative stem cell function of label retaining cells and MECs from the CD24$^+$/CD29$^+$ compartment, limiting dilutions of label-retaining CD24$^+$/CD29$^+$ cells, label-retaining non-CD24$^+$/CD29$^+$ cells and CD24$^+$/CD29$^+$ cells that had not retained H2BGFP were injected into the cleared fat pads of 3 week old NOD-SCID mice (Figure 3-

R26rtTA x H2BGFP	# cells	# glands	MRU frequency (C.I.)	n
Label retaining CD24$^+$/CD29$^+$ MECs	10^2	3/38	1/7,200 (3,100-16,000)	3
GFP$^+$/CD24$^+$/CD29$^+$	10^3	2/13		2
	10^4	3/6		1
Label retaining non-CD24$^+$/CD29$^+$ MECs	10^2	2/35	1/7,000 (2,200-23,000)	3
GFP$^+$, not CD24$^+$/CD29$^+$	10^3	1/18		2
Non-label retaining CD24$^+$/CD29$^+$ MECs	10^2	6/31	1/1,600 (820-2,900)	3
GFP$^-$/CD24$^+$/CD29$^+$	10^3	5/17		2

Figure 3- 12. Rosa26rtTA/H2BGFP Label Retention - Transplant Assays. Mammary epithelial cells were sorted from Rosa26rtTA/H2BGFP mice after a 6-8 week chase period, and injected into cleared fat pads of NOD-SCID mice at limiting dilutions.

12). I calculated the mammary repopulating unit (MRU) frequency of each population, using single-hit Poisson statistical methods [104].

Unexpectedly, the mammary repopulation rate for these injections was extremely low. The label retaining CD24$^+$/CD29$^+$ cells had a calculated MRU frequency of 1/7,200 and the label retaining non-CD24$^+$/CD29$^+$ cells had a MRU frequency of 1/7,000. Non-label retaining CD24$^+$/CD29$^+$ MECs had an MRU frequency of 1/6,000. As the LRC population was not enriched for stem cells, the non-label retaining CD24$^+$/CD29$^+$ cells were expected to have an MRU frequency comparable to what was previously published for the unfractionated CD24$^+$/CD29$^+$ compartment, 1/64 [12]. The outgrowths from these transplants were also observed to be significantly smaller than mammary glands grown from syngenic transplants (Figure 3-13).

There are several possible explanations for these results. Given the cellular heterogeneity of the mammary gland single cell suspensions used in FACS and the broad tissue spectrum of Rosa26rtTA activity, it is possible that the H2BGFP+ label retaining cells isolated from the Rosa26rtTA/H2BGFP cross are heavily contaminated with GFP$^+$ non-mammary cells. However, the repopulation activity of H2BGFP$^-$/CD24$^+$/CD29$^+$ cells in

a.

Label retaining CD24+/CD29+

b.

Label retaining non-CD24+/CD29+

c.

Non-label retaining CD24+/CD29+

d.

100 CD24+/CD29+ MECs

e.

1,000 unfractionated MECs
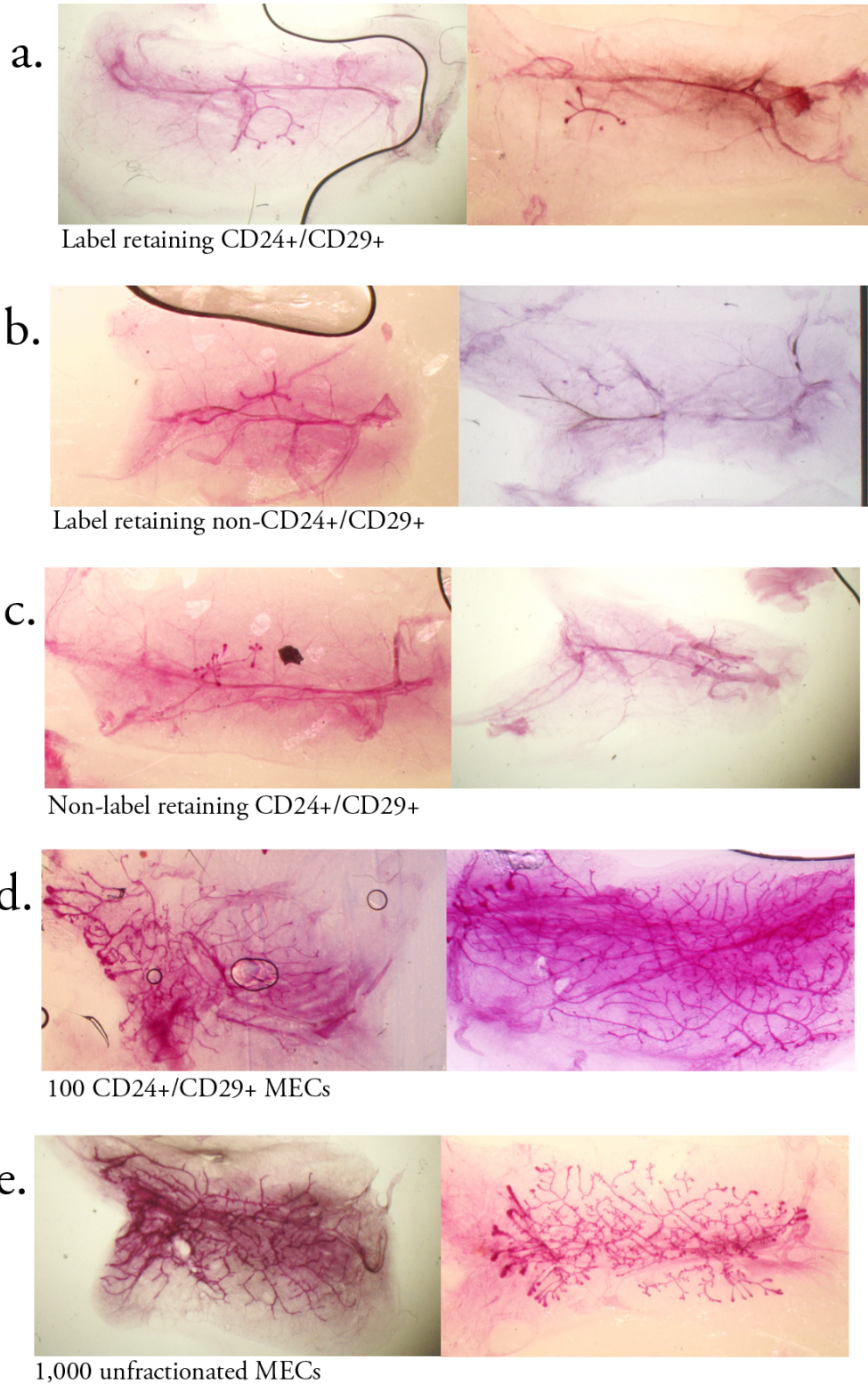
Figure 3- 13. Whole Mounts from Rosa26rtTA/H2BGFP label retention transplants. Mammary fat pad whole mounts from transplants of a) Rosa26rtTA/H2BGFP CD24+/CD29+ LRCs into NOD-SCID fat pads b) Rosa26rtTA/H2BGFP non-CD24+/CD29+ LRCs, into NOD-SCID fat pads c) Rosa26rtTA/H2BGFP CD24+/CD29+ non-LRCs, into NOD-SCID fat pads d) 100 CD24+/CD29+ MECs into syngenic fat pads e) 1,000 unfractionated MECs into syngeneic fat pads

44

NOD-SCID mice was much lower than was found in injections into syngeneic fat pads, which suggests the problem is with the assay, not the donor cells. As the Rosa26rtTA/H2BGFP MECs were derived from fully developed adult mammary glands, the growth defect is probably not caused by any intrinsic or genetic factors within the MECs. It also is unlikely that the problem is associated with Matrigel, or any other injection-related reagents, as successful cleared fat pad transplants were being performed concurrently with these experiments.

As this unusually low reconstitution rate occurred only when NOD-SCID mice were used, and all other transplants were performed by injecting MECs into syngeneic backgrounds, I concluded that the low reconstitution rate was the result of the NOD-SCID mammary fat pad environment. Although mouse mammary tumor cells are routinely injected into the cleared fat pads of NOD-SCID mice, it is possible that successful transplants of normal MECs require an immune component lacking in NOD-SCID mice; for example, macrophage activity, which is required for normal mammary development, is impaired in NOD-SCID mice [110, 111]. Alternatively, the mammary fat pads of NOD-SCID mice might be missing growth factors necessary to the engraftment or proliferation of normal mammary epithelial cells; human MECs grown in NOD-SCID mammary fat pads require the pre-implantation of human stromal cells for the creation of a viable environment [112]. NOD-SCID females are able to nurse their own pups, so this fat pad defect is either compensated for in NOD-SCID MECs or is critical only to mammary glands which are transplanted after birth.

Given the report of successful transplants of normal MECs into NOD-SCID mammary fat pads [35], it is possible that the mammary fat pad defect observed in my experiments were not general to all NOD-SCID mice, but to the specific mice used for these

experiments. NOD-SCID mice were primarily obtained from Charles River Laboratories, and it is possible that any mammary fat pad growth defect is caused by either the genetic sub-strain of the Charles River colony, or to the environmental conditions in which this colony was raised. Dietary alterations have been demonstrated to affect mammary development during puberty [113, 114].

This NOD-SCID problem could have been circumvented by crossing the Rosa26rtTA and H2BGFP transgenic strains onto the same inbred background, obviating the need for transplants into NOD-SCID mice. Alternatively, other immunodeficient strains (e.g. Nu/Nu, RAG-1) might be able to grow transplanted, non-tumor mammary cells. Concurrent experiments using the MMTVrtTA transgenic mouse demonstrated H2BGFP expression in the mammary gland at a significantly higher level than Rosa26rtTA. Additionally, MMTVrtTA induced minimal H2BGFP expression outside of the mammary gland, reducing the risk of contamination from other H2BGFP[+] cell types. Therefore, I discontinued the Rosa26rtTA/H2BGFP experiments in favor of the MMTVrtTA system.

MMTVrtTA induces H2BGFP preferentially in mammary epithelial cells expressing markers of stem cells and progenitors

The MMTVrtTA transgenic mouse was developed by Gunther et al. to express transgenes inducibly in the mammary gland. When crossed with transgenic mice carrying tet-inducible strains, doxycycline treatment reportedly induces transgene expression in the mammary gland, and at low levels in the salivary gland [65]. By contrast, other MMTV-driven transgenes reportedly are expressed in the seminal vesicles and lymphoid cells as well [60, 101]. These findings suggest that the tissue-specific activity of MMTV depends on its insertion site and can vary significantly between transgenic lines. In six week-old

MMTVrtTA/LacZ mice, 72 hours of doxycycline treatment was found to induce LacZ expression in the mammary gland in a dose-dependent, homogenous and completely penetrant fashion[65]. Because MMTVrtTA induction resulted in β-galactosidase activity in 100% of the mammary epithelium, this strain appeared ideal for a label retention study in the mammary epithelium.

I crossed the MMTVrtTA transgenic strain with H2BGFP mice. Because both the CMVrtTA and MMTVrtTA transgenic strains were on the FVB genetic background, the H2BGFP mice were backcrossed onto FVB, allowing syngeneic transplants of any label retaining cells from these crosses. MMTVrtTA/H2BGFP breeders and pups were maintained constantly on doxycycline until the pups were four weeks of age. Mammary glands were harvested from four week-old double transgenic MMTVrtTA/H2BGFP females and the induction of H2BGFP was assessed by immunofluorescence and flow cytometry at the beginning of the label retention experiment (Figure 3-14, 3-15, 3-16, 3-17, 3-18).

Unexpectedly, H2BGFP expression was observed in only a fraction (18 ±3.1%) of all MECs (Figure 3-14a). Doxycycline obtained from various sources was tested in induction experiments and found to evoke the same degree of H2BGFP expression (data not shown). To determine whether MMTVrtTA-induced H2BGFP expression correlated with specific MEC populations, H2BGFP$^+$ cells were analyzed for expression of the known mammary stem cell/progenitor markers CD24, CD29 and CD49f. Notably, all H2BGFP$^+$ MECs stained positive for markers of either the mammary epithelial stem cell (CD24$^+$/CD29$^+$, CD24$^+$/CD49f$^+$) or progenitor (CD24$^+$/CD29^{lo}, CD24$^+$/CD49f^{lo}) compartments (Figure 3-14d, g). Of the H2BGFP+ cells, 47±11% were CD24$^+$/CD29$^+$, 39±11% were CD24$^+$/CD29^{lo}. Of the CD24$^+$/CD29$^+$ and CD24$^+$/CD29^{lo} MECs, 55±6.7% and 15±4.4%

were H2BGFP$^+$, respectively (Figure 3-14e, f). (Averages and standard deviations were derived from an n = 10.)

By CD24/CD49f analysis, 36±7.1% were CD24$^+$/CD49f$^+$ and 50±1.7% were CD24$^+$/CD29^{lo} (Figure 3-14d, g). In the CD24$^+$/CD49f$^+$ compartment, 46±2.6% of MECs were H2BGFP$^+$, and 21±2.7% of CD24$^+$/CD49f^{lo} MECs were H2BGFP$^+$ (Figure 3-14h, i). While all H2BGFP+ subpopulations exhibited a range of H2BGFP expression levels, CD24$^+$/CD29^{lo} and CD24$^+$/CD49f^{lo} progenitor-containing populations were found to have a higher range of fluorescence intensity than CD24$^+$/CD29$^+$ and CD24$^+$/CD49f$^+$ stem cell-containing compartments. (Averages and standard deviations were derived from an n = 4.) To characterize the pattern of MMTVrtTA/H2BGFP expression *in situ*, mammary glands from four week-old double transgenic, doxycycline-induced females were sectioned and immunostained for CK8, CK14, p63, and β1 integrin (CD29). Consistent with the flow cytometry data, MMTVrtTA induced a mosaic pattern of H2BGFP expression, with a range of fluorescence levels. Luminal, myoepithelial and basal/cap cell populations contained some H2BGFP+ MECs (Figure 3-15). The majority of H2BGFP$^+$ MECs were detected within the basal layer of the ductal tree and the cap cells of the terminal end buds. These are known niches for mammary stem cells and correlate with our finding that approximately half of all CD24$^+$/CD29$^+$ cells were H2BGFP$^+$ [12]. Fewer H2BGFP$^+$ cells were detected within the luminal layer, which also is consistent with ~15% of the cells within the CD24$^+$/CD29^{lo} population being H2BGFP$^+$.

MMTVrtTA/H2BGFP mammary glands also were immunostained to detect expression of steroid hormone receptors, which is associated with differentiated MEC populations [12, 13, 40]. MMTVrtTA/H2BGFP induced mammary glands were sectioned
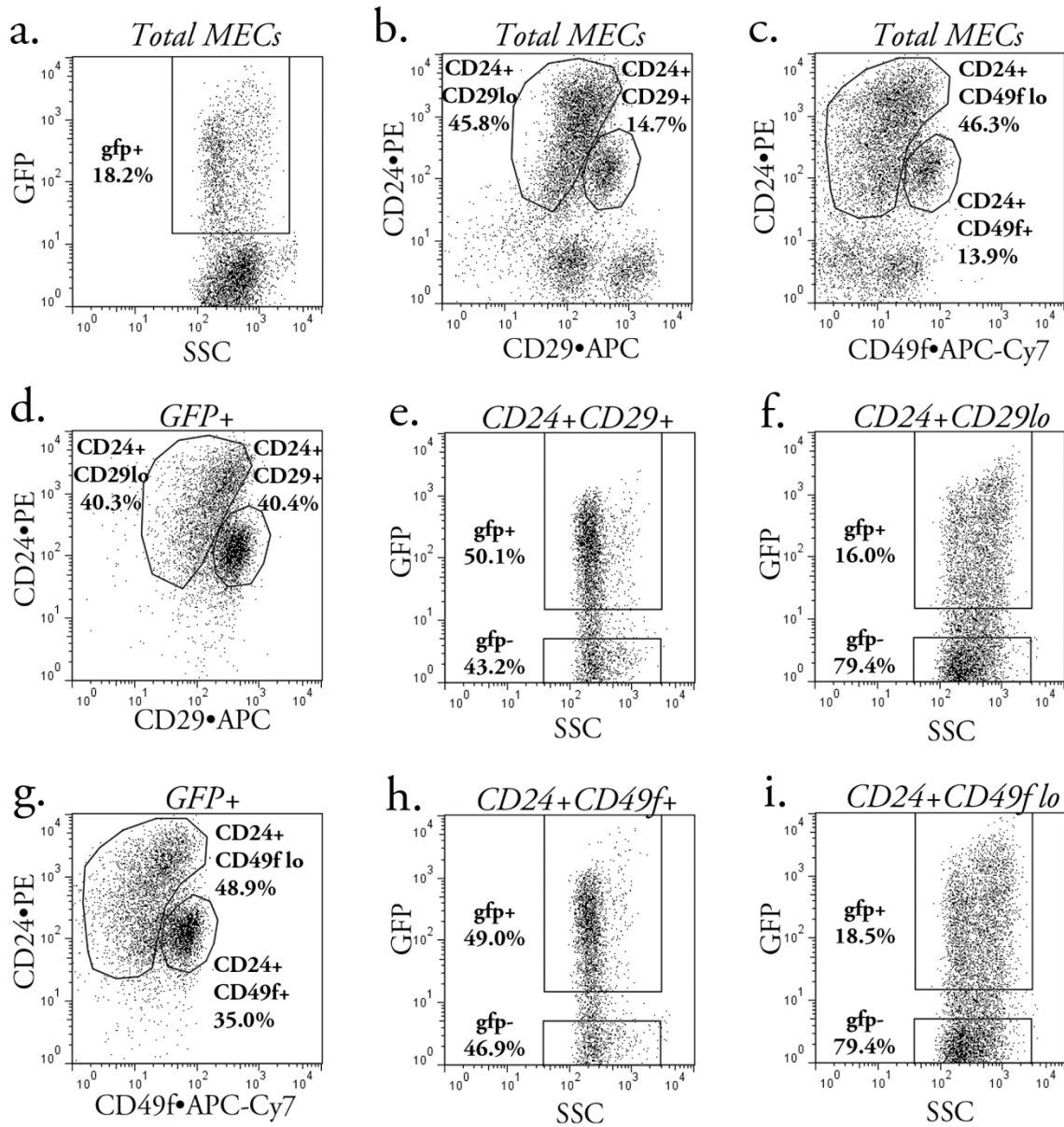
Figure 3- 14. . Flow cytometric analysis of MMTVrtTA/H2BGFP induction. Representative FACS plots from MMTVrtTA/H2BGFP induction mammary glands. Analysis of total MEC population by expression of a) H2BGFP b) CD24/CD29 c) CD24/CD49f. H2BGFP expression within the e) CD24+/CD29+ gate f) CD24+/CD29lo+ gate h) CD24+/CD49f+ gate i) CD24+/CD49f lo gate. Stem cell/progenitor marker expression within the H2BGFP+ population d) CD24/CD29 g) CD24/CD49f

and immunostained for ER (Figure 3-16), PR (Figure 3-17) and glucocorticoid receptor (GR) (Figure 3-18), which activates the MMTV promoter and plays a role in mammary proliferation during pregnancy. In these pubertal mice, the majority of cells in the ducts and TEBs were found to be ER$^+$ and GR$^+$. H2BGFP was co-expressed with ER and GR in some of these cells. Interestingly, H2BGFP$^+$ cells were consistently negative for PR staining (Figure 3-17).

MMTVrtTA label retention in the mammary gland

My discovery that MMTVrtTA induces H2BGFP expression principally in the mammary stem cell and progenitor compartments raised the possibility that LRCs found using the MMTVrtTA/H2BGFP system could represent novel subpopulations of mammary stem cells and/or progenitors and provide new details about the mammary stem cell hierarchy. Therefore, I conducted histone label retention studies in the mouse mammary gland using the MMTVrtTA/H2BGFP system.

MMTVrtTA/H2BGFP females were treated constantly with doxycycline until four weeks post-birth, at the beginning of the chase period. Experimental mice were kept from doxycycline for a six to eight week chase period. At the end of the chase period, mammary glands were harvested from experimental mice, and purified by FACS (Figure 3-19). H2BGFP$^+$ MECs post-chase were reduced in both number and intensity (Figure 3-19 b, h). After this chase period, 2±0.8% of all MECs were found to be H2BGFP$^+$. Of the CD24$^+$/CD29$^+$ cells analyzed, 4.8±1.9% were H2BGFP$^+$ LRCs, while 1.4±1.0% of CD24$^+$/CD29^{lo} cells were LRCs. This is consistent with an approximately ten-fold reduction of detectable H2BGFP+ cells across the entire mammary gland. Among the LRCs, 46.6±14.7% were found to be CD24$^+$/CD29$^+$, which corresponded with pre-chase
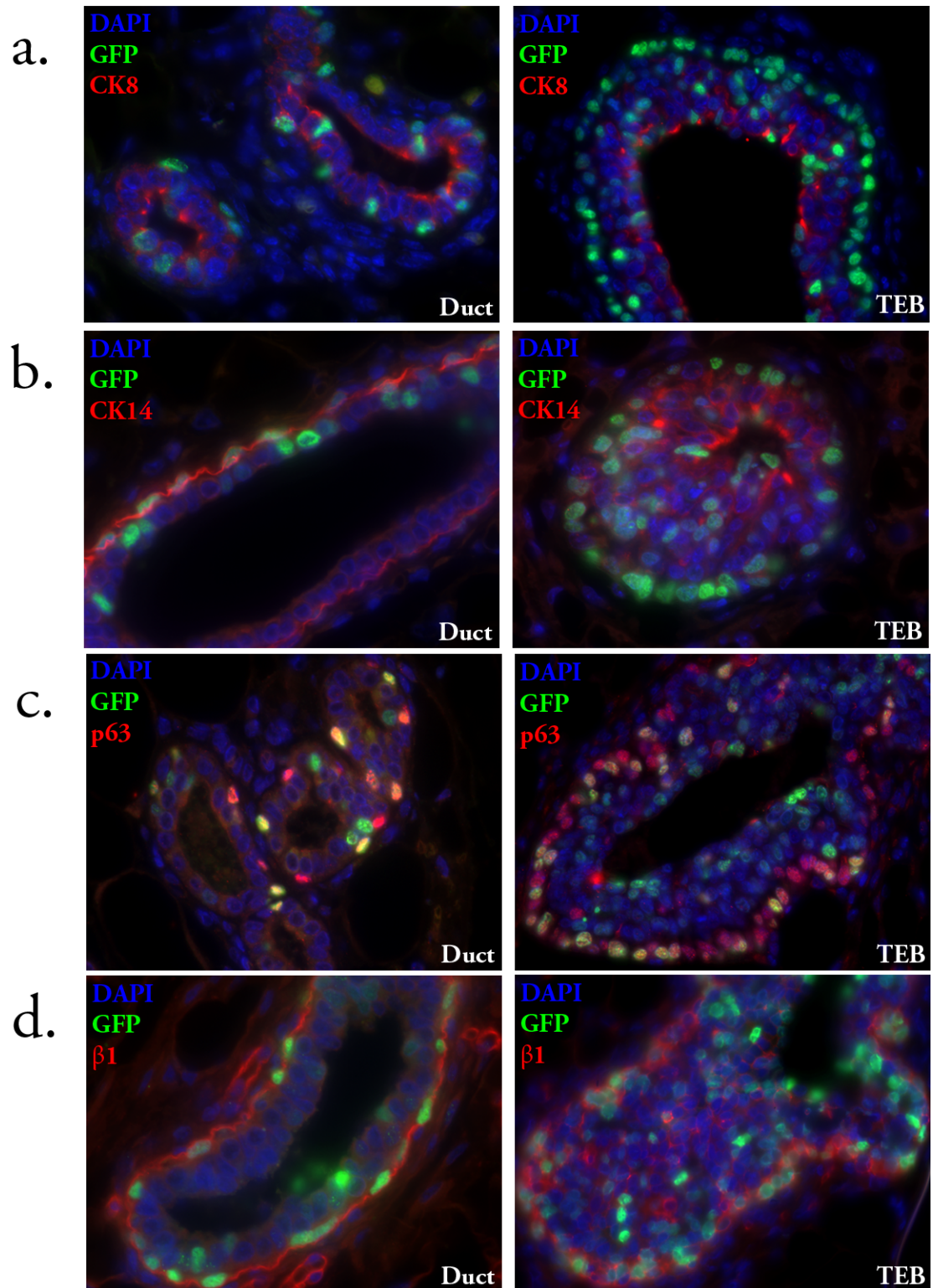
Figure 3- 15. Analysis of Lineage Marker Expression in MMTVrtTA induction of H2BGFP expression in the mammary glands. Representative immunostainings **of** mammary glands harvested from 4 week old double transgenic females treated with doxycycline, sectioned and stained with a) CK8 b) CK14 c) p63 d) β1 integrin. Photographs depict normal ducts (left) and terminal end buds (right).
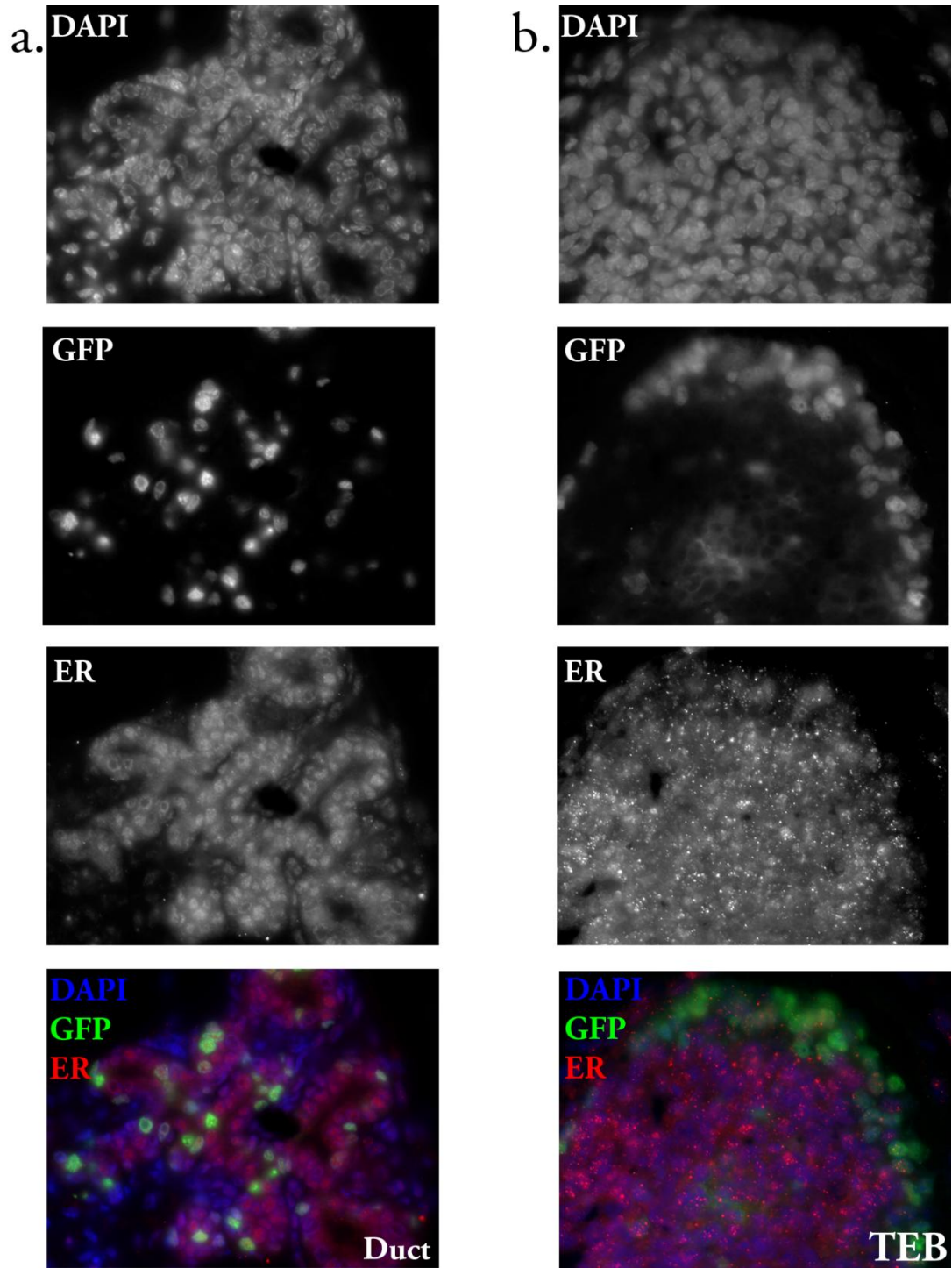
Figure 3- 16. Immunostaining of MMTVrtTA/H2BGFP Mammary Glands for Estrogen Receptor. Mammary glands from four week old doxycycline-treated females were sectioned and stained for estrogen receptor a) Mammary duct b) Terminal end bud
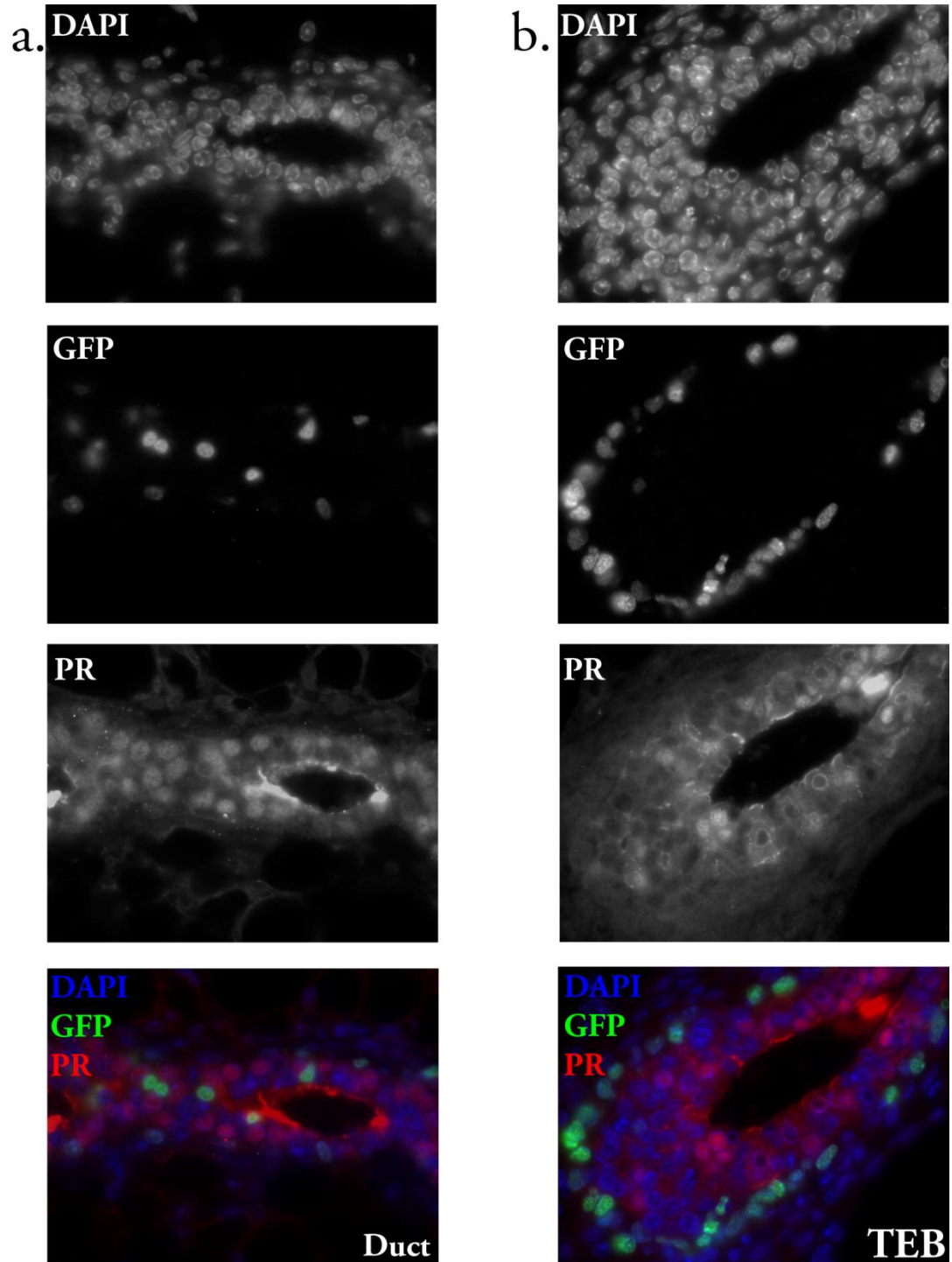
Figure 3- 17. Immunostaining of MMTVrtTA/H2BGFP Mammary Glands for Progesterone Receptor. Mammary glands from four week old doxycycline-treated females were sectioned and stained for progesterone receptor a) Mammary duct b) Terminal end bud
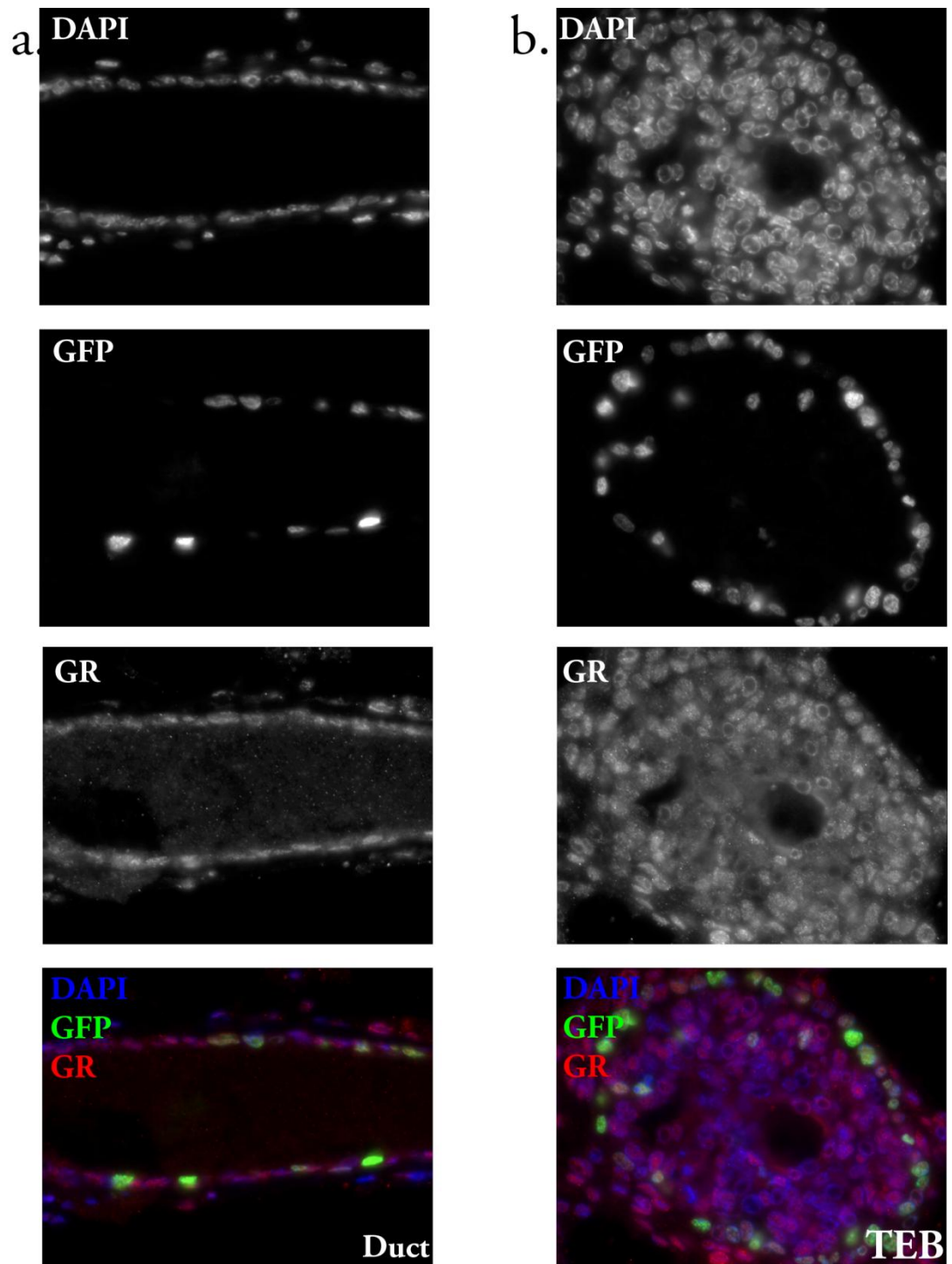
Figure 3- 18. Immunostaining of MMTVrtTA/H2BGFP Mammary Glands for Glucocorticoid Receptor. Mammary glands from four week old doxycycline-treated females were sectioned and stained for glucocorticoid receptor. a) Mammary duct b) Terminal end bud

analysis of H2BGFP$^+$ MECs. However, only 25.7±16.8% were CD24$^+$/CD29^{lo}, which is lower than the pre-chase proportion; this can be accounted for by considering the greater [proliferation activity and label dilution of CD24$^+$/CD29^{lo} progenitors (Figure 3-19g, 3-14d). (Averages and standard deviations were derived from an n = 12.)

Label retention within the CD24$^+$/CD29$^+$ stem cell compartment was expected, but the sizeable fraction of CD24$^+$/CD29^{lo} LRCs required some consideration of mammary gland dynamics. If the pubertal mammary gland follows the classical stem cell hierarchy, with stem cells generating progenitors and progenitors giving rise to large numbers of differentiated cells, active progenitors during puberty would not be expected to indefinitely retain an H2BGFP label. However, H2BGFP$^+$/CD24$^+$/CD29^{lo} MECs exhibited a higher range of fluorescence at 4 weeks than H2BGFP$^+$/CD24$^+$/CD29$^+$ MECs. Therefore, it is
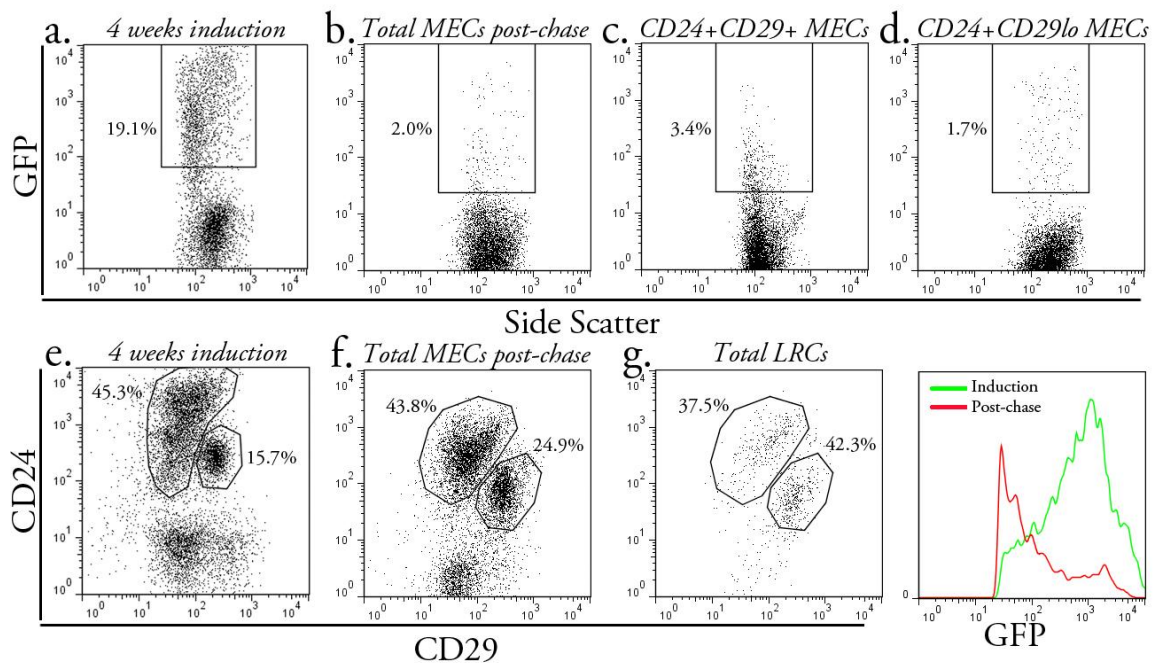
Figure 3- 19. MMTVrtTA/H2BGFP Label Retention. Doxycycline was removed from MMTVrtTA/H2BGFP females four weeks post birth. After 6-8 weeks of chase, mammary glands were harvested and analyzed for label retention. a) Total MECs from 4 weeks MMTVrtTA/H2BGFP induction b) Total MECs after 6-8 weeks of chase, total LRCs c) LRCs within the CD24+/CD29+ population d) LRCs within the CD24+/CD29lo population e) Total MECs from 4 weeks MMTVrtTA/H2BGFP induction f) Total MECs after 6-8 weeks chase g) CD24/CD29 expression of LRCs h) Comparison of H2BGFP intensity before (green) and after (red) label retention

possible that H2BGFP$^+$/CD24$^+$/CD29^{lo} cells had not gone through enough mitoses by the end of puberty to dilute H2BGFP below the threshold of detection in progenitors. Alternatively, the label-retaining H2BGFP$^+$/CD24$^+$/CD29^{lo} MECs might have been or become mitotically quiescent during puberty, suggesting a role for these cells other than that of active progenitor during puberty. Therefore, H2BGFP$^+$/CD24$^+$/CD29^{lo} LRCs could represent terminally differentiated cells, which maintained H2BGFP label because they had completed all of their allotted mitoses, or they could be label-retaining progenitor cells, which function at later stages of mammary development, such as estrus or pregnancy. Finally, it is possible that these CD24$^+$/CD29^{lo} LRCs are progenitors that retain label through asymmetric histone distribution, suggesting a novel mechanism for histone segregation in mammary stem cells and/or progenitors.

To assess the functional significance of the H2BGFP LRCs, label retaining and non-label retaining MECs from both the CD24$^+$/CD29$^+$ and CD24$^+$/CD29^{lo} compartments were sorted and transplanted into the cleared fat pads of syngenic mice. All populations were double-sorted with doublet discrimination to ensure purity, and were recounted by hemacytometer post-sort to obtain an accurate cell count. Recipient mice were maintained on doxycycline to continue transgene induction. Mammary fat pads were harvested after a six week growth period and stained with carmine alum to visualize mammary outgrowths. The resulting mammary glands were scored, and the mammary repopulating unit (MRU) frequency of each sorted population was calculated using single-hit Poisson statistics [104] (Figure 3-20).

Within the CD24$^+$/CD29$^+$ population, the LRCs were found to have a calculated MRU frequency of 1/160, with a 95% confidence interval of 1/110 to 1/240, and non-LRCs had an MRU frequency of 1/270, with a confidence interval of 1/160 to 1/460. Given the

overlapping confidence intervals, this 1.7-fold difference in mammary repopulation ability is unlikely to represent a significant functional difference between LRCs and non-LRCs in the $CD24^+/CD29^+$ compartment. (Averages and standard deviations were obtained from experimental n= 12)

Within the $CD24^+/CD29^{lo}$ population, the LRCs had an MRU frequency of 1/520, compared with the 1/1,900 frequency of non-LRC $CD24^+/CD29^{lo}$ MECs. These results were unexpected, as $CD24^+/CD29^{lo}$ cells were initially reported to have no *in vivo* repopulation ability[12]. In spite of various technical precautions, the small number of mammary outgrowths found in these $CD24^+/CD29^{lo}$ injections could have been the result

Population	# cells	# glands	MRU frequency (C.I.)
a. Label-retaining $CD24^+/CD29^+$	10	5/16	1/160 (110-240)
H2GFP+/CD24+/CD29+	20	3/20	
	50	8/19	
	100	6/11	
	200	10/22	
b. Non-LRC $CD24^+/CD29^+$	10	0/14	1/270 (160-460)
H2GFP/CD24+/CD29+	20	2/10	
	50	3/12	
	100	6/14	
	200	4/13	
c. Label-retaining $CD24^+/CD29^{lo}$	10	0/4	1/520 (160-1,600)
H2GFP+/CD24+/CD29lo	20	0/12	
	50	1/12	
	100	2/8	
	200	0/6	
d. Non-LRC $CD24^+/CD29^{lo}$	10	0/4	1/1,900 (460-7,600)
H2GFP/CD24+/CD29lo	20	0/15	
	50	0/12	
	100	0/4	
	200	2/13	

Figure 3- 20. MMTVrtTA/H2BGFP Label Retaining Cells - Repopulation Assays. Populations were sorted from MMTVrtTA/H2BGFP mammary glands after 6-8 weeks of chase. Sorted MECs were transplanted into cleared fat pads, grown for 6 weeks, harvested, stained with carmine alum and scored. Mammary repopulation unit frequencies were calculated using single-hit Poisson statistics, with 95% confidence intervals.

of contamination. However, because LRCs represented 1.4% of all CD24$^+$/CD29^{lo} MECs, it also was possible that I had enriched for a previously unknown sub-population with *in vivo* repopulating activity that had gone undetected in limiting dilution injections of the whole CD24$^+$/CD29^{lo} population.

Induction vs. Label Retention in the MMTVrtTA/H2BGFP model

Based on the above data, it was possible that I had isolated a unique mammary progenitor through H2BGFP label retention in the CD24$^+$/CD29^{lo} population. However, the induction of MMTVrtTA/H2BGFP in subpopulations of the CD24$^+$/CD29$^+$ and CD24$^+$/CD29^{lo} compartments meant that it was possible that any enrichment in stem cell/progenitor activity might be due to H2BGFP induction, not H2BGFP label retention. Although MMTV promoter activity is known to be dependent on its location within the genome, the MMTV promoter might be turned on preferentially in mammary stem cells and progenitors; from the perspective of viral evolution, stem cells and progenitors are able to effectively propagate the viral genome through their numerous progeny, making stem cell/progenitor-specific activity a useful survival strategy.

To determine whether H2BGFP label retention or induction was responsible for the observed mammary repopulation phenotype of LRCs, CD24$^+$/CD29$^+$ and CD24$^+$/CD29^{lo} populations with and without H2BGFP expression were isolated from doxycycline-treated MMTVrtTA/H2BGFP females four weeks post-birth, without any chase. MEC populations were purified by FACS and subjected to limiting dilution transplantation analysis (Figure 3-20). H2BGFP$^+$/CD24$^+$/CD29$^+$ MECs had an MRU frequency of 1/80, with a 95% confidence interval of 1/60 to 1/120 and H2BGFP$^-$/CD24$^+$/CD29$^+$ MECs had an MRU frequency of 1/100, with a confidence interval of 1/80 to 1/150. This minimal difference

Population	# cells	# glands	MRU frequency (C.I.)
a. GFP$^+$/CD24$^+$/CD29$^+$	10	4/16	1/80 (60-120)
GFP$^+$ MRUs	20	7/16	
	50	8/20	
	100	11/18	
	200	14/16	
b. GFP$^-$/CD24$^+$/CD29$^+$	10	5/20	1/100 (80-150)
GFP MRUs	20	5/20	
	50	7/20	
	100	12/20	
	200	13/18	
c. GFP$^+$/CD24$^+$/CD29^{lo}	10	1/20	1/710 (370-1,400)
GFP$^+$ progenitors	20	0/18	
	50	1/18	
	100	2/20	
	200	5/18	
d. GFP$^-$/CD24$^+$/CD29^{lo}	10	0/18	none
GFP progenitors	20	0/20	
	50	0/16	
	100	0/18	
	200	0/18	

Figure 3- 21. MMTVrtTA/H2BGFP Induction - Repopulation Assays. Populations were sorted from mammary glands of doxycycline-treated MMTVrtTA/H2BGFP females four weeks post-birth. Sorted MECs were transplanted into cleared fat pads, grown for 6 weeks, harvested, stained with carmine alum and scored. Mammary repopulation unit frequencies, with 95% confidence intervals, were calculated using single-hit Poisson statistics.

demonstrates that in primary transplants, there is no difference in the repopulation ability of H2BGFP$^+$ and H2BGFP$^-$ MECs in the CD24$^+$/CD29$^+$ compartment of induced MMTVrtTA/H2BGFP MECs. Surprisingly, induced H2BGFP$^+$/CD24$^+$/CD29^{lo} MECs had a calculated repopulation rate of 1/710, with a confidence interval of 1/370 to 1/1,400. Many of these mammary outgrowths were diminutive when compared to the glands produced by the CD24$^+$/CD29$^+$ populations (Figure 3-22). By contrast, H2BGFP$^-$/CD24$^+$/CD29^{lo} cells did not produce any mammary outgrowths, which is consistent with the lack of reported repopulating activity of bulk CD24$^+$/CD29^{lo} cells [12]. Therefore, the apparent improvement in mammary repopulating ability in H2BGFP$^+$/CD24$^+$/CD29^{lo} cells seen in label retention experiments was not actually due to enrichment by label retention, but
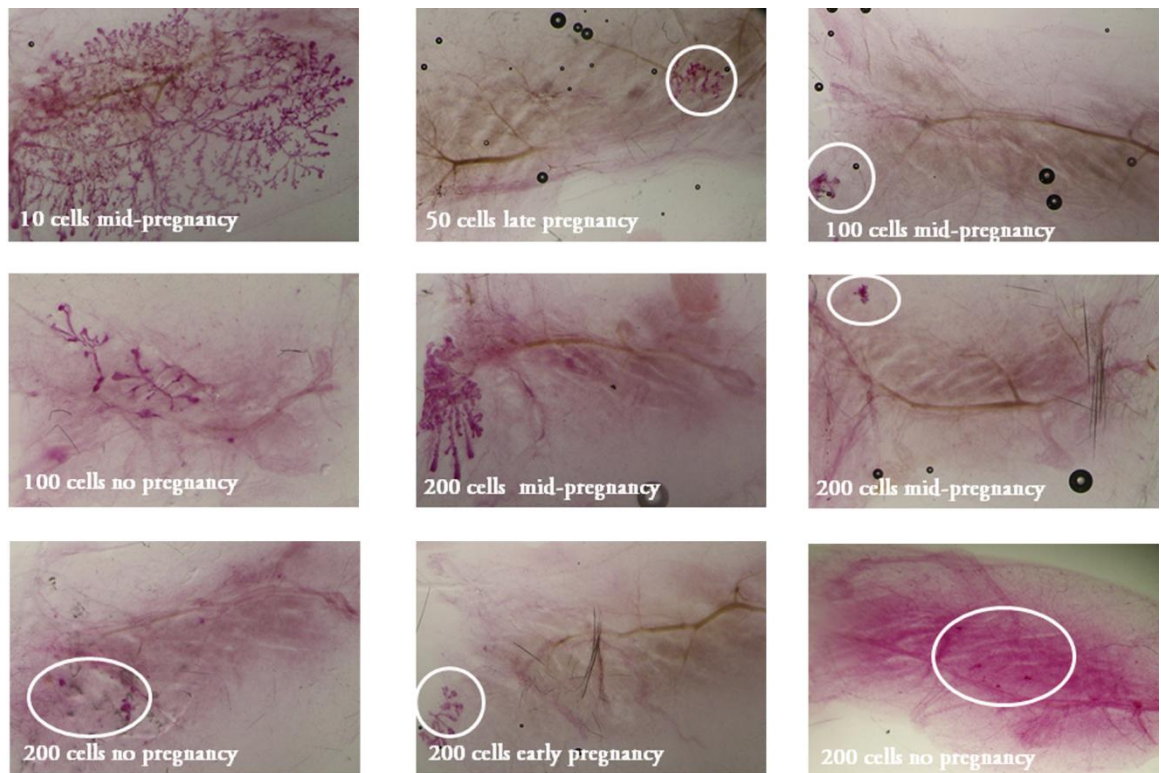
Figure 3- 22. H2BGFP+/CD24+/CD29lo Induction – Whole Mounts. Whole mount carmine alum stainings of mammary fat pads from injections of the H2BGFP+./CD24+/CD29lo population. Circles were drawn around particularly difficult-to-detect mammary outgrowths. All outgrowths were verified by sectioning and immunostaining

rather reflected differential properties of the H2BGFP$^+$/CD24$^+$/CD29^{lo} and H2BGFP$^-$/CD24$^+$/CD29^{lo} marked by MMTVrtTA/H2BGFP induction.

H2BGFP$^+$/CD24$^+$/CD29^{lo} MECs represent only 15% of the CD24$^+$/CD29^{lo} compartment, giving the repopulating cell a frequency of 1/4,700 within the CD24$^+$/CD29^{lo} MECs. This low frequency might mean that the H2BGFP$^+$/CD24$^+$/CD29^{lo} population contains a population of previously undetected mammary stem cells or progenitors. It also is possible that the mammary structures produced by this population were previously overlooked because of their size. In either case, the H2BGFP$^+$/CD24$^+$/CD29^{lo} population merited further examination, which is the topic of Chapter 3.

Discussion & Future Directions

Through the use of the tetracycline-inducible H2BGFP transgenic mouse model, I have investigated the possibility of identifying and isolating novel mammary stem cells and progenitors through histone label retention. Previous DNA label retention studies in the mammary gland have used pubertal proliferation, or a hormone-enhanced variant of the same, for label dilution studies [29, 86]. These studies identified LRCs with potentially interesting properties, but direct isolation of LRCs for growth assays was technically unfeasible.

My H2BGFP label retention studies were directed at the isolation and characterization of histone label retaining cells in the mammary gland. H2BGFP induction requires expression of a tetracycline transactivator, which, for such studies, ideally would be active in all mammary epithelial cells, and absent from any potentially contaminating lineages, such as fibroblasts, endothelial cells and circulating hematopoietic cells. Label retention assays, which require the isolation and characterization of a small population, are sensitive to contamination, particularly in heterogeneous tissues such as the mammary gland. I found that the CMVrtTA transgenic line did not express H2BGFP in the mammary gland. The MMTVtTA model was found to induce H2BGFP expression in ~6% of MECs, but was determined to be unsuitable for label retention due to a combination of low expression in the mammary gland and higher levels of H2BGFP expression in the lymphoid system.

Rosa26rtTA induced H2BGFP expression in 9% of MECs, and numerous other tissues; withdrawal of doxycycline in early puberty resulted in H2BGFP label dilution (Figure 3-10). However, I found that the calculated MRU frequency of $CD24^+/CD29^+$ MECs transplanted into NOD-SCID fat pads was almost 100x lower than expected (Figure 3-12). Because control transplants of MECs into syngenic mammary fat pads produced mammary

outgrowths at the expected frequency (Figure 3-11), I concluded that NOD-SCID mammary fat pads lack a critical component required for growth of exogenous MECs.

The MMTVrtTA/H2BGFP transgenic model resulted in H2BGFP expression in 18% of all MECs, as detected by flow cytometry. Unexpectedly, I discovered that MMTVrtTA induced H2BGFP expression principally within MECs expressing markers for mammary stem cells and progenitors. These findings contrasted with data from Gunther et al. who found MMTVrtTA activity in 100% of the mammary epithelium [65]. The most likely explanation for this discrepancy is that MMTVrtTA activity was monitored by expression of LacZ; the β-galactosidase assay is more sensitive than fluorescence detection.

Based on the lack of association between H2BGFP expression and mammary stem cell/progenitor markers in the Rosa26rtTA/H2BGFP model, I concluded that the unexpected expression pattern exhibited by the MMTVrtTA/H2BGFP model was unlikely to be caused by the H2BGFP transgene. Given that I detected MMTVrtTA induction exclusively in mammary stem cell and progenitor populations, it is possible that H2BGFP protein exists in all MECs, through inheritance from an H2BGFP-expressing progenitor, but at a level below the threshold of fluorescence detection. Alternatively, H2BGFP protein could be less stable than LacZ in differentiated cells. Nevertheless, my finding of mosaic MMTVrtTA activity in this transgenic line suggests that other studies that have utilized these mice might require reexamination, particularly if the conclusions drawn from these studies were dependent on homogenous transgene induction across the entire mammary epithelium. For example, studies where this MMTVrtTA transgene was used to induce tumorigenesis might be subject to different interpretation if these tumors arose exclusively from stem cell and progenitor populations.

The MMTVrtTA/H2BGFP induction data also differed from the expression pattern observed in the Rosa26rtTA/H2BGFP model, which found no correlation between H2BGFP expression and mammary lineage markers by either flow cytometry or immunostaining, even after label retention. Although the MMTVtTA/H2BGFP might be expected to have an expression pattern similar to that of MMTVrtTA/H2BGFP, MMTVtTA gene induction was found to be significantly lower in the mammary gland, and higher in the lymphoid system than in the MMTVrtTA system. This is most likely to be the result of different transgene locations, although it is possible that the different expression patterns are due to differences between the reverse tetracycline transactivator and tetracycline transactivator. The location of the MMTV promoter on the nucleosome has been previously reported to strongly affect MMTV promoter activity [58]. Unfortunately, at the time I was conducting experiments using the MMTVtTA mice, markers for mouse mammary stem cells and progenitors had not been published; therefore, I have no data to directly compare MMTVtTA induction with the MMTVrtTA induction in mammary stem cell/progenitor compartments. Although this remarkable pattern of MMTVrtTA induction of H2BGFP is most likely due to MMTVrtTA activity, I can draw no conclusion about whether the MMTV promoter itself, the transgene's location in the genome, or both, are directly responsible for the pattern of MMTVrtTA activity in the mammary epithelial stem cell/progenitor compartments.

The observed expression pattern in MMTVrtTA/H2BGFP MECs raised the possibility that any increased stem cell/progenitor activity in LRC populations was a product of H2BGFP label retention or induction. Therefore, I performed limiting dilution transplants of H2BGFP$^+$ and H2BGFP$^-$ MEC populations from mammary glands that had

been induced but not chased, as well as glands from label retention experiments. I observed no improvement in repopulation ability due to label retention.

Based on these experiments, I am unable to draw any conclusions about histone label retaining cells in the mammary gland. It remains possible that histone label retention assays could yield previously unknown mammary epithelial cell types. At present, the H2BGFP label retention system is limited by the available reagents for inducing H2BGFP expression in specific tissues.

Interestingly, I found that H2BGFP$^+$/CD24$^+$/CD29^{lo} MECs were able to produce mammary outgrowths while H2BGFP$^-$/CD24$^+$/CD29^{lo} cells were unable to do so (Figure 3-21, 3-22). I concluded that MMTVrtTA/H2BGFP induction in the mammary gland labels a subpopulation within the CD24$^+$/CD29^{lo} compartment which has different properties from the bulk of the CD24$^+$/CD29^{lo} cells, and might represent a novel multipotent progenitor with *in vivo* reconstitution ability. Characterization of the MEC populations labeled by MMTVrtTA/H2BGFP induction is covered in the next chapter of this thesis.

Chapter 4 Evidence for a novel multipotent mammary progenitor with pregnancy-specific activity

Introduction

Studies of mammary gland development have contributed to our understanding of the mammary stem cell hierarchy, which establishes the mammary architecture during puberty and gives rise to milk-producing alveoli during pregnancy. The existence of mammary stem cells was established by demonstrating that a single mammary epithelial cell can give rise to a fully functional mammary gland [12, 13, 25]. Lineage tracing and differentiation studies have provided evidence for lineage-specific mammary progentiors [12, 13, 38]. Although markers for mammary stem cells and progenitors have been identified, these populations have not been isolated to purity and our understanding of how they function in different stages of mammary development remains incomplete.

In the previous chapter of this thesis, I described experiments in which I attempted to isolate and characterize mammary stem cells and progenitors through isolation of cells that retain fluorescently tagged histone 2B after a chase period. I unexpectedly discovered that MMTVrtTA induced H2BGFP expression principally in the $CD24^+/CD29^+$ and $CD24^+/CD29^{lo}$ populations, which contain stem cells and progenitors, respectively. Furthermore, I found that the $H2BGFP^+/CD24^+/CD29^{lo}$ population was able to give rise to multi-lineage mammary outgrowths *in vivo*. The $CD24^+/CD29^{lo}$ population was originally reported to have no *in vivo* repopulation ability; however, while my work was in progress, other groups also reported that $CD24^+/CD29^{lo}$ MECs could give rise to limited mammary outgrowths [35, 36]. Additionally, $CD24^+/CD49f^{lo}$ MECs, which were also reported to have no *in vivo* potential, were found to give rise to mammary outgrowths able to form alveoli in pregnant recipients [35]. These studies suggested the existence of multipotent mammary progenitors in these compartments.

To determine whether MMTVrtTA/H2BGFP expression labels novel mammary stem cells or progenitors, I have assayed these MMTVrtTA/H2BGFP MEC populations for *in vivo* and *in vitro* growth ability and studied their gene expression profiles. This chapter reports evidence for a novel pregnancy-activated multipotent progenitor within the mouse mammary gland, and describes its functional properties.

Results

MMTVrtTA/H2BGFP expression in the CD24+/CD29+ compartment does not label long term mammary stem cells

In the hematopoietic system, stem cells have been sub-categorized based on their ability to reconstitute multi-lineage tissues over numerous serial transplants. Hematopoietic stem cells capable of sustaining developmental proliferation indefinitely are referred to as long-term stem cells, while stem cells that are only able to regenerate for only a few rounds of serial transplantation are known as short-term stem cells[115]. Analogous populations may exist in the mammary gland, but have not yet been positively identified.

Previous transplant experiments comparing MEC populations from mammary glands of induced MMTVrtTA/H2BGFP mice demonstrated that H2BGFP$^+$/CD24$^+$/CD29$^+$ and H2BGFP$^-$/CD24$^+$/CD29$^+$ MECs were functionally indistinguishable (Figure 3-21). Both populations repopulated the mammary gland at similar frequencies, which were consistent with previously published *in vivo* transplant frequencies of the unfractionated CD24$^+$/CD29$^+$ cells [12]. However, these assays did not address the long-term repopulation potential of these populations, as defined by the ability of these cells to serially transplant over many generations.

To test the long-term repopulating activity of MMTVrtTA/H2BGFP MECs, each of the four populations was sorted from the mammary glands of four week-old MMTVrtTA/H2BGFP females by flow cytometry. In each experiment, each MEC population was injected into 10 cleared fat pads of syngeneic mice in 500-cell aliquots. Recipient mice were treated with doxycycline to promote H2BGFP expression. After six weeks, transplanted fat pads were harvested and pooled according to transplanted cell type, analyzed by flow cytometry and re-transplanted. MMTVrtTA/H2BGFP populations were serially transplanted to secondary transplants in two experiments, and to a tertiary transplant in one experiment. $H2BGFP^+/CD24^+/CD29^+$ and $H2BGFP^-/CD24^+/CD29^+$ MECs gave rise to serially transplantable mammary glands (Figure 4-1c, d). The transplanted $CD24^+/CD29^+$ gave rise to smaller percentages of $CD24^+/CD29^+$ and $CD24^+/CD29^{lo}$ MECs than was found in the control glands; since serial transplants took place at six-week intervals, and mouse mammary fat pads are usually filled around eight to ten weeks post-birth, these percentages probably reflect incompletely filled mammary fat pads and higher percentages of non-epithelial cells. Surprisingly, only $H2BGFP^+/CD24^+/CD29^+$ cells gave rise to mammary glands expressing H2BGFP. This result suggested that H2BGFP expression was permanently turned off in the $H2BGFP^-/CD24^+/CD29^+$ populations. To eliminate the possibility that the apparent $H2BGFP^-/CD24^+/CD29^+$ outgrowths were actually the product of endogenous MECs from incompletely cleared mammary fat pads, genomic DNA was harvested from transplant mammary glands after tertiary transplants and tested by PCR for MMTVrtTA and H2BGFP transgenes. Both transgenes were present in $H2BGFP^+/CD24^+/CD29^+$ and $H2BGFP^-/CD24^+/CD29^+$-derived glands, demonstrating their transgenic origin. Therefore, both $CD24^+/CD29^+$ populations are capable of long term *in vivo* stem cell activity, but H2BGFP expression in the $CD24^+/CD29^+$ population is
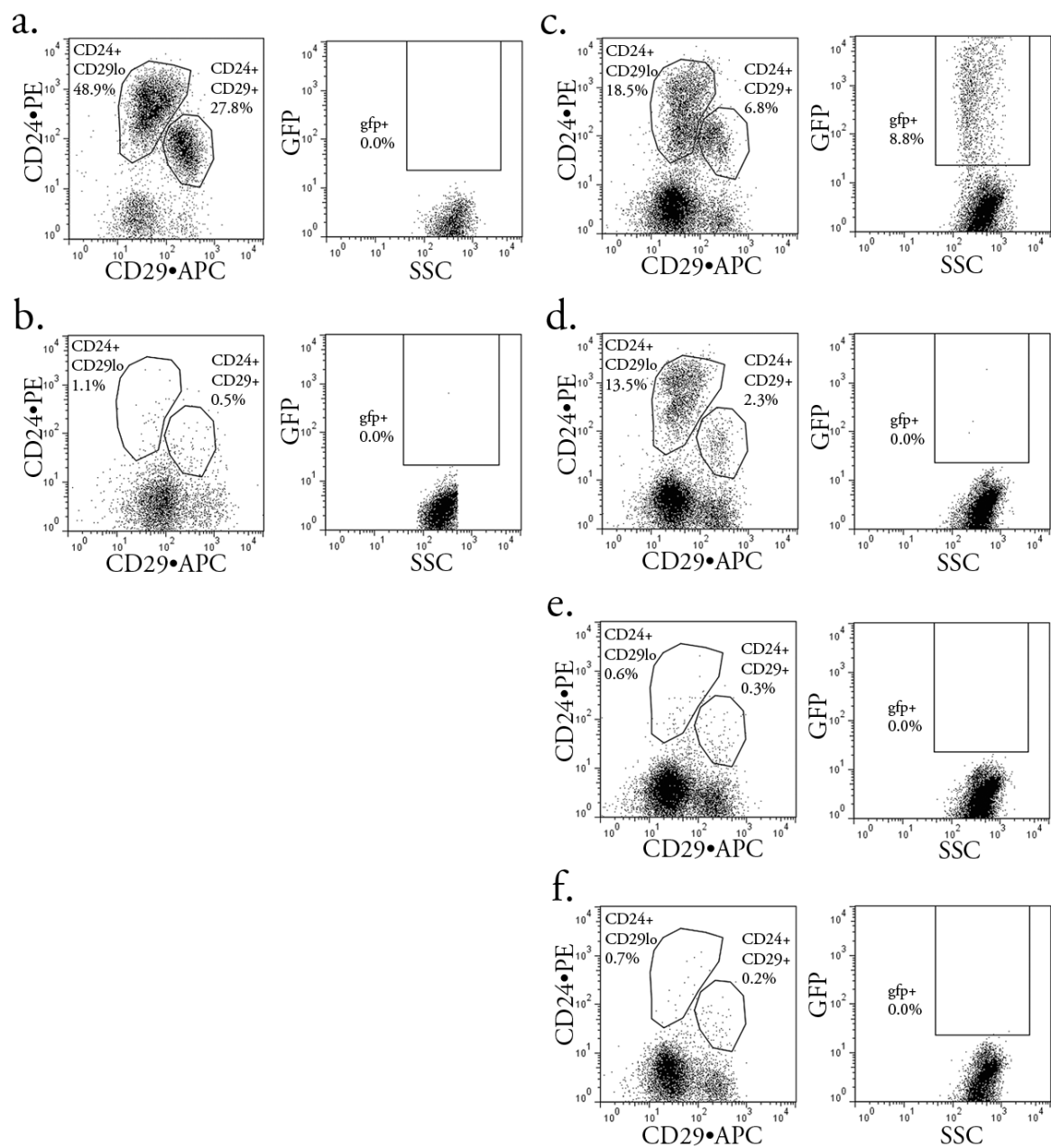
Figure 4- 1. Serial Transplants Analysis of MMTVrtTA/H2BGFP Populations. Representative flow cytomtetry plots of serial transplants. MMTVrtTA/H2BGFP MEC populations were sorted and transplanted at six week intervals; two experiments were carried out to secondary transplants, and one experiment was carried to tertiary transplant. Serially transplanted glands were analyzed by flow cytometry for expression of CD24/CD29 (left) and H2BGFP (right). Analysis of a) WT MECs b) empty mammary fat pads c) H2BGFP+/CD24+/CD29+ d) H2BGFP-/CD24+/CD29+ e) H2BGFP+/CD24+/CD29lo f) H2BGFP-/CD24+/CD29lo

epigenetically inherited and does not distinguish functionally different populations of CD24$^+$/CD29$^+$ cells.

Notably, the H2BGFP$^+$/CD24$^+$/CD29^{lo} population was unable to serially transplant, suggesting a progenitor origin for H2BGFP$^+$/CD24$^+$/CD29^{lo}-derived mammary outgrowths.

H2BGFP+/CD24+/CD29lo contain a population of pregnancy-activated multipotent mammary progenitors

In Chapter 3, I showed that H2BGFP$^+$/CD24$^+$/CD29^{lo} cell transplants were able to form small mammary glandular structures (Figure 3-21, 3-22). Although diminutive, these structures contained both luminal and myoepithelial/basal lineages and were able to produce milk, but had no serial transplantation ability (Figure 4-1). By contrast, H2BGFP$^-$/CD24$^+$/CD29^{lo} MECs were unable to produce any mammary outgrowths *in vivo*, suggesting different functions for H2BGFP$^+$ and H2BGFP$^-$ cells within the CD24$^+$/CD29^{lo} compartment. Therefore, MMTVrtTA induction of H2BGFP labels a CD24$^+$/CD29^{lo} sub-population containing a previously uncharacterized multipotent mammary progenitor with *in vivo* repopulation potential.

In the transplant experiments reported in Chapter 2, some transplant recipient mice were maintained as virgins and others were mated post- transplant to induce pregnancy and increase the size and visibility of the mammary outgrowths. To determine whether pregnancy affects the repopulation rate of MMTVrtTA/H2BGFFP populations, the limiting dilution data from virgin and pregnant mice were reanalyzed (Figure 4-2). Mammary outgrowths from these experiments were also scored for their size (Figure 4-3, Figure 4-4, Figure 3-22). The mammary repopulation abilities of the H2BGFP$^+$/CD24$^+$/CD29$^+$ and

H2BGFP$^-$/CD24$^+$/CD29$^+$ populations were similar in virgin and pregnant recipients (Figure 4-2a, b, e, f). Based on these data, I conclude that MMTVrtTA/H2BGFP expression in the CD24$^+$/CD29$^+$ compartment does not label MECs with different repopulating activity during pregnancy.

By contrast, the repopulating activity of H2BGFP$^+$/CD24$^+$/CD29^{lo} MECs was nearly five-fold higher in pregnant mice compared to virgins. The functional MRU frequency was 1/350 in pregnant mice, compared to 1/1,600 in virgins (Figure 4-2c, g). As described in Chapter 2, outgrowths from H2BGFP$^+$/CD24$^+$/CD29^{lo} MECs were smaller than glands derived from CD24$^+$/CD29$^+$ populations (Figures 3-22, 4-4, 4-5, 4-6), but still contained all mammary lineages and were able to produce milk (Figure 4-7). H2BGFP$^-$/CD24$^+$/CD29^{lo} MECs were unable to produce mammary outgrowths in either virgin or pregnant mice (Figure 4-2d, h).

To directly address whether H2BGFP$^+$/CD24$^+$/CD29^{lo} MECs selectively expand during pregnancy, I performed a controlled, separate series of cleared mammary fat pad transplants (n=3), focusing specifically on the H2BGFP$^+$/CD24$^+$/CD29^{lo} population. Half of the mice injected with H2BGFP$^+$/CD24$^+$/CD29^{lo} MECs were systematically made pregnant post-transplant for a direct comparison of H2BGFP$^+$/CD24$^+$/CD29^{lo} repopulation ability in virgin vs. pregnant mice (Figure 4-6). In these experiments, the calculated MRU frequency was 1/3,800 in virgin mice and 1/280 in pregnant mice. These data indicated that MMTVrtTA/H2BGFP expression in the CD24$^+$/CD29^{lo} compartment labels a population containing multi-potent progenitors that exhibit proliferative activity preferentially during pregnancy.

Shackleton et al. demonstrated that the CD24$^+$/CD29$^+$ and CD24$^+$/CD29^{lo} MEC populations could give rise to different structures when grown on a commercially available

Population	# cells	# glands	MRU frequency (confidence interval)
Virgin Recipients			
a. H2GFP$^+$/CD24$^+$/CD29$^+$	10	3/16	1/110 (70 – 160)
	20	5/12	
	50	3/12	
	100	6/10	
	200	9/12	
b. H2GFP$^-$/CD24$^+$/CD29$^+$	10	2/12	1/80 (60 – 130)
	20	2/14	
	50	5/12	
	100	9/12	
	200	9/10	
c. H2GFP$^+$/CD24$^+$/CD29^{lo}	10	0/14	1/1,600 (500 – 5,000)
	20	0/12	
	50	0/12	
	100	1/12	
	200	2/14	
d. H2GFP$^-$/CD24$^+$/CD29^{lo}	10	0/14	none
	20	0/12	
	50	0/12	
	100	0/14	
	200	0/14	
+ Pregnancy			
e. H2GFP$^+$/CD24$^+$/CD29$^+$	10	1/4	1/60 (34 – 100)
	20	3/6	
	50	5/8	
	100	5/8	
	200	6/6	
f. H2GFP$^-$/CD24$^+$/CD29$^+$	10	3/8	1/130 (80 – 240)
	20	3/6	
	50	2/8	
	100	4/8	
	200	4/8	
g. H2GFP$^+$/CD24$^+$/CD29^{lo}	10	1/6	1/350 (150 – 800)
	20	0/8	
	50	1/6	
	100	1/8	
	200	3/6	
h. H2GFP$^-$/CD24$^+$/CD29^{lo}	10	0/6	none
	20	0/8	
	50	0/6	
	100	0/6	
	200	0/6	

Figure 4- 2. MMTVrtTA/H2BGFP Populations in Virgin Vs. Pregnancy. Limiting dilution transplants in virgin recipients (a-d) and pregnant recipients (e-h) of MMTVrtTA/H2BGFP populations a,e) H2BGFP+/CD24+/CD29+ b,f) H2BGFP-/CD24+/CD29+ c,g) H2BGFP+/CD24+/CD29lo d,h) H2GFP-/CD24+/CD29lo

–
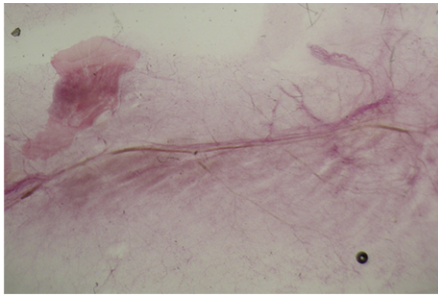
No epithelial outgrowth.
Only vasculature and fat pad striations.

~
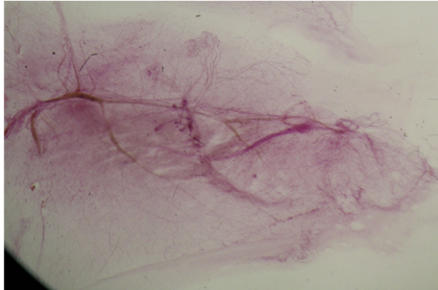
Small outgrowth(s), ranging from lone
TEBs to growths of 2-3 branched
ducts with TEBs.

+
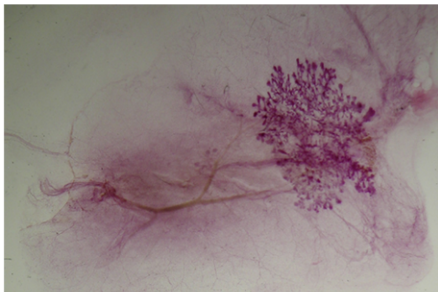
Outgrowths filling up to 1/3 of the
cleared fat pad.

++
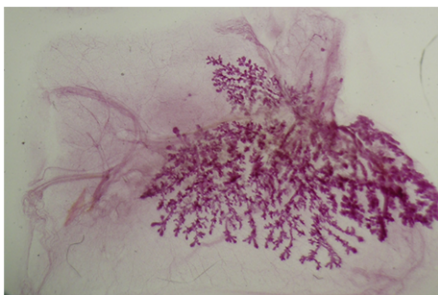
Outgrowths filling between 1/3 and
2/3 of the cleared fat pad.

+++
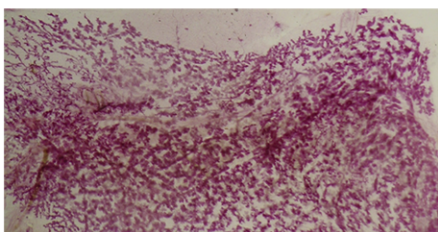
Outgrowths filling between 2/3 and
entire cleared fat pad.

Figure 4- 3. Mammary Outgrowth Size Scoring. Transplanted mammary fat pads were fixed, stained for carmine alum and scocred for size as follows.

Population	# cells	Outgrowth Size				
		-	~	+	++	+++
Virgin Recipients						
a. H2GFP+/CD24+/CD29+	10	13	1	2	0	0
	20	7	1	2	1	1
	50	9	1	1	0	1
	100	4	0	0	4	2
	200	3	2	4	2	1
b. H2GFP-/CD24+/CD29+	10	10	1	1	0	0
	20	12	1	0	0	1
	50	7	0	2	1	2
	100	3	1	4	3	1
	200	1	4	1	2	0
c. H2GFP+/CD24+/CD29lo	10	14	0	0	0	0
	20	12	0	0	0	0
	50	14	0	0	0	0
	100	11	1	0	0	0
	200	12	2	0	0	0
d. H2GFP-/CD24+/CD29lo	10	14	0	0	0	0
	20	12	0	0	0	0
	50	12	0	0	0	0
	100	14	0	0	0	0
	200	14	0	0	0	0
+ Pregnancy						
e. H2GFP+/CD24+/CD29+	10	3	0	0	1	0
	20	3	1	1	1	0
	50	3	1	0	1	3
	100	3	0	0	1	4
	200	0	0	3	2	3
f. H2GFP-/CD24+/CD29+	10	5	0	2	1	0
	20	5	2	0	0	1
	50	6	0	0	1	1
	100	4	0	1	2	1
	200	4	0	1	0	3
g. H2GFP+/CD24+/CD29lo	10	5	0	0	1	0
	20	8	0	0	0	0
	50	5	1	0	0	0
	100	7	1	0	0	0
	200	3	1	2	0	0
h. H2GFP-/CD24+/CD29lo	10	6	0	0	0	0
	20	8	0	0	0	0
	50	6	0	0	0	0
	100	6	0	0	0	0
	200	6	0	0	0	0

Figure 4- 4. Mammary Outgrowth Size Scoring of MMTVrtTA/H2BGFP Population Transplants. Outgrowths from MMTVrtTA/H2BGFP induction transplants were scored for size based on ability to fill the fat pad (see Figure 3-5) in virgin recipients (a-d) and pregnant recipients (e-h) of MMTVrtTA/H2BGFP populations a,e) H2BGFP+/CD24+/CD29+ b,f) H2BGFP-/CD24+/CD29+ c,g) H2BGFP+/CD24+/CD29lo d,h) H2GFP-/CD24+/CD29lo

	# cells					
a. H2GFP$^+$/CD24$^+$/CD29^{lo} *virgin*	10	0/14		1/3,800 (500 - 28,000)		
	20	0/12				
	50	1/12				
	100	0/12				
	200	0/8				
b. H2GFP$^+$/CD24$^+$/CD29^{lo} *+pregnancy*	10	2/12		1/280 (170 - 480)		
	20	2/14				
	50	4/14				
	100	4/14				
	200	4/14				

Size Scoring	# cells	-	~	+	++	+++
c. H2GFP$^+$/CD24$^+$/CD29^{lo} *virgin*	10	14	0	0	0	0
	20	12	0	0	0	0
	50	11	1	0	0	0
	100	12	0	0	0	0
	200	8	0	0	0	0
d. H2GFP$^+$/CD24$^+$/CD29^{lo} *+pregnancy*	10	10	2	0	0	0
	20	12	1	0	0	1
	50	10	4	0	0	0
	100	10	1	1	2	0
	200	10	1	2	0	1

Figure 4- 5. H2BGFP+/CD24+/CD29lo Transplants - Virgin vs. Pregnancy. H2BGFP+/CD24+/CD29lo MECs were sorted and transplanted in limiting dilutions. Mammary glands were scored for outgrowths (a, b) and size (c, d) in virgins (a, c) and pregnant mice (b, d)

reconstituted basement membrane gel, Matrigel™. CD24$^+$/CD29$^+$ MECs gave rise to

bilayer acinar structures, filled aciniar structures and tubular growths, while CD24$^+$/CD29^{lo}

MECs gave rise to single-layer acini which were consistently hollow. These Matrigel growth

phenotypes are believed to be reflective of the stem/progenitor fate of these MEC

populations. To test the 3D growth of MMTVrtTA/H2BGFP populations, MECs were

sorted and grown on Matrigel [12, 13]. H2BGFP$^+$/CD24$^+$/CD29$^+$ and H2BGFP$^-$

/CD24$^+$/CD29$^+$ MECs produced 11±5 and 13±3 acini per 1,000 cells cultured, respectively.

Within the CD24$^+$/CD29^{lo} population, H2BGFP$^+$ MECs gave rise to 100±11 and H2BGFP$^-$

/CD24$^+$/CD29^{lo} MEC gave rise to 126±17 acini per 1,000 cells cultured. Therefore, no

differences in 3D acini growth were detected in H2BGFP$^+$ and H2BGFP$^-$ subpopulations of
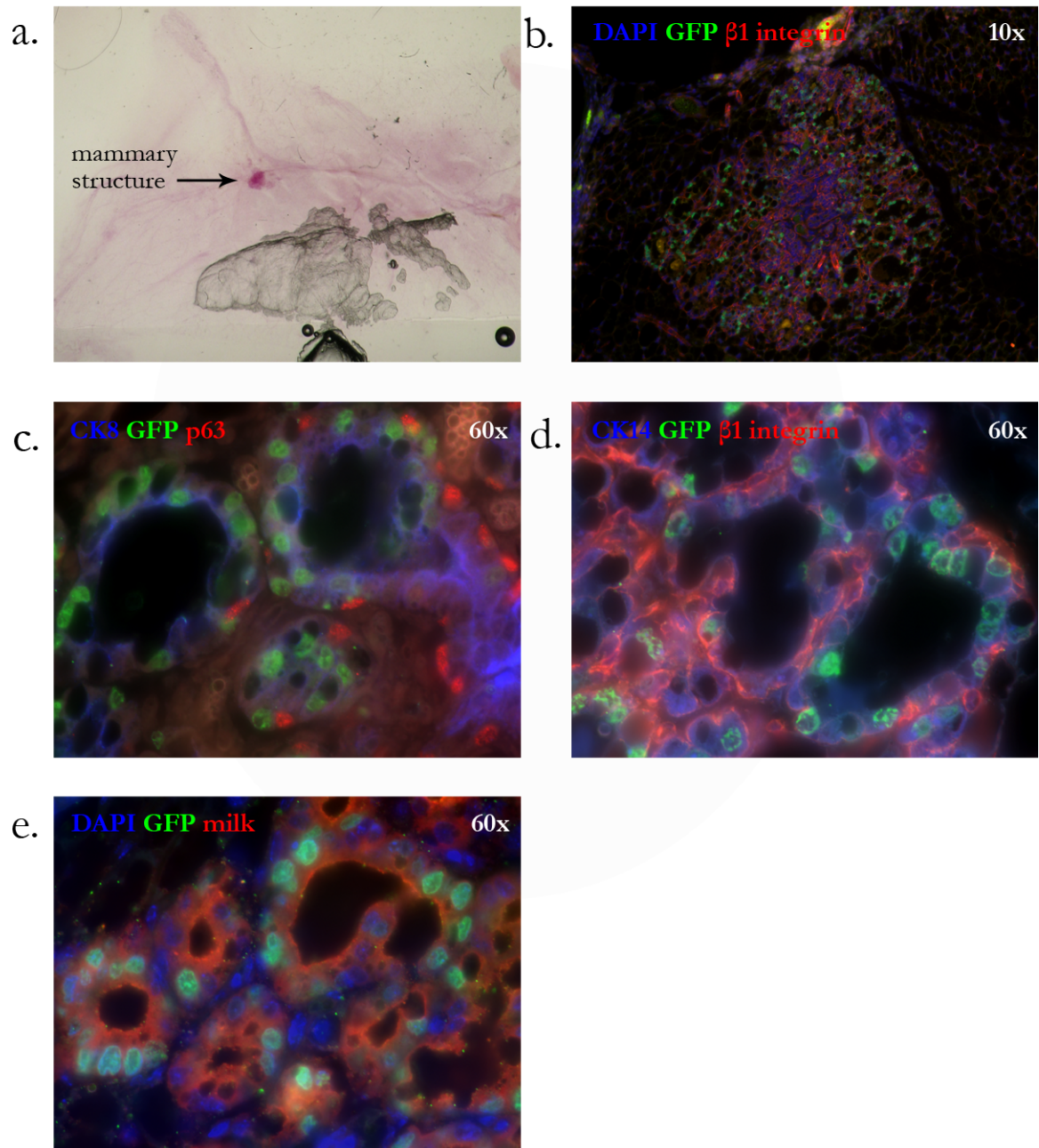
Figure 4- 6. Mammary Outgrowth from H2BGFP+/CD24+/CD29lo MECs. Transplanted fat pads were harvested, fixed and visualized by a) whole mounting, followed by sectioning and staining for b) GFP and β1 integrin (10x) c) CK8, GFP and p63 (60x) d) CK14, GFP and β1 integrin (60x) e) DAPI, GFP and milk
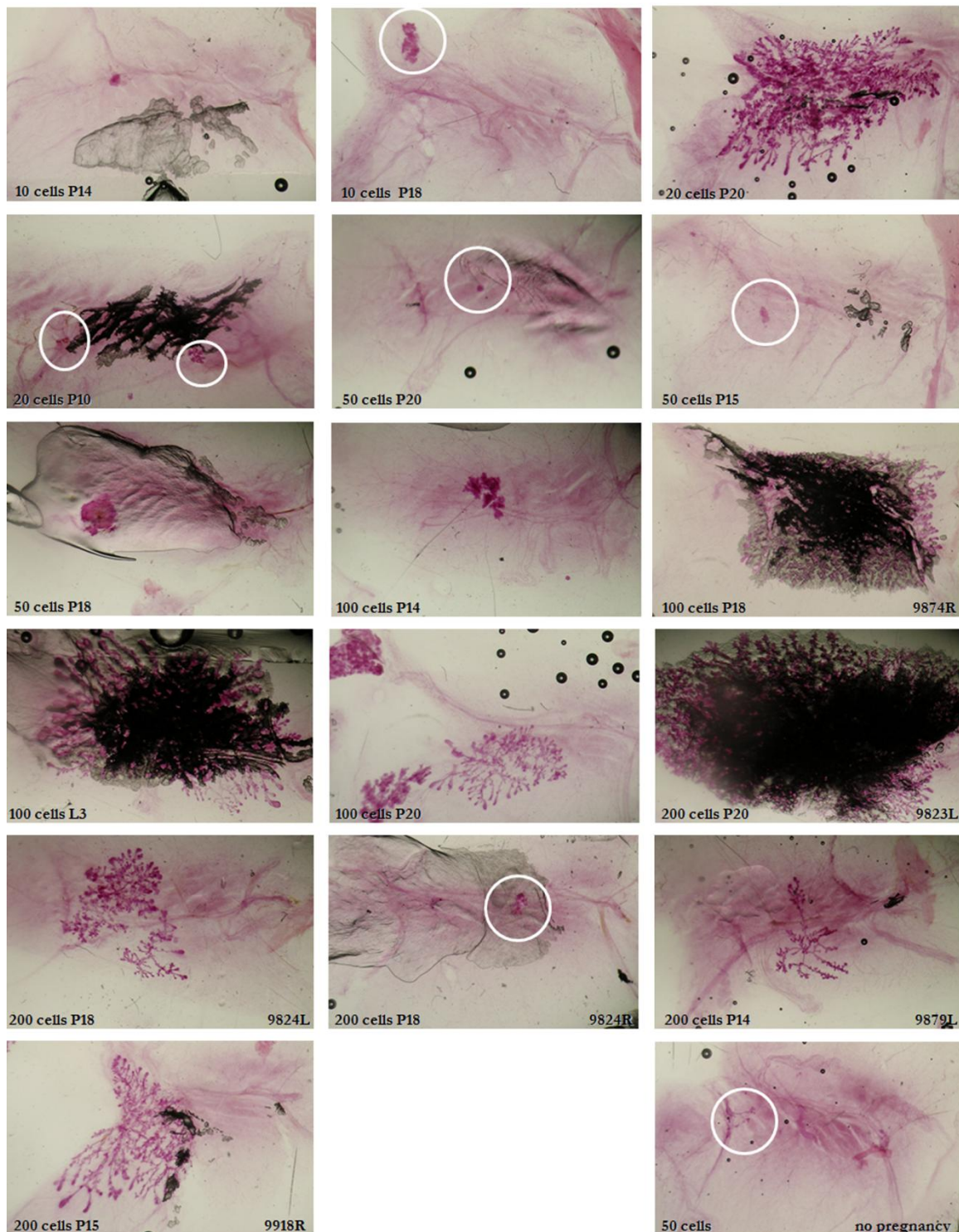
Figure 4- 7. H2BGFP+/CD24+/CD29lo Transplants – Second Set, Whole Mounts. Mammary fat pads injected with limiting dilutions of H2BGFP+/CD24+/CD29lo MECs were harvested, fixed and stained with carmine alum. Mice were either maintained as virgins (lower right fat pad) or made pregnant (all other whole mounts).

either $CD24^+/CD29^+$ or $CD24^+/CD29^{lo}$ MECs.

Gene expression analysis supports biologically distinct roles for H2BGFP+/CD24+/CD29lo and H2BGFP-/CD24+/CD29lo populations

The above data provides evidence that $H2BGFP^+$ $CD24^+/CD29^{lo}$ MECs contain a subpopulation of pregnancy-activated multipotent progenitors. Although the *in vivo* data was striking, it shed little light on the biochemical or molecular mechanisms of these progenitors. To further characterize the MMTVrtTA/H2BGFP MEC populations, RNA was isolated from each of the four MMTVrtTA/H2BGFP populations sorted from four week old double transgenic females and analyzed for differences in gene expression on the Illumina Mouse Microarray platform. Unsupervised clustering of the data sets segregated the samples into the original FACS-sorted populations, as predicted by H2BGFP expression and functional differences. Because I was unable to find any functional difference between the $CD24^+/CD29^+$ populations in primary transplants in virgin and pregnant mice, serial transplants and 3D *in vitro* growth assays, this gene expression segregation suggests that there may be a difference between the $H2BGFP^+/CD24^+/CD29^+$ and $H2BGFP^-/CD24^+/CD29^+$ populations which I have been unable to detect.

This analysis was focused on gene expression data from the $CD24^+/CD29^{lo}$ populations. Comparison of the gene expression levels of the $H2BGFP^+/CD24^+/CD29^{lo}$ and $H2BGFP^-/CD24^+/CD29^{lo}$ populations revealed that 257 probes showed statistically significant differences in expression between the $H2BGFP^+$ and $H2BGFP^-$ populations of the $CD24^+/CD29^{lo}$ compartments, based on the t-test p-value threshold of $p<0.05$. Fourteen of these probes, representing eleven genes, were associated with mammary gland development and differentiation as defined by the Gene Ontology database. Each of the

Figure 4- 8. Microarray Data for Mammary Development and Differentiation Genes. 257 probes were found to have statistically significant differences between H2BGFP+/CD24+/CD29lo and H2BGFP-/CD24+/CD29lo. The 14 probes displayed above are associated with mammary development and differentiation, according to the Gene Ontology database.

mammary-related transcripts, except for mucin 1 (Muc1), were expressed at much lower levels in the H2BGFP$^+$/CD24$^+$/CD29^{lo} population (Figure 4-8). These included well-documented mediators of mammary gland development, such as estrogen receptor 1, fibroblast growth factor receptor 2, prolactin receptor, and amphiregulin. To validate the microarray data, mRNA was harvested from sorted H2BGFP$^+$/CD24$^+$/CD29^{lo} and H2BGFP-/CD24+/CD29lo MECs from four week old double transgenic mice and analyzed by qPCR to determine the expression levels of genes of interest (Figure 4-9). The qPCR assays confirmed the microarray data for nine of the eleven mammary development genes: amphiregulin (AREG), caveolin 1 (Cav1), estrogen receptor 1 (Esr1), fibroblast growth factor receptor 2 (FGFR2), stem cell antigen 1 (Ly6a/Sca-1), mucin 1 (Muc1), prolactin receptor (PRLR), roundabout homolog 1 (Robo1) and wingless-type MMTV integration site family, member 5A (Wnt5a).

To compare the H2BGFP$^+$/CD24$^+$/CD29^{lo} and H2BGFP$^-$/CD24$^+$/CD29^{lo} populations with known mammary epithelial subtypes, data from this microarray was
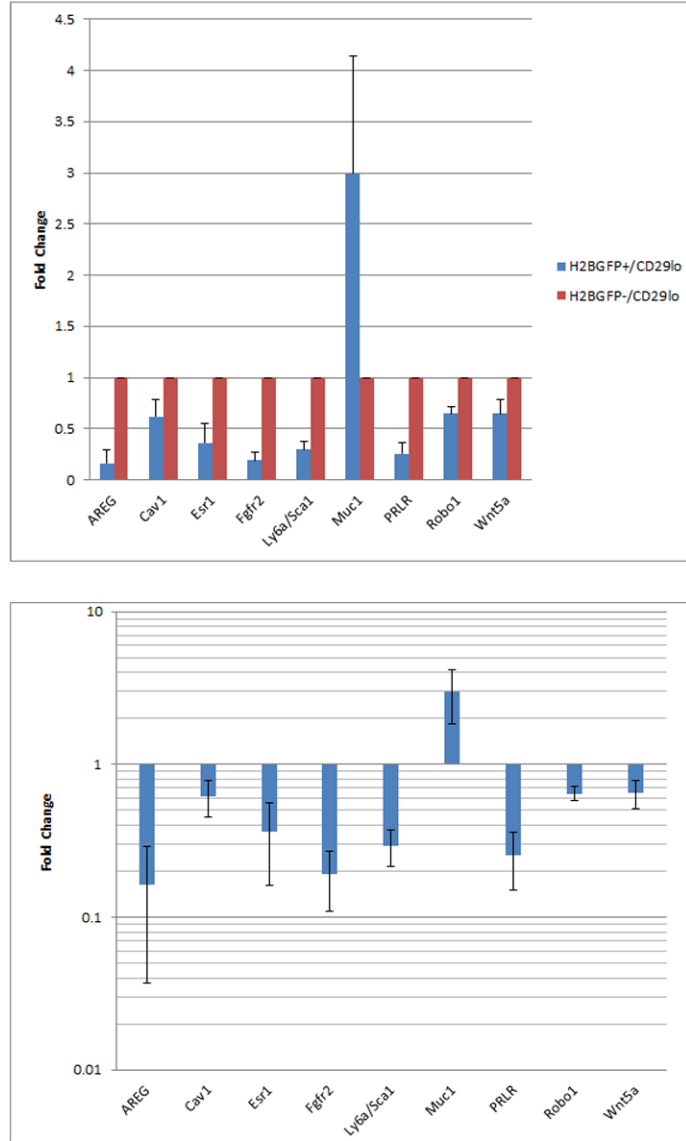
Figure 4- 9. Relative Fold Difference of Mammary Development and Differentiation Genes Identified by Microarray. Relative fold difference between transcripts in H2BGFP+/CD24+/CD29lo and H2BGFP-/CD24+/CD29lo cells. Results are displayed in a linear plot (top) and a log plot (bottom).

analyzed with previously reported data from mammary stem cells (CD24$^+$/CD29$^+$), luminal progenitors (CD24$^+$/CD29^{lo}/CD61$^+$) and mature luminal MECs (CD24$^+$/CD29^{lo}/CD61$^-$), focusing on the differentially expressed genes in H2BGFP$^+$/CD24$^+$/CD29^{lo} and H2BGFP$^-$/CD24$^+$/CD29^{lo} MECs [116] (Figure 4-10). Transcripts for these genes were significantly enriched (p = 2.8x10^{-35}) in genes that distinguished between the CD24$^+$/CD29$^+$, CD24$^+$/CD29^{lo}/CD61$^+$ and CD24$^+$/CD29^{lo}/CD61$^+$ subpopulations (p<0.05). This result

was expected since CD24 and CD29 were used in the isolation of both populations. However, transcripts expressed at higher levels in H2BGFP$^+$/CD24$^+$/CD29^{lo} are 3.6-fold enriched (p=2.5x10^{-16}) in genes which were also expressed highly in the CD24$^+$/CD29^{lo}/CD61$^+$ MECs, lower levels in CD24$^+$/CD29^{lo}/CD61$^-$ mature cells and lowest levels in the CD24$^+$/CD29$^+$ stem cell compartment. By contrast, the genes which were expressed at low levels in the H2BGFP$^+$/CD24$^+$/CD29^{lo} population were enriched (p=1.4x10^{-20}) in genes which also expressed at the lowest levels in CD24$^+$/CD29$^+$ MECs and the highest in the CD24$^+$/CD29^{lo}/CD61$^-$ mature luminal population. These data provide evidence that H2BGFP$^+$/CD24$^+$/CD29^{lo} cells share characteristics with both mammary stem cells and luminal-limited progenitors, a phenotype which could be expected in a multipotent progenitor. To further characterize the properties of MMTVrtT/H2BGFP MEC populations, the four populations were isolated by FACS, cytospun onto slides and immunostained for various mammary lineage markers (Figure 4-11). The immunostaining of β1 integrin was higher in both CD24$^+$/CD29$^+$ populations, confirming the flow cytometry data. CD24$^+$/CD29$^+$ populations were found to express higher levels of p63 and CK14 and CD24$^+$/CD29^{lo} populations were found to express more CK8. These data match previous observations on the unfractionated CD24$^+$/CD29$^+$ and CD24$^+$/CD29^{lo} populations [40]. Interestingly, the cytospin immunostainings confirmed the microarray and qPCR data that H2BGFP$^-$/CD24$^+$/CD29^{lo} cells express higher levels of AREG. H2BGFP$^-$/CD24$^+$/CD29^{lo} cells also expressed higher levels of PR and GR, which suggests a more differentiated fate for these cells. It is interesting to note that higher levels of PR and GR in an H2BGFP$^-$ population supports the hypothesis that the location of the MMTVrtTA transgene, not

H2BGFP+ H2BGFP-
CD24+   CD24+   CD24+   CD24+
CD29lo   CD29lo   CD24+   CD29lo   CD29lo
                   CD29+   CD61+   CD61-

PREDICTED: maltase-glucoamylase, transcript variant 1 (Mgam)
solute carrier family 1 (neuronal/epithelial high affinity glutamate transporter, system Xag)
cellular retinoic acid binding protein II (Crabp2)
prostaglandin E synthase (Ptges)
5530400B01Rik
suprabasin (Sbsn)
Csnk
adipose differentiation related protein (Adfp)
extracellular proteinase inhibitor (Expi)
sodium channel, nonvoltage-gated 1 beta (Scnn1b)
mucin 1, transmembrane (Muc1)
WAP four-disulfide core domain 3 (Wfdc3)
folate receptor 1 (adult) (Folr1)
CD14 antigen (Cd14)
Ctsh
Csnk
casein kappa (Csn3)
1500015A07Rik
angiopoietin 1 (Angpt1)
wingless-related MMTV integration site 5B (Wnt5b)
phospholipid scramblase 2 (Plscr2)
retinoblastoma 1 (Rb1)
protein phosphatase 1, regulatory (inhibitor) subunit 2 (Ppp1r2)
major facilitator superfamily domain containing 7B (Mfsd7b)
ceruloplasmin (Cp), transcript variant 2
D730046L02Rik
mucin 15 (Muc15)
microsomal glutathione S-transferase 1 (Mgst1)
A230079E18Rik
ribosomal protein S10 (Rps10)
neuropilin 1 (Nrp1)
LOC380930
solute carrier family 6 (neurotransmitter transporter, creatine), member 8 (Slc6a8)
Tmem5f1
thrombospondin 1 (Thbs1)
phosphodiesterase 4B, cAMP specific (Pde4b)
phosphodiesterase 4A, cAMP specific (Pde4a), transcript variant 5
kruppel-like factor 7 (ubiquitous) (Klf7)
diacylglycerol kinase zeta (Dgkz)
toll-like receptor 2 (Tlr2)
microtubule-associated protein 2 (Mtap2), transcript variant 2 XM_901527 XM_901529
complement component 4A (Rodgers blood group) (C4a)
complement component 4B (Childo blood group) (C4b) XM_921663 XM_921673 XM_921676 XM_921678
actin, alpha 2, smooth muscle, aorta (Acta2)
H19 fetal liver mRNA (H19), non-coding RNA.
polo-like kinase 2 (Drosophila) (Plk2)
fibroblast growth factor receptor 2 (Fgfr2), transcript variant 2
acid phosphatase-like 2 (Acpl2)
aldehyde dehydrogenase family 3, subfamily A2 (Aldh3a2)
prominin 2 (Prom2), transcript variant 2
microcephaly, primary autosomal recessive 1 (Mcph1)
death associated protein 3 (Dap3), nuclear gene encoding mitochondrial protein
death associated protein 3 (Dap3), nuclear gene encoding mitochondrial protein
caspase 8 (Casp8), transcript variant 1
AI987712
Mela
TOX high mobility group box family member 3 (Tox3)
C230068H16Rik
calcyphosine-like (Capsl)
fibroblast growth factor receptor 2 (Fgfr2), transcript variant 1
wingless-related MMTV integration site 5A (Wnt5a)
fibroblast growth factor receptor 2 (Fgfr2), transcript variant 2
predicted gene, EG240327 (EG240327)
PREDICTED: hypothetical protein LOC100041932 (LOC100041932)
ubiquitin-conjugating enzyme E2Q (putative) (Ube2q2)
growth factor receptor bound protein 14 (Grb14)
PREDICTED: LIM domain only 7, transcript variant 11 (Lmo7)
Il1r1
tetraspanin 13 (Tspan13)
vomeronasal 1 receptor, D6 (V1rd6)
catenin, beta like 1 (Ctnnbl1)
mediator complex subunit 30 (Med30)
proteasome (prosome, macropain) subunit, beta type 9 (large multifunctional peptidase 2) (Psmb9)
glucosamine (N-acetyl)-6-sulfatase (Gns)
kinesin family member 5C (Kif5c)
protein kinase, cAMP dependent regulatory, type II beta (Prkar2b)
xenotropic and polytropic retrovirus receptor 1 (Xpr1)
CD164 antigen (Cd164)
transglutaminase 2, C polypeptide (Tgm2)
solute carrier family 12, member 2 (Slc12a2)
lymphocyte antigen 6 complex, locus A (Ly6a)
major facilitator superfamily domain containing 7C (Mfsd7c)
Histihc
histone cluster 1, H1c (Hist1h1c)
solute carrier family 7 (cationic amino acid transporter, y+ system), member 2 (Slc7a2)
transmembrane anterior posterior transformation 1 (Tapt1)
RIKEN cDNA E030049G20 gene (E030049G20Rik), transcript variant 1
indoleamine-pyrrole 2,3 dioxygenase (Indo)
Il18r1
protocadherin alpha 7 (Pcdha7)
Col8a1
claudin 10 (Cldn10), transcript variant 1
membrane bound O-acyltransferase domain containing 1 (Mboat1)
forkhead box A1 (Foxa1)
claudin 6 (Cldn6)
AI987712
lymphocyte antigen 6 complex, locus D (Ly6d)
DnaJ (Hsp40) homolog, subfamily C, member 12 (Dnajc12)
RIKEN cDNA 9430028L06 gene (9430028L06Rik)
RIKEN cDNA 9430028L06 gene (9430028L06Rik)
stanniocalcin 2 (Stc2)
chemokine (C-X-C motif) ligand 15 (Cxcl15)
1110018J23Rik
RAS protein-specific guanine nucleotide-releasing factor 1 (Rasgrf1), transcript variant 2
RAS protein-specific guanine nucleotide-releasing factor 1 (Rasgrf1), transcript variant 1
Rasgrf1
angiogenin, ribonuclease A family, member 4 (Ang4)
protein C (Proc), transcript variant 3
dynein, axonemal, intermediate chain 1 (Dnaic1)
dynein, axonemal, intermediate chain 1 (Dnaic1)
estrogen-related receptor gamma (Esrrg)
Tcrd-V1
uroplakin 3A (Upk3a)
PREDICTED: similar to peptidylarginine deiminase, type II (LOC638935)
RIKEN cDNA 2200001I15 gene (2200001I15Rik)
apolipoprotein F (Apof)
WAP four-disulfide core domain 2 (Wfdc2)
tubulin, alpha 8 (Tuba8)
Tuba8
fibrinogen, gamma polypeptide (Fgg)
small proline-rich protein 1A (Sprr1a)
amphiregulin (Areg)
interleukin 33 (Il33)
activated leukocyte cell adhesion molecule (Alcam)
sterile alpha motif domain containing 5 (Samd5)
estrogen receptor 1 (alpha) (Esr1)
inter-alpha trypsin inhibitor, heavy chain 2 (Itih2)
PREDICTED: similar to WAP four-disulfide core domain 2 (LOC100048733)
solute carrier family 12, member 2 (Slc12a2)
arginase type II (Arg2)
glycerophosphodiester phosphodiesterase domain containing 1 (Gdpd1)
collagen, type VIII, alpha 1 (Col8a1)
solute carrier family 12, member 2 (Slc12a2)
prolactin receptor (Prlr)
transmembrane protein 56 (Tmem56)
claudin 10 (Cldn10), transcript variant 2
solute carrier family 35, member F3 (Slc35f3)
GIPC PDZ domain containing family, member 2 (Gipc2)
crystallin, mu (Crym)
cysteine dioxygenase 1, cytosolic (Cdo1)
PREDICTED: hypothetical protein LOC100042514 (LOC100042514)
chloride channel calcium activated 3 (Clca3)
Clca3
polyamine oxidase (exo-N4-amino) (Paox)
RIKEN cDNA 4930452B06 gene (4930452B06Rik)
2610305D13Rik
RIKEN cDNA 2610305D13 gene (2610305D13Rik)
centrosomal protein 55 (Cep55)
RIKEN cDNA 2900062L11 gene (2900062L11Rik), non-coding RNA.
PREDICTED: antigen identified by monoclonal antibody Ki 67 (Mki67)
DnaJ (Hsp40) homolog, subfamily B, member 4 (Dnajb4)
tubulin, alpha 1A (Tuba1a)
mannosidase 1, alpha (Man1a)
matrix metallopeptidase 14 (membrane-inserted) (Mmp14)
ecotropic viral integration site 5 (Evi5)
myristoylated alanine rich protein kinase C substrate (Marcks)
cyclin-dependent kinase inhibitor 2D (p19, inhibits CDK4) (Cdkn2d)
glypican 1 (Gpc1)
roundabout homolog 1 (Drosophila) (Robo1)
solute carrier organic anion transporter family, member 2a1 (Slco2a1)
S100 calcium binding protein A14 (S100a14)
PREDICTED: RIKEN cDNA 2310047A01 gene (2310047A01Rik)
GLI-Kruppel family member GLI3 (Gli3)
caveolin 1, caveolae protein (Cav1)
myelin protein zero (Mpz)
A630097K09Rik
Ptgcr3
glucosaminyl (N-acetyl) transferase 2, I-branching enzyme (Gcnt2), transcript variant 3
Sytl2
glutamine fructose-6-phosphate transaminase 2 (Gfpt2)
inhibin beta-A (Inhba)
epithelial mitogen (Epgn)
breast carcinoma amplified sequence 1 (Bcas1)
inhibitor of DNA binding 3 (Id3)
synaptotagmin-like 2 (Sytl2), transcript variant 5
glucoprotein (transmembrane) nmb (Gpnmb)

Figure 4- 10. Comparison of MMTVrtTA/H2BGFP Microarray Data with Visvader Microarray. Expression of genes which were differentially regulated between H2BGFP+/CD24+/CD29lo and H2BGFP-/CD24+/CD29lo (left columns) were analyzed previously published arrays of mammary stem cells (CD24+/CD29+), luminal progenitors (CD24+/CD29lo/CD61+) and mature luminal MECs (CD24+/CD29lo/CD61-).

Figure 4- 11. **Cytospin Analysis of MMTVrtTA/H2BGFP Populations.** MMTVrtTA/H2BGFP MECswere sorted, cytospun and immunostained for various markers.

MMTV promoter activity, is responsible for the labeling of CD24+/CD29lo cells with unique properties in vivo.

Discussion & Future Directions

Using the MMTVrtTA transgenic mouse to induce H2BGFP expression in the mammary gland, I have found that H2BGFP induction in the $CD24^+/CD29^{lo}$ progenitor-containing compartment labels a population which contains a multipotent progenitor that is specifically activated during pregnancy. This conclusion that GFP expression distinguishes two distinct populations of MECs is corroborated by data from mRNA expression analyses, which demonstrate that a large set of transcripts are differentially expressed in $H2BGFP^+/CD24^+/CD29^{lo}$ and $H2BGFP^-/CD24^+/CD29^{lo}$ cells. In contrast, I was unable to observe any functional differences between the $H2BGFP^+/CD24^+/CD29^+$ and $H2BGFP^-/CD24^+/CD29^+$ populations.

H2BGFP$^+$/CD24$^+$/CD29^{lo} MECs can form small mammary glandular structures *in vivo*, an ability which increases five- to ten-fold when the recipient mice are made pregnant post-transplant (Figure 4-2). H2BGFP$^-$/CD24$^+$/CD29^{lo} MECs are unable to form detectable mammary structures *in vivo*. H2BGFP$^+$/CD24$^+$/CD29^{lo}-derived outgrowths are significantly smaller than outgrowths from CD24+/CD29+ MECs, but have the same bilayer structure and cellular composition of normal mammary glands, and are able to produce milk; however, H2BGFP$^+$/CD24$^+$/CD29^{lo}-derived mammary structures cannot be serially transplanted. Expression profiling of these MEC populations suggests that they are distinct, and that H2BGFP$^+$/CD24$^+$/CD29^{lo} MECs are less differentiated than H2BGFP$^-$/CD24$^+$/CD29^{lo} MECs. This provides evidence that the H2BGFP$^+$/CD24$^+$/CD29^{lo} compartment contains a population of pregnancy-activated multipotent mammary progenitors.

These progenitors were identified in a population isolated from female mice during early puberty. The existence of pregnancy-activated progenitors in the mammary gland before sexual maturity indicates that these progenitors are produced during pubertal development and remain dormant until pregnancy. For the *in vivo* growth assays, cleared fat pad transplants were performed on three week old mice, and mammary fat pads were harvested six weeks later, at the end of puberty, or during late pregnancy. In H2BGFP$^+$/CD24$^+$/CD29^{lo} MEC transplants, few mammary outgrowths had developed in virgin mice by the end of puberty, suggesting that the progenitor cells are relatively unresponsive to the hormonal signals of puberty and require pregnancy hormones to develop an outgrowth detectable by carmine alum staining. Because pregnancy was induced 3-4 weeks post-transplant, these pregnancy-activated progenitors apparently survive in virgin

mice, but are for the most part unable to develop into detectable mammary epithelial structures in the mammary fat pads.

It is unknown whether H2BGFP$^-$/CD24$^+$/CD29^{lo} cells do not form mammary outgrowths *in vivo* because of a lack of proliferation or a failure to survive. Further studies using these MEC populations in combination with a powerful label, such as luciferase, which can be detected by imaging the live animal, could determine whether proliferation, survival or both are critical to the activity of mammary progenitors *in vivo*.

The evidence that a few mammary outgrowths were found in virgin mice suggests that either these H2BGFP$^+$/CD24$^+$/CD29^{lo} MECs can proliferate, albeit minimally, in response to pubertal signaling or that H2BGFP$^+$/CD24$^+$/CD29^{lo} MECs contain a mixed population of progenitors that respond to puberty and another larger number of progenitors that respond to pregnancy. As the existence of pregnancy-independent multipotent mammary progenitors has been reported [35, 36], and the calculated MRU frequencies of H2BGFP$^+$/CD24$^+$/CD29^{lo} cells suggest that these MECs represent a mixed population, either hypothesis could be correct. Further purification and *in vivo* testing of H2BGFP$^+$/CD24$^+$/CD29^{lo} MECs is required to determine whether this population contains more than one class of multipotent mammary progenitor.

The results from expression analysis of H2BGFP$^+$/CD24$^+$/CD29^{lo} MECs and H2BGFP$^-$/CD24$^+$/CD29^{lo} MECs supports the hypothesis that these populations are biologically distinct, and that H2BGFP expression labels a progenitor population within the CD24$^+$/CD29^{lo} compartment. H2BGFP$^+$/CD24$^+$/CD29^{lo} MECs express markedly lower levels of transcripts involved in mammary development and differentiation. These transcripts include Sca-1, which is upregulated in differentiated MECs [12], AREG, which is required for ductal elongation [117], PRLR and Cav1, which are involved in alveologenesis

[118, 119], and FGFR2, which is required for TEB development, mature luminal cell survival and alveologenesis [120, 121]. Interestingly, Muc1, which is associated with luminal cells, has increased transcript levels in H2BGFP$^+$/CD24$^+$/CD29^{lo} cells, contrasting with the multipotent progenitor function of the H2BGFP$^+$/CD24$^+$/CD29^{lo} population. Interestingly, when compared with populations of mammary stem cells, luminal progenitors and luminal cells as defined by expression of CD24, CD29 and CD61, the H2GFP$^+$/CD24$^+$/CD29^{lo} population bore characteristics of both stem cells and luminal progenitors. In particular, it is suggestive that genes expressed highly in H2BGFP+/ CD24+/CD29lo are enriched for luminal progenitor transcripts, while H2BGFP+/CD24+/CD29lo MECs share inhibited transcripts with mammary stem cells. This implies that the H2BGFP+/CD24+/CD29lo population has a common origin with, or may even give rise to CD24+/CD29lo/CD61+ MECs, but are less differentiated than luminal progenitors. These data support my hypothesis that H2BGFP$^+$/CD24$^+$/CD29^{lo} MECs contain multipotent progenitors.

The CD24$^+$/CD29$^+$ compartment has been reported to contain both mammary stem cells and myoepithelial-restricted progenitors [38]. Therefore, a subdivision of the CD24$^+$/CD29$^+$ population could represent the differentiation of functionally different MEC subtypes. Expression profiling data from H2BGFP+/CD24+/CD29+ and H2BGFP-/CD24+/CD29+ MECs independently segregated, suggesting a functional difference between these populations. However, functional proof of this difference has been elusive. Similar mammary repopulation rates and outgrowth morphologies of H2BGFP$^+$ and H2BGFP$^-$ MECs in the CD24$^+$/CD29$^+$ compartment suggest that MMTVrtTA/H2BGFP expression does not distinguish between these populations in primary transplants. Another possibility was that H2BGFP expression in the CD24$^+$/CD29$^+$ compartment delineates long

term and short term stem cells, which would be expected to have differential repopulation abilities in serial transplants. However, no difference in serial transplant ability was detected between these populations. Given that mammary epithelial cells have demonstrated a limit of between four and seven rounds of serial transplantation before they can no longer form a detectable gland [122], it is possible that more extensive experimentation could demonstrate currently undetected differences between these populations.

My unexpected finding from these experiments is that $CD24^+/CD29^+$ -derived glands maintain the H2BGFP expression of the parental population. Outgrowths from $H2BGFP^-/CD24^+/CD29^+$ MECs did not express H2BGFP, even when recipients were constantly treated with doxycycline. This result suggests that transcription of either rtTA or H2BGFP is epigenetically silenced in the stem/progenitor cells of this population and raises questions about the timing and initiation of MMTVrtTA induction of H2BGFP in the mammary gland. Because MECs were transplanted into pubertal females, this data suggests that MMTVrtTA/H2BGFP expression is determined (if not necessarily initiated) by three weeks of age, and that this fate is inherited by all descendants. At present, it is unknown whether MMTVrtTA induction of H2BGFP is a stochastic event or whether it is due to MMTV promoter activity and/or the insertion site of the MMTVrtTA transgene. However, the difference in *in vivo* repopulating activity and differential gene expression profiles of the $H2BGFP^+/CD24^+/CD29^{lo}$ and $H2BGFP^-/CD24^+/CD29^{lo}$ populations suggests that H2BGFP delineation of these two populations is not a random event.

A secondary goal of the microarray analysis was the identification of potential cell surface markers which could replace or even improve upon MMTVrtTA/H2BGFP expression for isolation of the $H2BGFP^+/CD24^+/CD29^{lo}$ population. As is discussed in the Appendix, 24 different candidate cell surface markers were selected from the microarray and

from known markers of the mammary stem cell hierarchy and tested for the ability to distinguish the H2BGFP$^+$/CD24$^+$/CD29^{lo} and H2BGFP$^-$/CD24$^+$/CD29^{lo} populations. Although no markers clearly separated these two populations, CD14 was identified as a promising potential marker for H2BGFP$^+$/CD24$^+$/CD29^{lo} MECs. While these experiments were being conducted, Visvader and colleagues also identified the CD24$^+$/CD29^{lo}/CD14$^+$/c-Kit$^-$ population as an alveolar progenitor population based on *in vitro* activity [32]. My findings support the hypothesis that CD14 might act as a marker for populations with pregnancy-specific activity. The CD24$^+$/CD29$^+$ compartment has been reported to contain both mammary stem cells and myoepithelial-restricted progenitors [38]. Therefore, a subdivision of the CD24$^+$/CD29$^+$ population could represent the differentiation of functionally different MEC subtypes. However, the similar mammary repopulation rates and outgrowth morphologies of H2BGFP$^+$ and H2BGFP$^-$ MECs in the CD24$^+$/CD29$^+$ compartment suggest that MMTVrtTA/H2BGFP expression does not distinguish between these populations. Another possibility was that H2BGFP expression in the CD24$^+$/CD29$^+$ compartment delineates long term and short term stem cells, which would be expected to have differential repopulation abilities in serial transplants. However, no difference in serial transplant ability was detected between these populations. Given that mammary epithelial cells have demonstrated a limit of between four and seven rounds of serial transplantation before they can no longer form a detectable gland [122], it is possible that more extensive experimentation could demonstrate currently undetected differences between these populations.

Unexpectedly, these experiments demonstrated that CD24$^+$/CD29$^+$ -derived glands maintain the H2BGFP expression of the parental population. H2BGFP$^-$/CD24$^+$/CD29$^+$ MECs were able to give rise to serially transplantable mammary outgrowths that did not

express H2BGFP, even when recipients were constantly treated with doxycycline. This result suggests that transcription of either rtTA or H2BGFP is epigenetically silenced in the stem/progenitor cells of this population and raises questions about the timing and initiation of MMTVrtTA induction of H2BGFP in the mammary gland. Because MECs were transplanted into pubertal females, this data suggests that MMTVrtTA/H2BGFP expression is determined (if not necessarily initiated) by three weeks of age, and that this fate is inherited by all descendants. At present, it is unknown whether MMTVrtTA induction of H2BGFP is a stochastic event or whether it is due to MMTV promoter activity and/or the insertion site of the MMTVrtTA transgene. However, the different *in vivo* repopulating activity and different gene expression profiles of the H2BGFP$^+$/CD24$^+$/CD29^{lo} and H2BGFP$^-$/CD24$^+$/CD29^{lo} populations suggests that H2BGFP delineation of these two populations is a non-random event.

Studies have demonstrated that disruption of specific signaling pathways can abrogate mammary development during either puberty without affecting alveologenesis, or vice versa [123-125]. This has established that mammary proliferation during puberty and pregnancy are separate processes, involving different biochemical mechanisms. The data discussed in this chapter of my thesis provides evidence that different mammary epithelial cell types are involved in these different modes of mammary development. While previously characterized stem cells are responsible for ductal elongation and formation of the mammary tree, a different population of pregnancy-activated progenitors could give rise to the milk-producing alveoli during pregnancy. This is supported by the evidence of Smith and colleagues, who found a population of parity-induced MECs (PI-MECs) which were able to contribute to alveoli during pregnancy, but were unable to form mammary ducts during puberty [42, 126]. Furthermore, Van Keymeulen et al., discovered in lineage tracing studies

of K8-expressing cells that some of these MECs were able to repeatedly give rise to alveoli, but that not all alveoli were derived from K8 lineage cells; this suggests that K8 expression identified some, but not all pregnancy-activated progenitors in the mammary gland [38]. My data contributes to evidence for a pregnancy-activated multipotent progenitor in the mammary gland.

Further purification and study of the multipotent pregnancy-activated progenitor population could further illuminate the dynamics of the mammary gland during pregnancy, providing valuable insights about mammary gland biology and breast cancer.

Chapter 5 Discussion & Future Directions

Thesis Summary

The original goal of my thesis research was to identify, isolate and characterize mouse mammary epithelial cells with stem cell or progenitor activity. My initial approach was to determine whether histone label retention enriches for mammary epithelial stem cells/progenitors. In Chapter 3 of this thesis, I examined transgenic models in which H2BGFP was induced in different tissue contexts, using the tetracycline transactivator or the reverse tetracycline transactivator under the control of four different promoters. I found that CMVrtTA did not express in the mammary gland. MMTVtTA and Rosa26rtTA were determined to be unsuitable for H2BGFP label retention experiments due to a combination of low H2BGFP induction in the mammary gland and potential contamination from non-mammary tissues expressing H2BGFP. In the course of these studies, I also observed that transplantation of normal MECs into the cleared fat pads of NOD-SCID mice resulted in low levels of mammary gland reconstitution, which led to the hypothesis that NOD-SCID mammary fat pads lack a critical factor for the development of transplanted MECs. The best model tested expressed the reverse tetracycline transactivator under control of the Mouse Mammary Tumor Virus promoter (MMTVrtTA). This model demonstrated mammary-specific induction of H2BGFP, as well as the highest level of H2BGFP expression in MECs.

Histone label retention experiments were performed using the MMTVrtTA/H2BGFP transgenic system. This led to the unexpected observation that MMTVrtTA-induced expression of H2BGFP in the mammary gland occurred exclusively in MECs within the $CD24^+/CD29^+$ and $CD24^+/CD29^{lo}$ compartments, which contain stem cells and mammary progenitors, respectively. When MMTVrtTA/H2BGFP label retaining cells were tested in transplant assays, they were found to have comparable *in vivo*

reconstitution activity as H2BGFP-expressing MECs prior to label retention. I concluded that histone label retention does not enrich for mammary stem cell/progenitor populations. However, MMTVrtTA/H2BGFP expression within the mammary stem cell and progenitor compartments could potentially label novel populations within these MEC compartments. Interestingly, I found that H2BGFP expression in the $CD24^+/CD29^{lo}$ compartment labeled a MEC population with the ability to develop into small mammary outgrowths *in vivo*. This suggested the existence of a subpopulation of multipotent progenitors in the $CD24^+/CD29^{lo}$ compartment. At the time of these experiments, $CD24^+/CD29^{lo}$ MECs had demonstrated no *in vivo* repopulation ability, and therefore this was a notable finding.

In Chapter 4 of this thesis, I described my investigations of the functional properties of $H2BGFP^+/CD24^+/CD29^+$, $H2BGFP^-/CD24^+/CD29^+$, $H2BGFP^+/CD24^+/CD29^{lo}$ and $H2BGFP^-/CD24^+/CD29^{lo}$ cells. I found that $H2BGFP^+$ and $H2BGFP^-$ populations in the $CD24^+/CD29^+$ compartment could not be distinguished based on the repopulation activity of primary transplants in virgin or pregnant mice, the ability to be serially transplanted or behavior in 3D spheroid growth assays. However, $H2BGFP^+$ cells within the $CD24^+/CD29^{lo}$ compartment had the ability to develop mammary outgrowths *in vivo*, while $H2BGFP^-/CD24^+/CD29^{lo}$ MECs were unable to do so. Although these outgrowths were significantly smaller than the glands derived from $CD24^+/CD29^+$ MECs and were unable to serially transplant, they contained luminal and myoepithelial/basal cells and were able to produce milk. Further investigations revealed that the repopulating ability of $H2BGFP^+/CD24^+/CD29^{lo}$ MECs is five- to ten-fold higher when recipient mice were made pregnant. Expression analysis of $H2BGFP^+/CD24^+/CD29^{lo}$ MECs compared to $H2BGFP^-/CD24^+/CD29^{lo}$ MECs confirmed that these populations were significantly different, and revealed that $H2BGFP^+/CD24^+/CD29^{lo}$ MECs expressed lower levels of transcripts

involved in mammary development and differentiation. Taken together, these data support

the hypothesis that the H2BGFP$^+$/CD24$^+$/CD29^{lo} compartment contains a heretofore

uncharacterized population containing a multipotent, pregnancy-activated mammary

progenitor. Further study of the H2BGFP$^+$/CD24$^+$/CD29^{lo} population is required to

determine which signals trigger pregnancy-activated proliferation, and the function of these

cells in repeated pregnancies.

In the Appendix of this thesis, I described further experiments to evaluate candidate

cell surface markers for isolation of the pregnancy-activated multipotent progenitors

contained within the H2BGFP$^+$/CD24$^+$/CD29^{lo} population. These markers were selected

from genes that are differentially regulated in H2BGFP$^+$/CD24$^+$/CD29^{lo} and H2BGFP$^-$

/CD24$^+$/CD29^{lo} cells as assessed by my microarray experiments, and from previously

identified markers of the mammary stem cell hierarchy. Unfortunately, no single marker or

combination of tested markers was able to separate the H2BGFP$^+$/CD24$^+$/CD29^{lo} and

H2BGFP$^-$/CD24$^+$/CD29^{lo}. However, six markers (CD14, CD49b, EpCAM, FGF2, Jag1

and Sca-1) demonstrated some degree of separation between the H2BGFP$^+$/CD24$^+$/CD29^{lo}

and H2BGFP$^-$/CD24$^+$/CD29^{lo} populations, suggesting that these markers could be used

alone or in combination to separate the pregnancy-activated multipotent progenitor

population from the bulk of the CD24$^+$/CD29^{lo} MECs. Further flow cytometry analysis

demonstrated that CD14 alone was the most promising candidate marker. Unfortunately,

transplants of CD24$^+$/CD29^{lo}/CD14$^+$ and CD24$^+$/CD29^{lo}/CD14$^-$ MECs in virgin and

pregnant mice resulted in a mammary repopulation rate far greater than was predicted based

on analysis of CD14 expression in the CD24$^+$/CD29^{lo} compartment and my previous

transplant experiments. This result might have been due to an unusually high concentration

of growth factors or other biochemical components within the Matrigel used for these

injections. More extensive experiments are required to determine which critical factors in Matrigel encourage mammary development, and whether or not they have a physiological role. Simultaneous with these experiments, another group reported that CD24^{+}/CD29^{lo}/CD14^{+}/c-Kit^{-} MECs can rise to lactogenic colonies *in vitro* [32], providing evidence for CD14 as a strong candidate marker for isolation of pregnancy-activated multipotent progenitors in the mammary gland.

My findings contribute to the increasing body of work on the mammary epithelial stem cell hierarchy, and provide evidence that mammary development during puberty and pregnancy are separate processes, involving not only different signaling pathways, but different target cells.

Histone Label Retention in the Mammary Gland

Evidence for label retaining cells with stem/progenitor function in the mammary epithelium was first provided by the work of Smith and colleagues through experiments in which DNA-based labels and estrogen-enhanced pubertal proliferation were utilized to identify mammary LRCs [86]. These LRCs were found to be actively cycling, which was interpreted as evidence for immortal strand retention, and to express ER and PR [89]. These LRCs also were found to contribute to alveologenesis during successive pregnancies [89]. Notably, subsequent work demonstrated that expression of steroid hormone receptors is absent in mammary stem cells (CD24^{+}/CD29^{+} and CD24^{+}/CD49f^{+}), whereas ~40% of the more differentiated CD24^{+}/CD29^{lo} compartment expresses ER and/or PR [40]. These results suggest that either DNA label retention identifies a new class of mammary stem cells with steroid hormone receptor expression and activity in pregnancy, or that these LRCs are progenitor cells, with persistent proliferation capacity during pregnancy.

Label retention assays have been used previously to identify putative stem cells and stem cell niches [72, 76, 77]; however, label retention can be technically difficult and functionally limited. Adult stem cells are believed to retain label due to either relative mitotic quiescence or asymmetric division of labeled molecules. In either case, label dilution can still occur, resulting in a difficult-to-detect signal, particularly if the tissue in question does not have a niche containing a concentration of stem cells, such as the epidermal bulge. Additionally, DNA label retention using molecules such as BrdU or tritiated thymidine does not permit the isolation of live LRCs, limiting the ability to test the functional properties of LRCs. New developments in DNA labeling, such as the use of nucleotide analogs with native fluorescence, might eventually eliminate this difficulty [127].

Currently, the best tool for isolation of LRCs is the tetracycline-inducible H2BGFP transgenic mouse. However, as demonstrated in Chapter 2, H2BGFP pulse-chase experiments are limited by the availability of transgenic models able to direct expression of H2BGFP in the desired tissue. Rosa26rtTA and MMTVtTA were able to induce H2BGFP expression in the mammary gland, but not exclusively. Unfortunately, the mammary gland is a highly heterogeneous tissue and label retention experiments necessarily result in the isolation of a small percentage of cells; therefore, H2BGFP$^+$ non-epithelial cells in the mammary gland are a potential source of contamination. This problem could be circumvented by transplanting H2BGFP-induced MECs into the cleared fat pad of a non-H2BGFP mouse, and monitoring H2BGFP label dilution during pubertal expansion; this would, however, greatly increase the expense and difficulty of generating enough LRCs for stem cell/progenitor assays.

I performed H2BGFP label retention experiments using the Rosa26rtTA and MMTVrtTA transgenic systems. Transplants of the Rosa26rtTA/H2BGFP LRCs produced

disappointing results, most likely due to a defect in the NOD-SCID mammary fat pad. However, these transgenic mice might still be used to isolate mammary LRCs, after a backcross of both strains into the same genetic background and with due consideration for potential contamination from non-mammary lineages. LRCs isolated from the MMTVrtTA/H2BGFP system demonstrated no enrichment in mammary stem cells/progenitors after pubertal dilution of H2BGFP signal. However, given the evidence that pubertal, estrous and pregnancy-associated expansion of the mammary gland are separate processes [35, 123, 124, 128, 129], it is possible that label retention assays conducted using repeated estrus cycles or pregnancies could result in the isolation of LRCs with novel stem/progenitor functions.

Alternatively, future H2BGFP label retention experiments could utilize tetracycline-inducible strains distinct from the ones that I examined in this thesis research. For example, a model where the $CD24^+/CD29^+$ compartment was completely labeled at the beginning of a label retention experiment could allow the isolation of functionally significant LRCs in this compartment. However, each of these transgenic models would require thorough characterization and testing to ensure that the desired pulse-chase kinetics are achieved. For example, one study has reported the use of CK14rtTA to induce H2BGFP in the mammary gland, resulting in induction only in the myoepithelial/basal layer [130]; use of this strain would result in myoepithelial lineage-specific LRCs. The reverse tetracycline transactivator driven by the cytokeratin 5 promoter (CK5rtTA) was used for H2BGFP label retention in the epidermis, and could also be used in the mammary gland, as early mammary epithelial lineages are known to express CK5 [85]; however, lineage tracing studies have suggested that K5 is also active exclusively in the myoepithelial layer of the adult mammary gland, which could limit use of K5rtTA in H2BGFP LRC studies [38]. Tetracycline transactivators under

the control of pregnancy/lactation-dependent promoters, such as BLG, would require pregnancy and lactation for induction, and possibly for label dilution as well; a label retention study using the WAPrtTA/H2BGFP system has been reported, with inconclusive results on the survival of LRCs after involution [87, 131].

The lack of a reliably mammary-specific promoter with pre-pregnancy activity has been a long-standing technical difficulty in mammary gland research. However, this drawback could result in adaptations of the label retention assay that could lead to new discoveries. For example, label dilution through mammary proliferation during estrus or pregnancy could be explored productively. Alternatively, tetracycline transactivator strains under the control of lineage-specific promoters such as CK14 could identify myoepithelial or luminal LRCs. It remains possible that H2BGFP label retention could provide valuable new insights into the mammary stem cell hierarchy, but thorough consideration of the technical and scientific limitations is required for productive experimentation and analysis of label retention in the mammary gland.

Evidence for a pregnancy-activated multipotent progenitor in the H2BGFP+/CD24+/CD29lo population

Investigations of mammary development have found evidence for a mammary stem cell hierarchy, consisting of stem cells capable of reconstituting the original mammary gland [12, 13], multipotent progenitors capable of giving rise to more than one mammary subtype [35, 38], unipotent progenitors committed to producing single-lineage MECs [32, 38] and differentiated cells with limited to no proliferation capacity [38, 116]. The roles that these MEC populations play during different stages of mammary development are still being characterized. Mammary stem cells are involved in the establishment of the mammary

architecture during puberty, and studies demonstrating the expansion of the $CD24^+/CD49f^+$ stem cell compartment during estrus and pregnancy suggest that mammary stem cells also proliferate during estrus and pregnancy expansion [2, 132]. However, a lineage-tracing study found that non-stem populations within the $CD24^+/CD29^+$ compartment, which corresponds with the $CD24^+/CD49f^+$ population, include myoepithelial cells that can expand during pregnancy [38]. Additionally, mammary glands that are missing luminal progenitor populations, as a consequence of the deletion of Stat5A/5B or expression of mutant cyclin D1, can form normal mammary glands but were unable to undergo alveologenesis [35, 123, 124]. If pregnancy proliferation was only dependent on stem cells, the loss of a pre-pregnancy progenitor population should not affect alveologenesis. These data support the rival hypothesis that while stem cells are involved in mammary pubertal proliferation, progenitors give rise to alveoli during pregnancy.

Studies that have examined the disruption of signaling pathways in the mammary gland have established that mammary proliferation during puberty and pregnancy are separate functions. Pubertal mammary development is dominated by estrogen signaling, whereas estrus and pregnancy proliferation in the mammary gland are progesterone-dependent. Loss of Stat5A/5B or CyclinD1 in the mammary gland results in the development of morphologically normal glands that are unable to develop alveoli during pregnancy; both Stat5A/5B- and CyclinD1- deficient mammary glands lack $CD24^+/CD29^{lo}/CD61^+$ luminal progenitors [35, 123, 124]. Interestingly, mice missing Stat5A in the mammary gland or expressing mutant CyclinD1 demonstrate increased latency in the development of mammary tumors, suggesting that these missing progenitors could be important for tumorigenesis [35, 133]. Mice expressing a dominant negative form of ErbB2 in the mammary gland develop normally, but form incomplete alveoli during pregnancy and

cannot lactate [128]. Conversely, mammary glands that overexpress Tgfβ and or lack amphiregulin are severely defective in ductal development, but can form alveoli in response to pregnancy [117, 129]. In some of these studies, it was not established conclusively that the observed defect was due to a missing mammary cell population; however, further examination of these mammary development models might reveal which mammary stem/progenitor cells are directly responsible for pubertal vs. pregnancy proliferation.

The goal of my studies was to identify and characterize novel mammary stem cell/progenitor populations and investigate their role in various stages of mammary development. Although puberty-mediated label retention in the MMTVrtTA/H2BGFP transgenic system did not enrich for mammary stem cells or progenitors in the LRCs, I made the serendipitous discovery that the H2BGFP$^+$/CD24$^+$/CD29^{lo} population could give rise to diminutive mammary structures *in vivo*. These outgrowths reproduced the original mammary cell composition and structure, and could produce milk when recipient mice were made pregnant (Figure 4-7). At the time these experiments were conducted, this finding was unexpected because CD24$^+$/CD29^{lo} MECs were initially reported to contain luminal progenitors and to have no *in vivo* repopulation activity [12]. Because H2BGFP$^+$/CD24$^+$/CD29^{lo} MECs were found to have a mammary repopulating unit frequency of 1/710 in the initial experiments (Figure 3-21), and these MECs comprised only ~15% of the CD24$^+$/CD29^{lo} compartment (Figure 3-14), these cells would have gone undetected in the limiting dilution transplants described by Shackleton et al. [12].

When the H2BGFP$^+$/CD24$^+$/CD29^{lo} transplant data were analyzed with respect to the pregnancy status of the recipient mice, I found that pregnancy increased the mammary repopulation ability of these MECs five- to ten-fold (Figure 4-2, 4-6). These data, in combination with the fact that these structures could not serially transplant (Figure 4-1),

suggested that MMTVrtTA-induced H2BGFP expression in the CD24$^+$/CD29^{lo} compartment labeled a population containing pregnancy-activated multipotent progenitors. Because this population was isolated from female mice during early puberty, and because immunofluorescence data suggests that H2BGFP$^+$/CD24$^+$/CD29^{lo} MECs are located at intervals in the luminal layer of the mammary gland, I surmise that these pregnancy-activated progenitors are established in the mammary gland along with the rest of the ductal architecture, but remain dormant until stimulated by signals generated during pregnancy.

Because mammary outgrowths were detected in both virgin and pregnant mammary glands, although at drastically different rates, it also is possible that the H2BGFP$^+$/CD24$^+$/CD29^{lo} population contains two types of progenitors, one that helps mammary gland growth during puberty, and a progenitor that is present in higher numbers and is active only during pregnancy. The studies that reported *in vivo* mammary proliferation in CD24$^+$/CD29^{lo} and CD24$^+$/CD49f^{lo} cells were performed in virgin mice, suggesting the existence of puberty-activated multipotent mammary progenitors [35, 36]. Because pregnancy would occur after the bulk of pubertal mammary development had taken place, the data from my pregnancy experiments would include outgrowths from both puberty- and pregnancy-specific progenitors. One method that could be employed to address whether more than one progenitor is present in the H2BGFP$^+$/CD24$^+$/CD29^{lo} population would be to express a more readily detectable biomarker, such as luciferase, in the H2BGFP$^+$/CD24$^+$/CD29^{lo} cells prior to transplant. Regular body scans of H2BGFP$^+$/CD24$^+$/CD29^{lo} transplant recipient mice could detect the dynamics of H2BGFP$^+$/CD24$^+$/CD29^{lo}-derived outgrowths, and determine whether these cells proliferate in response to puberty and pregnancy, or only pregnancy. Alternatively, co-transplantation of H2BGFP$^+$/CD24$^+$/CD29^{lo} and unlabeled CD24$^+$/CD29$^+$ MECs,

followed by tracing the contribution of H2BGFP$^+$/CD24$^+$/CD29^{lo}-derived cells to the mammary gland during puberty and pregnancy could determine whether or not the H2BGFP$^+$/CD24$^+$/CD29^{lo} population contains puberty progenitors. At present, I can conclude only that H2BGFP$^+$/CD24$^+$/CD29^{lo} contains a population of multipotent progenitors with preferential proliferation during pregnancy.

Evidence for the existence of pregnancy-specific progenitors has been reported by the Smith and Wagner labs, who utilized the WAP-cre/LacZ transgenic system to carry out lineage tracing of pregnancy-activated cells. This resulted in the labeling of parity-induced MECs (PI-MECs) which were found to give rise to alveoli over multiple pregnancies [42]. As was the case with the H2BGFP$^+$/CD24$^+$/CD29^{lo} pregnancy-activated progenitors, PI-MECs were found to exist in the mammary gland prior to pregnancy, suggesting that their cell fate was established during puberty [43]. Although PI-MECs were initially reported to have no mammary repopulating ability *in vivo*, a later study found that they could occasionally give rise to fully functional mammary glands and that they contained a small population of CD24$^+$/CD49f$^+$ stem cells [44]. The H2BGFP$^+$/CD24$^+$/CD29^{lo} population might contain more than one kind of mammary progenitor, but all of my experiments have indicated that these MECs have no self-renewal capacity, as is indicated by their lack of serial transplant activity. Because transplant recipient mice were made pregnant only once, I can draw no conclusion about whether the H2BGFP$^+$/CD24$^+$/CD29^{lo} progenitor can give rise to repeated mammary outgrowths *in vivo*. Experiments that track the *in vivo* kinetics of the transplanted H2BGFP+/CD24+/CD29lo population across multiple pregnancies, similar to the one described above to determine whether this population contains puberty-specific progenitors, could determine whether these pregnancy-activated progenitors can proliferate during multiple pregnancies.

It is notable that expression of CD61, which has been found to distinguish between luminal progenitors and mature luminal cells within the $CD24^+/CD29^{lo}$ compartment [116], did not differ between the $H2BGFP^+/CD24^+/CD29^{lo}$ and $H2BGFP^-/CD24^+/CD29^{lo}$ populations (Figure A-3i). This result, in combination with comparison of gene expression profiles of $CD24^+/CD29^{lo}$ MECs distinguished by CD61 expression (Figure 4-10) provides convincing support for the idea that H2BGFP expression in the $CD24^+/CD29^{lo}$ identifies a different and probably novel mammary progenitor. It is possible that MMTVrtTA/H2BGFP expression in the $CD24^+/CD29^{lo}$ compartment labels pregnancy progenitors, whereas CD61 expression identifies $CD24^+/CD29^{lo}$ progenitors with activity during puberty. Interestingly, Jeselsohn et al. found that $CD24^+/CD49f^{lo}$ MECs, which were also initially found to have no *in vivo* repopulating ability, could give rise to mammary outgrowths in both pregnant and virgin hosts, also suggesting the existence of mammary progenitors which do not require the stimulus of pregnancy for *in vivo* repopulation activity; it is also notable that development of these outgrowths required co-injection of Matrigel. The pregnancy activation experiments described in this thesis and by Jeselsohn et al. could be applied to other MEC populations to discover any pregnancy-specific activities of other mammary progenitor populations [35].

In contrast to the differential cell activity found in the $CD24^+/CD29^{lo}$ populations, my studies found no functional difference in the $H2BGFP^+/CD24^+/CD29^+$ and $H2BGFP^-/CD24^+/CD29^+$ populations. $H2BGFP^+/CD24^+/CD29^+$ and $H2BGFP^-/CD24^+/CD29^+$ MECs had similar mammary repopulation rates in pregnancy and in virgin mice (Figure 4-2) and the same serial transplantation ability (Figure 4-1). The main difference between these populations was that their descendants inherited the H2BGFP status of the original stem cell. This raises the question of how H2BGFP was induced in the $CD24^+/CD29^+$

compartment and whether this affects H2BGFP expression in the downstream

$CD24^+/CD29^{lo}$ compartment. All of the functional evidence points to distinct differences

between the $H2BGFP^+/CD24^+/CD29^{lo}$ and $H2BGFP^-/CD24^+/CD29^{lo}$ populations,

making it more likely that H2BGFP expression is induced rather than epigenetically inherited

in the $CD24^+/CD29^{lo}$ population. Additionally, expression analysis was able to separate the

$H2BGFP^+/CD24^+/CD29^+$ and $H2BGFP^-/CD24^+/CD29^+$ populations, suggesting that

these populations might have different functions which have not been detected by the assays

already conducted. Although further studies could discover a functional difference between

the $CD24^+/CD29^+$ populations, I conclude, based on the current evidence, that the most

likely possibility is that MMTVrtTA/H2BGFP expression in this compartment is stochastic

and without significance to the mammary epithelial stem cell hierarchy.

Expression analysis also provides evidence that the $H2BGFP^+/CD24^+/CD29^{lo}$

population contains a population of progenitors distinct from the bulk $H2BGFP^-$

$/CD24^+/CD29^{lo}$ population. A significant number of genes involved in mammary

development and differentiation are expressed at lower levels in the

$H2BGFP^+/CD24^+/CD29^{lo}$ population, which is consistent with biological differences

between the two $CD24^+/CD29^{lo}$ populations. For example, Esr1 and AREG are required

for ductal elongation, a process limited to pubertal proliferation [117, 129]. An analysis of

genes which differ between $H2BGFP^+/CD24^+/CD29^{lo}$ and $H2BGFP^-/CD24^+/CD29^{lo}$

MECs in a previously reported microarray of mammary stem, luminal progenitor and mature

luminal populations found that $H2BGFP^+/CD24^+/CD29^{lo}$ expression had striking

commonalities with both stem cells and luminal progenitors[116].

$H2BGFP^+/CD24^+/CD29^{lo}$ MECs express genes highly in common with

CD24+/CD29lo/CD61+ luminal progenitors, but repress other transcripts in common with

the mammary stem cell compartment, suggesting the possibility that they either share a common origin with or give rise to luminal progenitors. This analysis supports the role of H2BGFP$^+$/CD24$^+$/CD29^{lo} MECs as a multipotent mammary progenitor. In all of the mammary transplant studies described in this thesis, MEC populations were co-injected with basement membrane matrix, growth factor reduced Matrigel™. This is notable because although CD24$^+$/CD29^{lo} MECs were originally observed to have *in vivo* activity, Valliant et al. later observed that CD24$^+$/CD29^{lo} MECs could form small mammary outgrowths if co-injected with Matrigel [36]. Another study found that CD24$^+$/CD49f^{lo} MECs, which also were also originally reported to have no *in vivo* activity, formed lobular-alveolar structures in both virgin and pregnant mice in the presence of Matrigel [35]. These data contribute to a growing body of evidence for an unknown component or growth factor in Matrigel that increases transplant uptake, by assisting either cell survival or proliferation [134]. Additionally, lineage tracing demonstrated that myoepithelial-limited progenitors could give rise to mammary gland structures *in vivo*, but only if co-injected with a critical ratio of luminal cells, suggesting that paracrine signals can alter progenitor cell activity *in vivo* [38]. It is notable that in previous studies, neither Matrigel nor the addition of other mammary cells was able to affect the mammary growth protential of the stem cell compartments identified by expression of CD24$^+$/CD29$^+$ or CD24$^+$/CD49f$^+$ [12, 36]. Determining which additional components required for *in vivo* progenitor activity are fulfilled by the addition of Matrigel, and whether these components are involved in normal mammary development, would contribute to our understanding of mammary development.

Altogether, this thesis provides evidence that H2BGFP$^+$/CD24$^+$/CD29^{lo} MECs contain a population of pregnancy-activated multipotent mammary progenitors. Future directions for this project could include experiments to understand the basis for the

pregnancy-specific activity of H2BGFP$^+$/CD24$^+$/CD29^{lo} MECs; mice transplanted with H2BGFP$^+$/CD24$^+$/CD29^{lo} MECs could be treated with pregnancy hormones, such as progesterone and prolactin, to determine which signals trigger H2BGFP$^+$/CD24$^+$/CD29^{lo} outgrowths. Alternatively, H2BGFP$^+$/CD24$^+$/CD29^{lo} MECs could be co-transplanted with defined extracellular matrix components and/or growth factors to determine which are most crucial to mammary progenitor activity *in vivo*. H2BGFP$^+$/CD24$^+$/CD29^{lo} MECs could also be co-transplanted with unlabeled populations of different MEC subtypes, such as CD24$^+$/CD29$^+$ cells or CD24$^+$/CD29^{lo}/CD61$^{\pm}$ populations to determine if paracrine signaling from these MECs can affect the *in vivo* repopulating ability of H2BGFP$^+$/CD24$^+$/CD29^{lo} MECs. Additionally, co- transplantation of H2BGFP$^+$/CD24$^+$/CD29^{lo} MECs with unlabeled CD24$^+$/CD29$^+$ cells could determine the contribution of H2BGFP$^+$/CD24$^+$/CD29^{lo} MECs to the mammary gland during puberty and pregnancy. Additionally, *in vivo* development of H2BGFP$^+$/CD24$^+$/CD29^{lo} MECs could be monitored to elucidate the dynamics of H2BGFP$^+$/CD24$^+$/CD29^{lo} activity during different stages mammary development.

Although the ability to repopulate the cleared mammary fat pad remains the best in vivo assay for mammary stem cells/progenitors, the development of mammary glands from transplanted MECs is a non-physiological phenomenon. Transplanted MECs do not undergo any of the stages of mammary development prior to three weeks of age. Therefore, mammary fat pad transplants might detect progenitors responsible for mammary proliferation during puberty, rather than stem cells. Serial transplant studies have found that normal mammary glands can be transplanted 4-7 times, and that later transplants give rise to outgrowths of diminishing size [122]. As stem cells theoretically can propagate indefinitely, this gradual decrease in proliferative ability suggests that transplant assays either select for

progenitor-derived outgrowths, or that the transplantation process itself causes stem cells to terminally differentiate.

The lineage tracing study conducted by Van Keymeulen et al. found that all mammary lineages are descended from embryonic MECs expressing CK14. However, they were unable to identify a post-natal MEC population which gave rise to more than a single mammary lineage, without transplantation. Under the physiological conditions of mammary development, this study found no evidence of a post-natal mammary stem cell, and demonstrated that a bipotent cell fate can be artificially induced in a myoepithelial progenitor when transplanted with luminal cells [38]. It is possible that H2BGFP$^+$/CD24$^+$/CD29^{lo} repopulation is the result of contamination and co-transplantation, and that furthermore, the pregnancy activation observed is the result of increased paracrine signaling between luminal cells and myoepithelial progenitors. Since the myoepithelial progenitors described by Van Keymeulen et al. are CD24$^+$/CD29$^+$, this is unlikely, but still possible.

The best strategy to eliminate the posibility of artificial differentiation through transplantation in the H2BGFP$^+$/CD24$^+$/CD29^{lo} MECs would be to conduct a lineage tracing study. However, the only tool for investigating the H2BGFP+/CD24+/CD29lo population at present is the MMTVrtTA/H2BGFP model. Unfortunately, use of the MMTVrtTA transgenic system in a lineage tracing study is unlikely to be informative, since MMTVrtTA is active in CD24$^+$/CD29$^+$ populations as well as CD24$^+$/CD29^{lo} populations. This consideration also precludes use of the MMTVrtTA model to selectively kill, transform or otherwise manipulate the H2BGFP$^+$/CD24$^+$/CD29^{lo} population. Unless other methods are found to identify the H2BGFP$^+$/CD24$^+$/CD29^{lo} population, study of these MECs is limited to use of the MMTVrtTA/H2BGFP system and transplantation assays.

Candidate Cell Surface Markers for the H2BGFP+/CD24+/CD29lo

population

Although mammary epithelial subpopulations have been identified by various

indirect means, such as histology [26] and mammary outgrowth analysis [37], isolation of

MEC populations through the use of cell surface markers and FACS remains the most

reliable tool for characterization of MEC subtypes. MEC subpopulations that have been

identified by cell surface markers include stem cells (CD24$^+$/CD29$^+$, CD24$^+$/CD49^f) [12,

13], luminal progenitors (CD24$^+$/CD29^{lo}/CD61$^+$) [116], myoepithelial progenitors (non-

stem CD24$^+$/CD29$^+$, CD24^{lo}CD49f$^+$) [13, 38], mature luminal cells (CD24$^+$/CD29^{lo}/CD61$^-$)

[116] and alveolar progenitors (CD24$^+$/CD29^{lo}/CD14$^+$/c-Kit$^-$) [33].

In the Appendix of this thesis, I describe the testing and evaluation of various

candidate cell surface markers for the H2BGFP$^+$/CD24$^+$/CD29^{lo} population. Candidates

were selected from cell surface markers identified in microarray experiments and from

markers already known to identify populations of interest in the mammary gland. Of the

twenty-four candidate markers tested, six displayed differences in expression between

H2BGFP$^+$/CD24$^+$/CD29^{lo} and H2BGFP$^-$/CD24$^+$/CD29^{lo} cells, and only one, CD14, was

found to express in the majority of the H2BGFP$^+$/CD24$^+$/CD29^{lo} population.

Unfortunately, *in vivo* testing of this marker was inconclusive because of an unusually high

repopulation rate of transplanted MECs, which might be the result of an anomalous lot of

Matrigel. Repetition of these experiments with a different lot of Matrigel would probably

demonstrate that CD14 is able to isolate pregnancy-specific mammary progenitors.

The identification of CD14 as an upregulated transcript and potential cell surface

marker for the H2BGFP$^+$/CD24$^+$/CD29^{lo} population has interesting implications. Asselin-

Labat et al have identified CD24$^+$/CD29^{lo}/CD14$^+$/c-Kit$^-$ MECs as alveolar progenitors [32,

33]. However, this classification is based on *in vitro* testing and immunostaining of mammary glands, and has not yet been verified *in vivo*. One possible future experiment could involve lineage tracing, using the CD14 promoter to identify these cells and their descendants *in situ*. Further studies may identify other markers which, in combination with CD14, can isolate the pregnancy-activated multipotent progenitors within the H2BGFP+/CD24+/CD29lo population.

Final Note

Although much progress has been made, the mammary epithelial stem cell hierarchy remains incompletely understood. In this thesis, I have presented evidence for a pregnancy-activated multipotent mammary progenitor. This supports the hypothesis that different cell types as well as different signaling pathways are activated during the fundamentally distinct processes of pubertal mammary proliferation and pregnancy-mediated alveologenesis. Future directions for this project include identifying other cell surface markers for isolation of this population, elucidating unknown factors involved in progenitor activity such as Matrigel, and studying the dynamics of pregnancy-activated progenitors *in vivo*.

Appendix A Testing Candidate Cell Surface Markers for Independent Isolation of the H2BGFP+/CD24+/CD29lo Population by FACS

Introduction

In the course of histone label retention experiments, I found that MMTVrtTA-induced expression H2BGFP in the mammary gland labeled a sub-population of the CD24$^+$/CD29^{lo} compartment that contained a novel multipotent progenitor with pregnancy-specific activity. Further study of this progenitor could provide valuable new insights into the mechanisms of proliferation in the mammary gland at different stages of development. However, studies of the H2BGFP$^+$/CD24$^+$/CD29^{lo} population are currently limited by the need to use the MMTVrtTA/H2BGFP transgenic mouse system to isolate these MECs.

To further characterize these progenitors, I carried out transcription profiling of the H2BGFP$^+$/CD24$^+$/CD29^{lo} and H2BGFP$^-$/CD24$^+$/CD29^{lo} populations, as was described in Chapter 3. A secondary goal of these microarrays was to identify cell surface proteins that might be candidate markers for separating these populations by FACS. Ideally, such a marker would be strongly expressed in the cell subtype of interest, allowing for positive selection, and have commercially available antibodies already shown to be effective for flow cytometry. As the H2BGFP$^+$/CD24$^+$/CD29^{lo} population is mixed and additional purity could be obtained from a more selective marker, a marker that labeled only a fraction of H2BGFP$^+$/CD24$^+$/CD29^{lo} cells would be considered a strong candidate marker. Alternatively, two or more markers could be combined to isolate the population. Based on the microarray data, I tested candidate cell surface markers for the H2BGFP$^+$/CD24$^+$/CD29^{lo} population. This appendix reports the results of these experiments and additional considerations for future research on the mammary epithelial stem cell hierarchy.

Results

Candidate cell surface markers for independent isolation of

H2BGFP+/CD24+/CD29lo MECs

Candidate cell surface markers for separation of the $H2BGFP^+/CD24^+/CD29^{lo}$ population from the $H2BGFP^-/CD24^+/CD29^{lo}$ MECs were selected based on various factors. These selection criteria included differential expression detected by microarray, availability of commercial antibodies, previous identification as a marker in the mammary stem cell hierarchy and identification as a marker in other adult stem cells/progenitors or developmental pathways.

In order to identify potential cell surface markers, the 256 microarray probes demonstrating statistically significant differences between $H2BGFP^+/CD24^+/CD29^{lo}$ and $H2BGFP^-/CD24^+/CD29^{lo}$ populations were surveyed for cell surface proteins as identified by the Gene Ontology database (Figure A-1). Candidate markers selected from this group included mucin 1 (Muc1, expressed in luminal cells), Alcam, CD86, Ly6a/Sca-1 (expressed in differentiated MECs [12]), FGFR2 and Il1R1. Other candidate markers not on the Gene Ontology list were identified from the microarray (Figure A-2), including CD138/syndecan, CD14, CD55, CD164, CXCL16, interleukin 33 (Il33), jagged 1 (Jag1), osteoactivin, AREG and PRLR. Markers selected on the basis of previous identification in the mammary stem cell hierarchy or other adult stem cell populations include CD44 [135], CD49b [31], CD61 [136], EpCam [137], E-cadherin and c-Kit. A different CD24 antibody from the one used in previous assays was selected based on evidence that mammary progenitors and stem cells could be distinguished by their level of CD24 expression using this clone(i.e. $CD24^{mid}$ vs. $CD24^{hi}$) [34, 35].

To test the selected antibodies, MECs were isolated from four week-old MMTVrtTA/H2BGFP mice and stained with the antibodies for candidate cell surface

Figure A-1. Expression of Cell Surface Markers in CD24+/CD29lo Populations. Of the 257 probes found to demonstrate statistically significant differences between H2BGFP+/CD24+/CD29lo and H2BGFP-/CD24+/CD29lo populations, these probes were identified as cell surface proteins by the Gene Ontology database.

markers, in addition to the markers used in the original analysis. The

H2BGFP$^+$/CD24$^+$/CD29^{lo} and H2BGFP$^-$/CD24$^+$/CD29^{lo} populations were gated and

analyzed for staining of the experimental antibody; histograms of isotype controls or MECs

stained only with secondary antibodies were used as control curves for comparison. A total

of twenty-four candidate cell surface markers were assayed in at least three different

experiments (Figure A-3).

Of the twenty-four markers tested, none demonstrated a complete separation of

H2BGFP$^+$/CD24$^+$/CD29^{lo} cells from the H2BGFP$^-$/CD24$^+$/CD29^{lo} population, nor were

any identified as marking only part of the H2BGFP$^+$/CD24$^+$/CD29^{lo} population. Thirteen

antigens (AlCAM, AREG, CD44, CD55, CD86, CD138, CD164, CXCL16, E-cadherin, Il33,

Muc1, osteoactivin, PRLR) showed equivalent levels of expression between

H2BGFP$^+$/CD24$^+$/CD29^{lo} and H2BGFP$^-$/CD24$^+$/CD29^{lo} cells. Five candidate markers

(CD24, CD49f, CD61, c-Kit, IL1R1) demonstrated minimal differences in expression level

between the two populations. Because all of these antibodies, except for the IL1R1
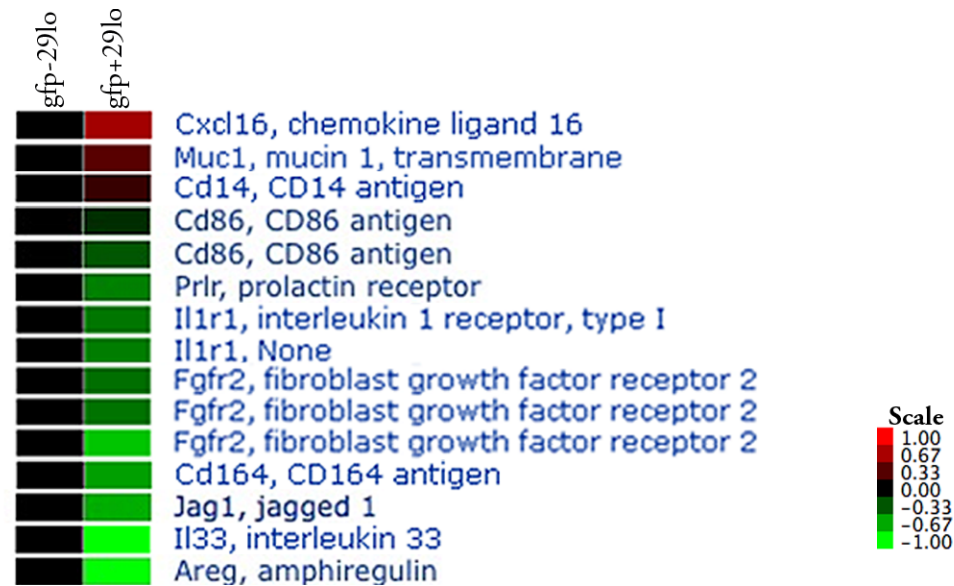
Figure A-2. Expression of Candidate Cell Surface Markers in CD24+/CD29lo Populations. Transcripts identified as candidate stem cell markers for separation of H2BGFP+/CD24+/CD29lo and H2BGFP-/CD24+/CD29lo populations in the MMTVrtTA/H2BGFP microarray.

antibody, have been used repeatedly in flow cytometric studies, it can be concluded that these data accurately represent the protein expression level of these candidate markers on the cell surface of the tested MEC populations.

Six markers (CD14, CD49b, EpCAM, FGFR2, Jag1, Sca-1) were expressed differentially in the H2BGFP$^+$/CD24$^+$/CD29^{lo} and H2BGFP$^-$/CD24$^+$/CD29^{lo} populations. Although none of these antibodies clearly distinguished the H2BGFP$^+$ from the H2BGFP$^-$ populations, the histograms for these antibodies suggested possibly different sub-populations with distinct properties. For example, most H2BGFP$^+$/CD24$^+$/CD29^{lo} MECs were CD14$^+$, whereas the H2BGFP$^-$/CD24$^+$/CD29^{lo} compartment contained a mixed population of CD14$^+$ and mostly CD14$^-$ MECs. H2BGFP$^+$/CD24$^+$/CD29^{lo} MECs were found to be Sca-1$^-$, but H2BGFP$^-$/CD24$^+$/CD29^{lo} MECs contained both Sca-1$^+$ and Sca-1$^-$ cells. H2BGFP$^+$/CD24$^+$/CD29^{lo} MECs expressed higher levels of CD49b than H2BGFP$^-$/CD24$^+$/CD29^{lo} MECs, but there was no obvious separation of CD49b subpopulations
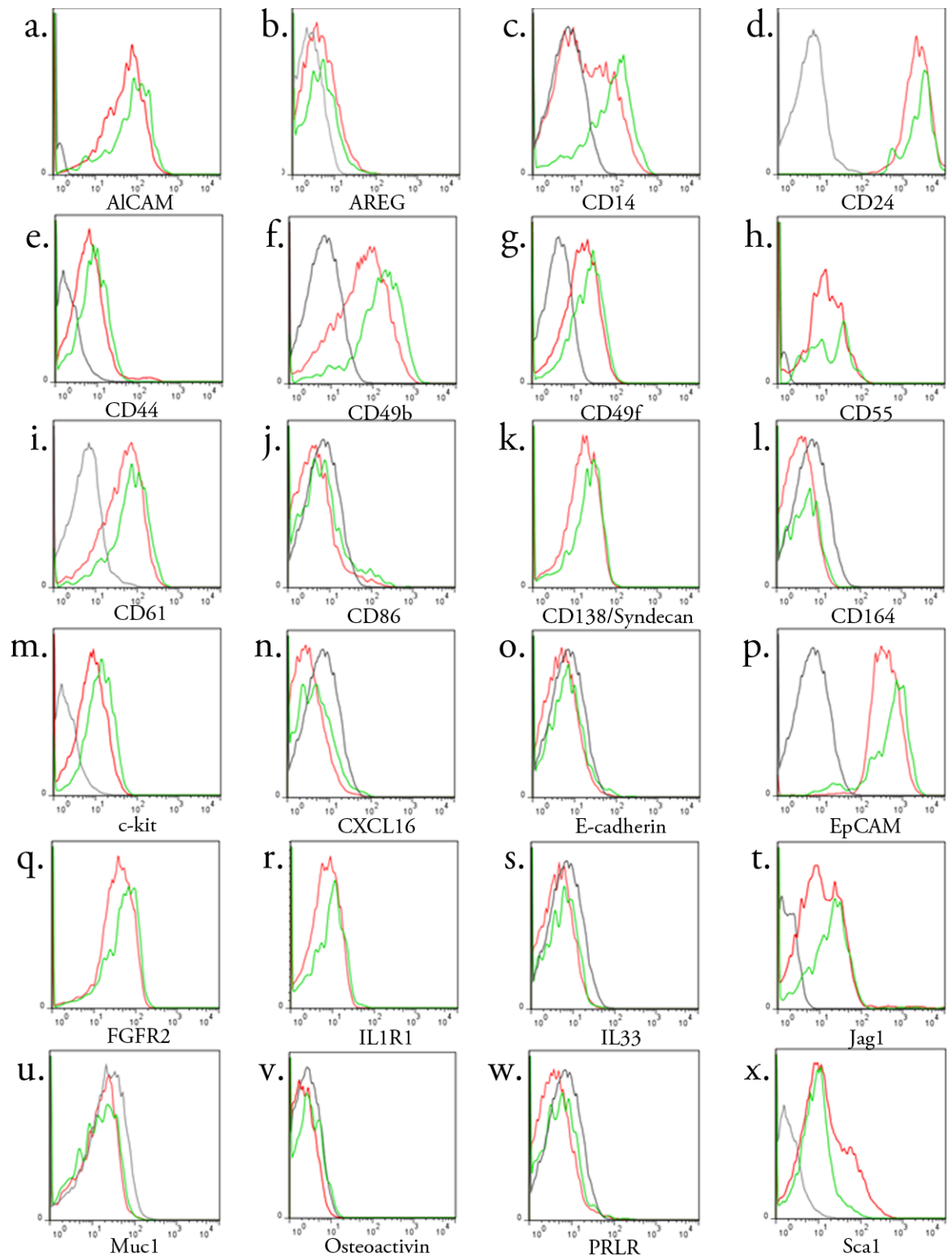
Figure A-3. Flow Cytometric Analysis of Candidate Cell Surface Markers. MMTVrtTA/H2BGFP MECs were stained for antibodies for candidate cell surface markers. Staining was compared between H2BGFP+/CD24+/CD29lo (green) MECs, H2BGFP-/CD24+/CD29lo (red) MECs and control (gray).

within these compartments. The EpCAM, FGFR2 and Jag1 histograms also suggested a mixed H2BGFP-/CD24+/CD29lo population, but these differences were not sufficiently large for FACS isolation to be attempted. Based on this data, I concluded that CD14 and CD49b were the best candidates for cell surface markers able to enrich for H2BGFP$^+$/CD24$^+$/CD29^{lo} MECs.

To determine whether these were suitable markers for alternative isolation of H2BGFP$^+$/CD24$^+$/CD29^{lo} MECs, CD14 and CD49b were tested, both individually and in combination, for their ability to enrich for H2BGFP$^+$ cells in the CD24$^+$/CD29^{lo} CD14 as a marker of pregnancy-activated multipotent progenitors in the mammary epithelium. Based on the above experiments, I determined that CD14 was the most promising candidate cell surface marker for isolation of the multipotent pregnancy-activated progenitors within the H2BGFP$^+$/CD24$^+$/CD29^{lo} population. In the microarray, CD14 transcript levels were found to be slightly elevated in H2BGFP+/CD24+/CD29lo MECs compared with H2BGFP$^-$/CD24$^+$/CD29^{lo} MECs. This is consistent with the flow cytometry data, which found that H2BGFP$^+$/CD24$^+$/CD29^{lo} cells were almost entirely CD14$^+$, whereas H2BGFP$^-$/CD24$^+$/CD29^{lo} cells contained a mixed population of CD14$^+$ and CD14$^-$ cells (Figure A-3c). populations (Figure A-4). In these experiments, 21±4.7% of CD24$^+$/CD29^{lo} MECs were GFP$^+$. The GFP$^+$ population was 33±4.4% of CD24$^+$/CD29^{lo}/CD14$^+$ MECs and 35±2.5% of CD24$^+$/CD29^{lo}/CD49b$^+$ cells (Figure A-4f, i). (Averages and standard deviations were derived from n= 3) However, CD24$^+$/CD29^{lo}/CD14$^+$/CD49b$^+$ MECs were 35±6.3% GFP$^+$, demonstrating no additional enrichment when CD14 and CD49b were used in combination. CD14 was determined to be the better marker for subdivision of the CD24$^+$/CD29^{lo} compartment because CD14 divides
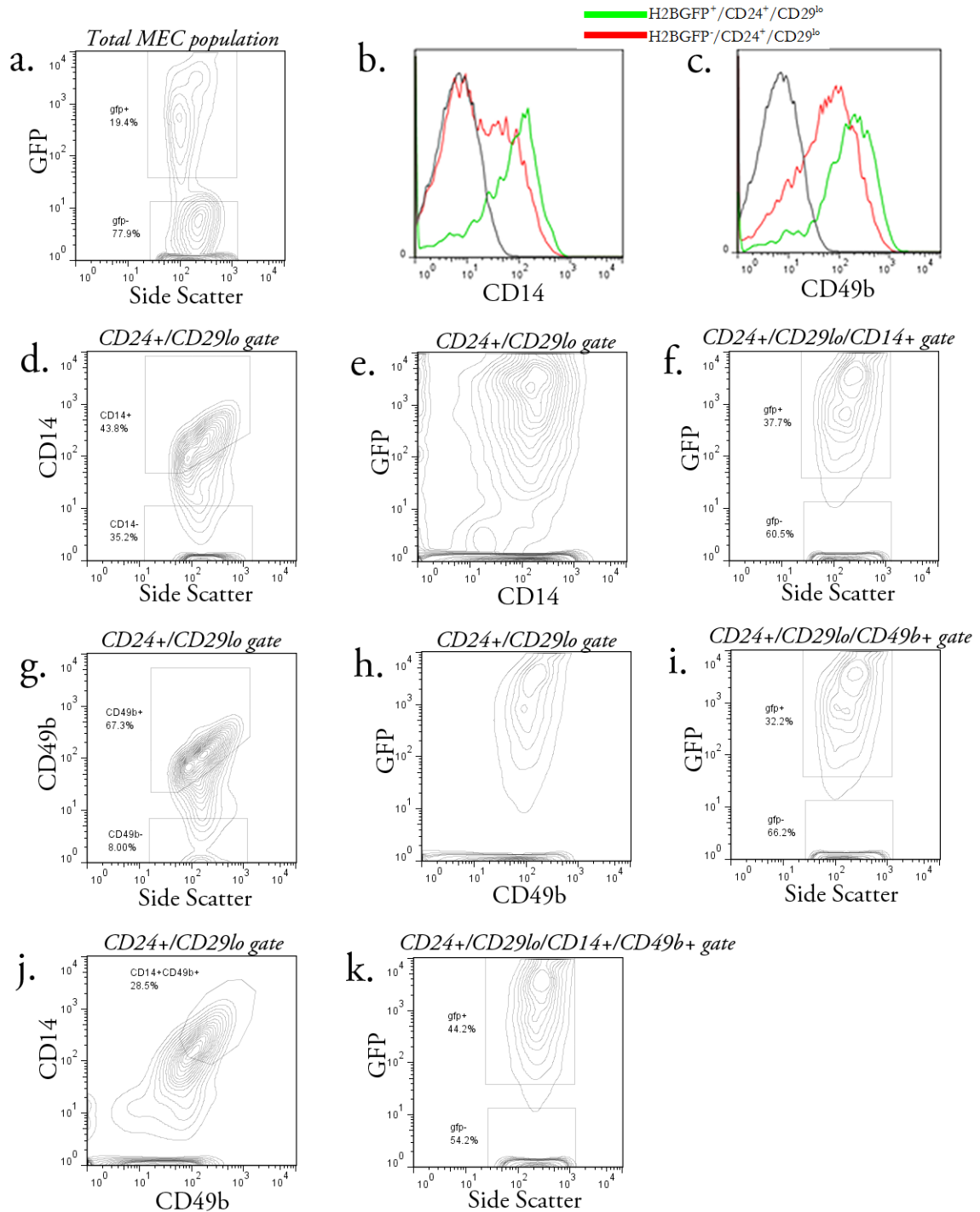
Figure A-4. CD14 and CD49b as markers for H2BGFP+/CD24+/CD29lo MECs. CD14 and CD49b were tested separately and in combination as potential markers for isolation of H2BGFP+/CD24+/CD29lo MECs. Analysis of a) GFP expression in total MECs b) CD14 expression in H2BGFP+ vs. H2BGFP- populations c) CD49b expression in H2BGFP+ vs. H2BGFP- populations d) CD14 expression in CD24+/CD29lo population e) correlation of GFP and CD14 in CD24+/CD29lo population f) GFP expression in CD24+/CD29lo/CD14+ g) CD49b expression in CD24+/CD29lo population h) correlation of GFP and CD49b in CD24+/CD29lo population i) GFP expression in CD24+/CD29lo/CD49b+ j) CD14 and CD49b expression in CD24+/CD29lo population k) GFP expression in CD24+/CD29lo/CD14+/CD49b+

the CD24$^+$/CD29^{lo} population into distinct CD14$^+$ and CD14$^-$ populations, whereas CD49b expression was less distinct (Figure A-4b, c). (Averages and standard deviations were derived from an n = 4)

The CD24$^+$/CD29^{lo}/CD14$^+$ population contained 78±6.2% of the H2BGFP$^+$/CD24$^+$/CD29^{lo} population; however, 63±3.5% of the CD24$^+$/CD29^{lo}/CD14$^+$ population was H2BGFP$^-$/CD24$^+$/CD29^{lo} cells. Therefore, CD14 clearly is not an ideal marker for isolating the multipotent pregnancy-activated progenitor within the CD24$^+$/CD29^{lo} population. Nevertheless, an imperfect marker is still less cumbersome than the requirement for two strains of transgenic mice, and can be used more broadly to test changes in the pregnancy progenitor population in studies of other transgenic mice with mammary phenotypes. Therefore, I tested the ability of CD24$^+$/CD29^{lo}/CD14$^+$ MECs to form mammary structures *in vivo* compared to the CD24$^+$/CD29^{lo}/CD14$^-$ population, in both virgin and pregnant recipients.

Surprisingly, all transplants produced far more outgrowths than were anticipated based on published studies and my multiple previous experiments, resulting in calculated MRU frequencies much higher than expected. CD24$^+$/CD29^{lo}/CD14$^+$ MECs had a calculated MRU frequency of 1/460 in virgin recipients and 1/180 in pregnant recipients (Figure A-5a, c). CD24$^+$/CD29^{lo}/CD14$^-$ MECs had a calculated MRU frequency of 1/1,300 in virgins and 1/220 in pregnant mice (Figure A-5b, d). In order to eliminate any possibility of contamination from H2BGFP- populations, mammary outgrowths were sectioned and immunostained, and only outgrowths that stained positive for GFP were counted. The recalculated MRU frequency for CD24$^+$/CD29^{lo}/CD14$^+$ cells was 1/1,100 in virgins and1/550 in pregnant mice, whereas CD24$^+$/CD29^{lo}/CD14$^-$ cells did not give rise to GFP$^+$ outgrowths in virgins and had a calculated MRU frequency of 1/880 in pregnant mice.

Population	# cells	# glands	MRU frequency (C.I.)
a. CD24⁺/CD29ˡᵒ/ CD14⁺ *virgin*	10	0/16	1/1,100 (460 – 2,700)
	20	0/16	
	50	1/14	
	100	1/16	
	200	3/16	
b. CD24⁺/CD29ˡᵒ/ CD14⁺ *+pregnancy*	10	1/14	1/550 (280 – 1,100)
	20	0/16	
	50	1/14	
	100	3/16	
	200	4/14	
c. CD24⁺/CD29ˡᵒ/ CD14- *virgin*	10	0/14	N/A
	20	0/16	
	50	0/16	
	100	0/16	
	200	0/14	
d. CD24⁺/CD29ˡᵒ/ CD14- *+pregnancy*	10	0/16	1/880 (380 – 2,000)
	20	1/14	
	50	3/16	
	100	2/14	
	200	0/14	

Population	Cell #	Outgrowth Size					
		-	~	+	++	+++	++++
a. CD24⁺/CD29ˡᵒ/ CD14⁺ *virgin*	10	16	0	0	0	0	0
	20	16	0	0	0	0	0
	50	13	0	1	0	0	0
	100	15	0	1	0	0	0
	200	13	2	0	1	0	0
b. CD24⁺/CD29ˡᵒ/CD14⁺ *+pregnancy*	10	13	0	1	0	0	0
	20	16	0	0	0	0	0
	50	13	0	1	0	0	0
	100	13	2	1	0	0	0
	200	10	1	1	2	0	0
c. CD24⁺/CD29ˡᵒ/ CD14- *virgin*	10	14	0	0	0	0	0
	20	16	0	0	0	0	0
	50	16	0	0	0	0	0
	100	16	0	0	0	0	0
	200	14	0	0	0	0	0
d. CD24⁺/CD29ˡᵒ/CD14- *+pregnancy*	10	16	0	0	0	0	0
	20	13	1	0	0	0	0
	50	13	0	3	0	0	0
	100	12	2	0	0	0	0
	200	14	0	0	0	0	0

Figure A-5. Limiting Dilution Transplants of CD14 Populations in Virgins and Pregnant Mice. MECs were isolated from four week old MMTVrtTA/H2BGFP females and CD24+/CD29lo/CD14+ and CD24+/CD29lo/CD14- populations were sorted and transplanted into mice which were left virgin (a, c) or made pregnant (b, d). Mammary glands were counted (upper) and scored for size (lower).

Population	# cells	# glands	MRU frequency (C.I.)
a. CD24+/CD29lo/ CD14+ *virgin*	10	0/16	1/460 (250 – 840)
	20	0/16	
	50	2/14	
	100	2/16	
	200	7/16	
b. CD24+/CD29lo/ CD14+ *+pregnancy*	10	4/14	1/180 (120 – 280)
	20	2/16	
	50	2/14	
	100	7/16	
	200	8/14	
c. CD24+/CD29lo/ CD14- *virgin*	10	0/14	1/1,300 (490 – 3,600)
	20	0/16	
	50	0/16	
	100	1/16	
	200	3/14	
d. CD24+/CD29lo/ CD14- *+pregnancy*	10	3/16	1/220 (140 – 350)
	20	4/14	
	50	6/16	
	100	5/14	
	200	3/14	

Population	Cell #	Outgrowth Size					
		-	~	+	++	+++	++++
a. CD24+/CD29lo/ CD14+ *virgin*	10	16	0	0	0	0	0
	20	16	0	0	0	0	0
	50	12	1	1	0	0	0
	100	14	1	1	0	0	0
	200	9	5	2	0	0	0
b. CD24+/CD29lo/CD14+ *+pregnancy*	10	10	0	2	0	1	1
	20	14	1	0	0	1	0
	50	12	1	1	0	0	0
	100	9	2	2	2	1	0
	200	5	2	1	5	0	0
c. CD24+/CD29lo/ CD14- *virgin*	10	14	0	0	0	0	0
	20	16	0	0	0	0	0
	50	16	0	0	0	0	0
	100	15	1	0	0	0	0
	200	11	2	0	0	0	1
d. CD24+/CD29lo/CD14- *+pregnancy*	10	13	2	0	1	0	0
	20	10	2	1	1	0	0
	50	10	1	5	0	0	0
	100	9	3	1	1	0	0
	200	11	1	2	0	0	0

Figure A-6. Limiting Dilution Transplants of CD14 Transplants - GFP+ glands only. Data from Figure A-5 was filtered to include only mammary glands which demonstrated GFP+ expression.

These recalculated repopulation rates are still well above the expected repopulation rates of the injected CD24$^+$/CD29^{lo} subpopulations.

Discussion & Future Directions

In the search for a cell surface marker that could isolate the pregnancy-activated multipotent progenitor within the H2BGFP$^+$/CD24$^+$/CD29^{lo} population independently of MMTVrtTA/H2BGFP transgene activity, twenty-four antibodies were tested by flow cytometry. These antigens were selected from the microarray comparing the H2BGFP$^+$/CD24$^+$/CD29^{lo} cells with H2BGFP$^-$/CD24$^+$/CD29^{lo} cells, and from known markers of the mammary stem cell hierarchy. For eighteen of these antibodies, I found no difference or minimal differences in staining between H2BGFP$^+$/CD24$^+$/CD29^{lo} and H2BGFP$^-$/CD24$^+$/CD29^{lo} populations. Whether these assays accurately represent the expression of these proteins on the cell surface, or whether these antibodies did not function in flow cytometry is unknown. Some of the antibodies (AREG, CD164, Il33, Muc1, PRLR) used were not previously tested in flow cytometry, or were tested in non-physiological conditions, such as transgenic overexpression of the antigen, that could have resulted in the apparent success of a relatively weak antibody.

Notably, CD61 did not differentiate between the H2BGFP$^+$ and H2BGFP$^-$ subpopulations of the CD24$^+$/CD29^{lo} compartment. On the basis of *in vitro* assays, CD24$^+$/CD29^{lo}/CD61$^+$ cells have been reported to represent luminal progenitors, whereas CD24$^+$/CD29^{lo}/CD61$^-$ cells were reported to be a more differentiated cell population. Because CD61 expression did not differ significantly between H2BGFP$^+$/CD24$^+$/CD29^{lo}

and H2BGFP$^-$/CD24$^+$/CD29^{lo} MECs, H2BGFP$^+$ cells must represent a distinct sub-division of functional mammary cells within the CD24$^+$/CD29^{lo} compartment.

The H2BGFP$^+$/CD24$^+$/CD29^{lo} and H2BGFP$^-$/CD24$^+$/CD29^{lo} populations demonstrated different flow cytometry profiles for six of the antibodies tested. For these antibodies, the data suggested that either the H2BGFP$^+$ or H2BGFP$^-$ compartments contained distinct subpopulations with different expression of the tested cell surface markers. These results were not surprising, as the CD24$^+$/CD29^{lo} subpopulations are expected to be mixed, based on quantitative transplantation studies and *in vivo* assays. Of the candidate cell surface markers displaying differences within the CD24$^+$/CD29^{lo} populations, the differences in EpCAM, FGFR2 and Jag1 were deemed too small to be useful for cell separation; however, the future development of more effective antibodies against these antigens could potentially be used for isolation of the H2BGFP$^+$/CD24$^+$/CD29^{lo} populations. The H2BGFP$^-$/CD24$^+$/CD29^{lo} population was found to contain a Sca-1$^+$ subpopulation, which was expected, as Sca-1 is expressed in differentiated MECs [12]; however, this confirmation of previously reported data was not useful for separation of the H2BGFP$^+$/CD24$^+$/CD29^{lo} and H2BGFP$^-$/CD24$^+$/CD29^{lo} cells, because the Sca-1$^+$ and Sca-1$^-$ populations overlapped significantly. CD49b and CD14 were tested, separately and in combination, as possible markers for isolation of H2BGFP$^+$/CD24$^+$/CD29^{lo} MECs; CD14 was found to be the more effective marker because of its ability to distinguish distinct CD14$^+$ and CD14$^-$ populations, and was therefore used to isolate CD24$^+$/CD29^{lo} subpopulations that were tested for pregnancy-specific activity.

The results of the cleared fat pad transplants followed the predicted mammary outgrowth pattern only insofar as CD24$^+$/CD29^{lo}/CD14$^+$ cells had a higher repopulation rate than CD24$^+$/CD29^{lo}/CD14$^-$ cells, and that pregnancy increased the calculated MRU rate

of both populations. However, the mammary repopulation rates for transplants of

$CD24^+/CD29^{lo}/CD14^+$ and $CD24^+/CD29^{lo}/CD14^-$ cells were very high. Even when the

data were filtered to include only GFP^+ outgrowths, the mammary repopulation rate

remained far higher than expected. Because $H2BGFP^+/CD24^+/CD29^{lo}$ MECs had a

calculated MRU frequency of ~1/300 in pregnant recipients (Figures 3-4, 3-8), and because

approximately 30% of the $CD24^+/CD29^{lo}/CD14^+$ cells were $H2BGFP^+$, the expected MRU

frequency of $CD24^+/CD29^{lo}/CD14^+$ MECs was ~1/1,000. Because the

$CD24^+/CD29^{lo}/CD14^-$ population also contained ~20% of the $H2BGFP^+/CD24^+/CD29^{lo}$

cells, it was possible, if unlikely, that the multipotent mammary progenitors were contained

in the CD14$^-$ population. Yet, neither of these possibilities explains the extremely high rate

of fat pad repopulation observed in these transplants. This result is surprising, particularly

because the $CD24^+/CD29^{lo}$ compartment is believed to contain no stem cells and was

originally reported to have no repopulation activity. Because my numerous previous

transplant experiments have agreed with published data concerning mammary repopulation

rates (Figures 2-11, 3-4, 3-8), I concluded that this anomalous result is not due to problems

with the mammary fat pad transplants.

There are several possible explanations for these unexpected data. One possibility is

that some minor change in the enzymatic digestion conditions or cell sorting protocol has

resulted in the addition of doublets (i.e. stem cells adhering to progenitors or mature

mammary cells) or other contaminating cells to the population of MECs sorted for

transplant. Because the digestive enzymes used in these experiments have changed lots

repeatedly over the years, with no noticeable change in mammary repopulation rate, and

because the same cell sorting protocols and FACS machines were used for all experiments in

this thesis, this explanation is possible, but unlikely. It is also unlikely that the transplant

recipient mice, which were obtained from commercial vendors, had different circulating hormone levels or otherwise provided a better *in vivo* environment for growth of mammary structures.

The most likely explanation for this dramatic increase in mammary repopulation ability of the $CD24^+/CD29^{lo}$ population is a change in the Matrigel co-injected with transplanted MECs. All MECs transplanted in my experiments were co-injected with growth factor reduced Matrigel (see Chapter 2, Materials & Methods). Matrigel can vary widely between lots, and contains growth factors or other molecules able to affect cell proliferation and differentiation [105]. Valliant et al. reported that $CD24^+/CD29^{lo}$ cells were unable to form mammary structures *in vivo* unless co-injected with Matrigel [36]; therefore, it is highly likely that different lots of Matrigel could affect the rate of repopulation in $CD24^+/CD29^{lo}$ cells. (The $CD24^+/CD29^+$ stem cell compartment was unaffected by addition of Matrigel [36].) Because my *in vivo* transplantation data was heretofore consistent across numerous lots of Matrigel, the batch used in these latest experiments was probably anomalous, containing unusually high levels of mammary growth-promoting components. Transplants of $CD24^+/CD29^{lo}/CD14^+$ and $CD24^+/CD29^{lo}/CD14^-$ populations using a different lot of Matrigel would probably result in the predicted mammary repopulation rate.

The fact that Matrigel can so dramatically affect the *in vivo* growth ability of $CD24^+/CD29^{lo}$ cells raises the question of what Matrigel components cause this change. Van Keymeulen et al. recently reported that myoepithelial progenitors could give rise to fully functional mammary structures when transplanted with a critical concentration of luminal cells, and speculated that paracrine signaling between the populations was responsible for this phenomenon. It is plausible that the growth factors responsible for such signaling might be contained within certain formulations of Matrigel. Alternatively, previous studies

have demonstrated that extracellular matrix stiffness can affect the differentiation of mesenchymal stem cells [138]. It is possible that the mechanical structure provided by Matrigel, which polymerizes at body temperature, might result in the activation of different proliferation or differentiation programs depending on the stiffness of the Matrigel in which the transplanted MECs are embedded. Positive identification of the factor(s) in Matrigel that promotes *in vivo* mammary growth and development could provide a significant contribution to our understanding of mammary development.

The identification of CD14 as a likely marker for the pregnancy-activated multipotent mammary progenitor subpopulation within the $CD24^+/CD29^{lo}$ compartment is interesting. CD14 is a co-receptor for bacterial lipopolysaccharide and mediates the immune response to bacterial infections. A truncated form of CD14 is secreted into breast milk, which has been hypothesized to mediate infant gut-bacterial interactions [139]. CD14 also is expressed at high levels in the mammary gland during involution, possibly as a signal to the immune system to assist in clearing apoptotic cells [140]. Various groups have identified CD14 as a potential marker for alveolar progenitors [32, 33]; for example, $CD24^+/CD29^{lo}/CD14^+/c\text{-Kit}^-$ MECs can form lactogenic colonies *in vitro*. Mice that are null for the CD14 gene have no reported mammary phenotype; however, study of MEC populations in these mice could provide further details about the mechanisms of mammary development [141].

My data suggests that CD14 is a marker for multipotent, pregnancy-activated mammary progenitors, but until the effect of Matrigel on the *in vivo* assays can be clarified, the *in vivo* role of CD14 populations will remain incompletely understood. In any event, CD14 does not provide complete purification of the $H2BGFP^+/CD24^+/CD29^{lo}$ population.

Future studies could identify the other markers that are required in combination with CD14,

CD24 and CD29 to isolate these pregnancy-activated progenitors.

Bibliography

1. Visvader, J.E., *Keeping abreast of the mammary epithelial hierarchy and breast tumorigenesis.* Genes & development, 2009. **23**(22): p. 2563-77.
2. Joshi, P.A., H.W. Jackson, A.G. Beristain, M.A. Di Grappa, P.A. Mote, C.L. Clarke, J. Stingl, P.D. Waterhouse, and R. Khokha, *Progesterone induces adult mammary stem cell expansion.* Nature, 2010. **465**(7299): p. 803-7.
3. Brisken, C., *Hormonal control of alveolar development and its implications for breast carcinogenesis.* Journal of mammary gland biology and neoplasia, 2002. **7**(1): p. 39-48.
4. Smalley, M. and A. Ashworth, *Stem cells and breast cancer: A field in transit.* Nature reviews. Cancer, 2003. **3**(11): p. 832-44.
5. Beato, M., *Chromatin structure and the regulation of gene expression: remodeling at the MMTV promoter.* Journal of molecular medicine, 1996. **74**(12): p. 711-24.
6. Cole, H., *The Mammary Gland of the Mouse, during Oestrus Cycle, Pregnancy and Lactation.* Proceedings of the Royal Society of London: Biological Sciences, 1933. **114**: p. 136-161.
7. Tiede, B. and Y. Kang, *From milk to malignancy: the role of mammary stem cells in development, pregnancy and breast cancer.* Cell research, 2011. **21**(2): p. 245-57.
8. Hennighausen, L. and G.W. Robinson, *Signaling pathways in mammary gland development.* Developmental cell, 2001. **1**(4): p. 467-75.
9. Kouros-Mehr, H., E.M. Slorach, M.D. Sternlicht, and Z. Werb, *GATA-3 maintains the differentiation of the luminal cell fate in the mammary gland.* Cell, 2006. **127**(5): p. 1041-55.
10. Smith, G.H., T. Mehrel, and D.R. Roop, *Differential keratin gene expression in developing, differentiating, preneoplastic, and neoplastic mouse mammary epithelium.* Cell growth & differentiation : the molecular biology journal of the American Association for Cancer Research, 1990. **1**(4): p. 161-70.
11. Barbareschi, M., L. Pecciarini, M.G. Cangi, E. Macri, A. Rizzo, G. Viale, and C. Doglioni, *p63, a p53 homologue, is a selective nuclear marker of myoepithelial cells of the human breast.* The American journal of surgical pathology, 2001. **25**(8): p. 1054-60.
12. Shackleton, M., F. Vaillant, K.J. Simpson, J. Stingl, G.K. Smyth, M.L. Asselin-Labat, L. Wu, G.J. Lindeman, and J.E. Visvader, *Generation of a functional mammary gland from a single stem cell.* Nature, 2006. **439**(7072): p. 84-8.
13. Stingl, J., P. Eirew, I. Ricketson, M. Shackleton, F. Vaillant, D. Choi, H.I. Li, and C.J. Eaves, *Purification and unique properties of mammary epithelial stem cells.* Nature, 2006. **439**(7079): p. 993-7.
14. Watson, C.J. and W.T. Khaled, *Mammary development in the embryo and adult: a journey of morphogenesis and commitment.* Development, 2008. **135**(6): p. 995-1003.
15. Bocchinfuso, W.P. and K.S. Korach, *Mammary gland development and tumorigenesis in estrogen receptor knockout mice.* Journal of mammary gland biology and neoplasia, 1997. **2**(4): p. 323-34.
16. Williams, J.M. and C.W. Daniel, *Mammary ductal elongation: differentiation of myoepithelium and basal lamina during branching morphogenesis.* Developmental biology, 1983. **97**(2): p. 274-90.
17. Mailleux, A.A., M. Overholtzer, T. Schmelzle, P. Bouillet, A. Strasser, and J.S. Brugge, *BIM regulates apoptosis during mammary ductal morphogenesis, and its absence reveals alternative cell death mechanisms.* Developmental cell, 2007. **12**(2): p. 221-34.
18. Fata, J.E., V. Chaudhary, and R. Khokha, *Cellular turnover in the mammary gland is correlated with systemic levels of progesterone and not 17beta-estradiol during the estrous cycle.* Biology of reproduction, 2001. **65**(3): p. 680-8.
19. Virgo, B.B. and G.D. Bellward, *Serum progesterone levels in the pregnant and postpartum laboratory mouse.* Endocrinology, 1974. **95**(5): p. 1486-90.
20. Richert, M.M., K.L. Schwertfeger, J.W. Ryder, and S.M. Anderson, *An atlas of mouse mammary gland development.* Journal of mammary gland biology and neoplasia, 2000. **5**(2): p. 227-41.

21.   Oakes, S.R., H.N. Hilton, and C.J. Ormandy, *The alveolar switch: coordinating the proliferative cues and cell fate decisions that drive the formation of lobuloalveoli from ductal epithelium.* Breast cancer research : BCR, 2006. **8**(2): p. 207.

22.   Brisken, C. and R.D. Rajaram, *Alveolar and lactogenic differentiation.* Journal of mammary gland biology and neoplasia, 2006. **11**(3-4): p. 239-48.

23.   Smith, A., *A glossary for stem-cell biology.* Nature, 2006. **441**.

24.   Deome, K.B., L.J. Faulkin, Jr., H.A. Bern, and P.B. Blair, *Development of mammary tumors from hyperplastic alveolar nodules transplanted into gland-free mammary fat pads of female C3H mice.* Cancer research, 1959. **19**(5): p. 515-20.

25.   Kordon, E.C. and G.H. Smith, *An entire functional mammary gland may comprise the progeny from a single cell.* Development, 1998. **125**(10): p. 1921-30.

26.   Chepko, G. and G.H. Smith, *Three division-competent, structurally-distinct cell populations contribute to murine mammary epithelial renewal.* Tissue & cell, 1997. **29**(2): p. 239-53.

27.   Welm, B.E., S.B. Tepera, T. Venezia, T.A. Graubert, J.M. Rosen, and M.A. Goodell, *Sca-1(pos) cells in the mouse mammary gland represent an enriched progenitor cell population.* Developmental biology, 2002. **245**(1): p. 42-56.

28.   Booth, B.W., C.A. Boulanger, L.H. Anderson, L. Jimenez-Rojo, C. Brisken, and G.H. Smith, *Amphiregulin mediates self-renewal in an immortal mammary epithelial cell line with stem cell characteristics.* Experimental cell research, 2010. **316**(3): p. 422-32.

29.   Kenney, N.J., G.H. Smith, E. Lawrence, J.C. Barrett, and D.S. Salomon, *Identification of Stem Cell Units in the Terminal End Bud and Duct of the Mouse Mammary Gland.* Journal of biomedicine & biotechnology, 2001. **1**(3): p. 133-143.

30.   Asselin-Labat, M.L., K.D. Sutherland, H. Barker, R. Thomas, M. Shackleton, N.C. Forrest, L. Hartley, L. Robb, F.G. Grosveld, J. van der Wees, G.J. Lindeman, and J.E. Visvader, *Gata-3 is an essential regulator of mammary-gland morphogenesis and luminal-cell differentiation.* Nature cell biology, 2007. **9**(2): p. 201-9.

31.   Li, W., B.J. Ferguson, W.T. Khaled, M. Tevendale, J. Stingl, V. Poli, T. Rich, P. Salomoni, and C.J. Watson, *PML depletion disrupts normal mammary gland development and skews the composition of the mammary luminal cell progenitor pool.* Proceedings of the National Academy of Sciences of the United States of America, 2009. **106**(12): p. 4725-30.

32.   Asselin-Labat, M.L., K.D. Sutherland, F. Vaillant, D.E. Gyorki, D. Wu, S. Holroyd, K. Breslin, T. Ward, W. Shi, M.L. Bath, S. Deb, S.B. Fox, G.K. Smyth, G.J. Lindeman, and J.E. Visvader, *Gata-3 negatively regulates the tumor-initiating capacity of mammary luminal progenitor cells and targets the putative tumor suppressor caspase-14.* Molecular and cellular biology, 2011. **31**(22): p. 4609-22.

33.   Stingl, J., *Detection and analysis of mammary gland stem cells.* The Journal of pathology, 2009. **217**(2): p. 229-41.

34.   Sleeman, K.E., H. Kendrick, A. Ashworth, C.M. Isacke, and M.J. Smalley, *CD24 staining of mouse mammary gland cells defines luminal epithelial, myoepithelial/basal and non-epithelial cells.* Breast cancer research : BCR, 2006. **8**(1): p. R7.

35.   Jeselsohn, R., N.E. Brown, L. Arendt, I. Klebba, M.G. Hu, C. Kuperwasser, and P.W. Hinds, *Cyclin D1 kinase activity is required for the self-renewal of mammary stem and progenitor cells that are targets of MMTV-ErbB2 tumorigenesis.* Cancer cell, 2010. **17**(1): p. 65-76.

36.   Vaillant, F., G.J. Lindeman, and J.E. Visvader, *Jekyll or Hyde: does Matrigel provide a more or less physiological environment in mammary repopulating assays?* Breast cancer research : BCR, 2011. **13**(3): p. 108.

37.   Smith, G.H., *Experimental mammary epithelial morphogenesis in an in vivo model: evidence for distinct cellular progenitors of the ductal and lobular phenotype.* Breast cancer research and treatment, 1996. **39**(1): p. 21-31.

38.   Van Keymeulen, A., A.S. Rocha, M. Ousset, B. Beck, G. Bouvencourt, J. Rock, N. Sharma, S. Dekoninck, and C. Blanpain, *Distinct stem cells contribute to mammary gland development and maintenance.* Nature, 2011. **479**(7372): p. 189-93.

39. B. MacMahon, P.C., T. M. Lin, C. R. Lowe, A. P. Mirra, B. Ravnihar, E. J. Salber, V. G. Valaoras, and S. Yuasa, *Age at first birth and breast cancer risk.* Bull World Health Organ, 1970. **43**(2): p. 209-221.

40. Asselin-Labat, M.L., M. Shackleton, J. Stingl, F. Vaillant, N.C. Forrest, C.J. Eaves, J.E. Visvader, and G.J. Lindeman, *Steroid hormone receptor status of mouse mammary stem cells.* Journal of the National Cancer Institute, 2006. **98**(14): p. 1011-4.

41. Tiede, B.J., L.A. Owens, F. Li, C. DeCoste, and Y. Kang, *A novel mouse model for non-invasive single marker tracking of mammary stem cells in vivo reveals stem cell dynamics throughout pregnancy.* PloS one, 2009. **4**(11): p. e8035.

42. Boulanger, C.A., K.U. Wagner, and G.H. Smith, *Parity-induced mouse mammary epithelial cells are pluripotent, self-renewing and sensitive to TGF-beta1 expression.* Oncogene, 2005. **24**(4): p. 552-60.

43. Booth, B.W., C.A. Boulanger, and G.H. Smith, *Alveolar progenitor cells develop in mouse mammary glands independent of pregnancy and lactation.* Journal of cellular physiology, 2007. **212**(3): p. 729-36.

44. Matulka, L.A., A.A. Triplett, and K.U. Wagner, *Parity-induced mammary epithelial cells are multipotent and express cell surface markers associated with stem cells.* Developmental biology, 2007. **303**(1): p. 29-44.

45. Cardiff, R.D. and N. Kenney, *Mouse mammary tumor biology: a short history.* Advances in cancer research, 2007. **98**: p. 53-116.

46. Nusse, R. and H.E. Varmus, *Many tumors induced by the mouse mammary tumor virus contain a provirus integrated in the same region of the host genome.* Cell, 1982. **31**(1): p. 99-109.

47. Jhappan, C., D. Gallahan, C. Stahle, E. Chu, G.H. Smith, G. Merlino, and R. Callahan, *Expression of an activated Notch-related int-3 transgene interferes with cell differentiation and induces neoplastic transformation in mammary and salivary glands.* Genes & development, 1992. **6**(3): p. 345-55.

48. Callahan, R. and G.H. Smith, *Common integration sites for MMTV in viral induced mouse mammary tumors.* Journal of mammary gland biology and neoplasia, 2008. **13**(3): p. 309-21.

49. Donehower, L.A., A.L. Huang, and G.L. Hager, *Regulatory and coding potential of the mouse mammary tumor virus long terminal redundancy.* Journal of virology, 1981. **37**(1): p. 226-38.

50. Geisse, S., C. Scheidereit, H.M. Westphal, N.E. Hynes, B. Groner, and M. Beato, *Glucocorticoid receptors recognize DNA sequences in and around murine mammary tumour virus DNA.* The EMBO journal, 1982. **1**(12): p. 1613-9.

51. Cato, A.C., R. Miksicek, G. Schutz, J. Arnemann, and M. Beato, *The hormone regulatory element of mouse mammary tumour virus mediates progesterone induction.* The EMBO journal, 1986. **5**(9): p. 2237-40.

52. Bruggemeier, U., L. Rogge, E.L. Winnacker, and M. Beato, *Nuclear factor I acts as a transcription factor on the MMTV promoter but competes with steroid hormone receptors for DNA binding.* The EMBO journal, 1990. **9**(7): p. 2233-9.

53. Kim, M.H. and D.O. Peterson, *Oct-1 protein promotes functional transcription complex assembly on the mouse mammary tumor virus promoter.* The Journal of biological chemistry, 1995. **270**(46): p. 27823-8.

54. Lefebvre, P., D.S. Berard, M.G. Cordingley, and G.L. Hager, *Two regions of the mouse mammary tumor virus long terminal repeat regulate the activity of its promoter in mammary cell lines.* Molecular and cellular biology, 1991. **11**(5): p. 2529-37.

55. von der Ahe, D., S. Janich, C. Scheidereit, R. Renkawitz, G. Schutz, and M. Beato, *Glucocorticoid and progesterone receptors bind to the same sites in two hormonally regulated promoters.* Nature, 1985. **313**(6004): p. 706-9.

56. Scheidereit, C., S. Geisse, H.M. Westphal, and M. Beato, *The glucocorticoid receptor binds to defined nucleotide sequences near the promoter of mouse mammary tumour virus.* Nature, 1983. **304**(5928): p. 749-52.

57. Truss, M., J. Bartsch, A. Schelbert, R.J. Hache, and M. Beato, *Hormone induces binding of receptors and transcription factors to a rearranged nucleosome on the MMTV promoter in vivo.* The EMBO journal, 1995. **14**(8): p. 1737-51.

58. Richard-Foy, H. and G.L. Hager, *Sequence-specific positioning of nucleosomes over the steroid-inducible MMTV promoter.* The EMBO journal, 1987. **6**(8): p. 2321-8.

59. Selbert, S., D.J. Bentley, D.W. Melton, D. Rannie, P. Lourenco, C.J. Watson, and A.R. Clarke, *Efficient BLG-Cre mediated gene deletion in the mammary gland.* Transgenic research, 1998. **7**(5): p. 387-96.

60. Wagner, K.U., R.J. Wall, L. St-Onge, P. Gruss, A. Wynshaw-Boris, L. Garrett, M. Li, P.A. Furth, and L. Hennighausen, *Cre-mediated gene deletion in the mammary gland.* Nucleic acids research, 1997. **25**(21): p. 4323-30.

61. Muller, W.J., E. Sinn, P.K. Pattengale, R. Wallace, and P. Leder, *Single-step induction of mammary adenocarcinoma in transgenic mice bearing the activated c-neu oncogene.* Cell, 1988. **54**(1): p. 105-15.

62. Guy, C.T., R.D. Cardiff, and W.J. Muller, *Induction of mammary tumors by expression of polyomavirus middle T oncogene: a transgenic mouse model for metastatic disease.* Molecular and cellular biology, 1992. **12**(3): p. 954-61.

63. Stewart, T.A., P.K. Pattengale, and P. Leder, *Spontaneous mammary adenocarcinomas in transgenic mice that carry and express MTV/myc fusion genes.* Cell, 1984. **38**(3): p. 627-37.

64. Neel, B., *Personal communication.*

65. Gunther, E.J., G.K. Belka, G.B. Wertheim, J. Wang, J.L. Hartman, R.B. Boxer, and L.A. Chodosh, *A novel doxycycline-inducible system for the transgenic analysis of mammary gland biology.* The FASEB journal : official publication of the Federation of American Societies for Experimental Biology, 2002. **16**(3): p. 283-92.

66. Huettner, C.S., P. Zhang, R.A. Van Etten, and D.G. Tenen, *Reversibility of acute B-cell leukaemia induced by BCR-ABL1.* Nature genetics, 2000. **24**(1): p. 57-60.

67. Hennighausen, L., *Personal Communication.*

68. Schwartz, M.S., G.H. Smith, and D. Medina, *The effect of parity, tumor latency and transplantation on the activation of int loci in MMTV-induced, transplanted C3H mammary pre-neoplasias and their tumors.* International journal of cancer. Journal international du cancer, 1992. **51**(5): p. 805-11.

69. Anisimov, V.N., I.G. Popovich, I.N. Alimova, M.A. Zabezhinski, A.V. Semenchenko, and A.I. Yashin, *Number of pregnancies and ovariectomy modify mammary carcinoma development in transgenic HER-2/neu female mice.* Cancer letters, 2003. **193**(1): p. 49-55.

70. Jamerson, M.H., M.D. Johnson, P.A. Furth, and R.B. Dickson, *Early parity significantly elevates mammary tumor incidence in MMTV-c-myc transgenic mice.* Transgenic research, 2003. **12**(6): p. 747-50.

71. Pina, B., U. Bruggemeier, and M. Beato, *Nucleosome positioning modulates accessibility of regulatory proteins to the mouse mammary tumor virus promoter.* Cell, 1990. **60**(5): p. 719-31.

72. Potten, C.S., W.J. Hume, P. Reid, and J. Cairns, *The segregation of DNA in epithelial stem cells.* Cell, 1978. **15**(3): p. 899-906.

73. Potten, C.S., G. Owen, and D. Booth, *Intestinal stem cells protect their genome by selective segregation of template DNA strands.* Journal of cell science, 2002. **115**(Pt 11): p. 2381-8.

74. Cairns, J., *Somatic stem cells and the kinetics of mutagenesis and carcinogenesis.* Proceedings of the National Academy of Sciences of the United States of America, 2002. **99**(16): p. 10567-70.

75. Cheng, H. and C.P. Leblond, *Origin, differentiation and renewal of the four main epithelial cell types in the mouse small intestine. V. Unitarian Theory of the origin of the four epithelial cell types.* The American journal of anatomy, 1974. **141**(4): p. 537-61.

76. Montgomery, R.K. and D.T. Breault, *Small intestinal stem cell markers.* Journal of anatomy, 2008. **213**(1): p. 52-8.

77. Braun, K.M. and F.M. Watt, *Epidermal label-retaining cells: background and recent applications.* The journal of investigative dermatology. Symposium proceedings / the Society for Investigative Dermatology, Inc. [and] European Society for Dermatological Research, 2004. **9**(3): p. 196-201.

78. Barker, N., J.H. van Es, J. Kuipers, P. Kujala, M. van den Born, M. Cozijnsen, A. Haegebarth, J. Korving, H. Begthel, P.J. Peters, and H. Clevers, *Identification of stem cells in small intestine and colon by marker gene Lgr5.* Nature, 2007. **449**(7165): p. 1003-7.

79. Sato, T., R.G. Vries, H.J. Snippert, M. van de Wetering, N. Barker, D.E. Stange, J.H. van Es, A. Abo, P. Kujala, P.J. Peters, and H. Clevers, *Single Lgr5 stem cells build crypt-villus structures in vitro without a mesenchymal niche.* Nature, 2009. **459**(7244): p. 262-5.

80. Montgomery, R.K., D.L. Carlone, C.A. Richmond, L. Farilla, M.E. Kranendonk, D.E. Henderson, N.Y. Baffour-Awuah, D.M. Ambruzs, L.K. Fogli, S. Algra, and D.T. Breault, *Mouse telomerase reverse transcriptase (mTert) expression marks slowly cycling intestinal stem cells.* Proceedings of the National Academy of Sciences of the United States of America, 2011. **108**(1): p. 179-84.

81. Morris, R.J. and C.S. Potten, *Slowly cycling (label-retaining) epidermal cells behave like clonogenic stem cells in vitro.* Cell proliferation, 1994. **27**(5): p. 279-89.

82. Morris, R.J. and C.S. Potten, *Highly persistent label-retaining cells in the hair follicles of mice and their fate following induction of anagen.* The Journal of investigative dermatology, 1999. **112**(4): p. 470-5.

83. Braun, K.M., C. Niemann, U.B. Jensen, J.P. Sundberg, V. Silva-Vargas, and F.M. Watt, *Manipulation of stem cell proliferation and lineage commitment: visualisation of label-retaining cells in wholemounts of mouse epidermis.* Development, 2003. **130**(21): p. 5241-55.

84. Bickenbach, J.R. and E. Chism, *Selection and extended growth of murine epidermal stem cells in culture.* Experimental cell research, 1998. **244**(1): p. 184-95.

85. Tumbar, T., G. Guasch, V. Greco, C. Blanpain, W.E. Lowry, M. Rendl, and E. Fuchs, *Defining the epithelial stem cell niche in skin.* Science, 2004. **303**(5656): p. 359-63.

86. Smith, G.H., *Label-retaining epithelial cells in mouse mammary gland divide asymmetrically and retain their template DNA strands.* Development, 2005. **132**(4): p. 681-7.

87. Creamer, B.A., A.A. Triplett, and K.U. Wagner, *Longitudinal analysis of mammogenesis using a novel tetracycline-inducible mouse model and in vivo imaging.* Genesis, 2009. **47**(4): p. 234-45.

88. Fernandez-Gonzalez, R., I. Illa-Bochaca, B.E. Welm, M.C. Fleisch, Z. Werb, C. Ortiz-de-Solorzano, and M.H. Barcellos-Hoff, *Mapping mammary gland architecture using multi-scale in situ analysis.* Integrative biology : quantitative biosciences from nano to macro, 2009. **1**(1): p. 80-9.

89. Booth, B.W. and G.H. Smith, *Estrogen receptor-alpha and progesterone receptor are expressed in label-retaining mammary epithelial cells that divide asymmetrically and retain their template DNA strands.* Breast cancer research : BCR, 2006. **8**(4): p. R49.

90. Booth, B.W., C.A. Boulanger, and G.H. Smith, *Selective segregation of DNA strands persists in long-label-retaining mammary cells during pregnancy.* Breast cancer research : BCR, 2008. **10**(5): p. R90.

91. Seale, R.L., *Studies on the mode of segregation of histone nu bodies during replication in HeLa cells.* Cell, 1976. **9**(3): p. 423-9.

92. Leffak, I.M., R. Grainger, and H. Weintraub, *Conservative assembly and segregation of nucleosomal histones.* Cell, 1977. **12**(3): p. 837-45.

93. Bonne-Andrea, C., M.L. Wong, and B.M. Alberts, *In vitro replication through nucleosomes without histone displacement.* Nature, 1990. **343**(6260): p. 719-26.

94. Jamai, A., R.M. Imoberdorf, and M. Strubin, *Continuous histone H2B and transcription-dependent histone H3 exchange in yeast cells outside of replication.* Molecular cell, 2007. **25**(3): p. 345-55.

95. Blanpain, C., W.E. Lowry, A. Geoghegan, L. Polak, and E. Fuchs, *Self-renewal, multipotency, and the existence of two cell populations within an epithelial stem cell niche.* Cell, 2004. **118**(5): p. 635-48.

96. Oliver, J.A., A. Klinakis, F.H. Cheema, J. Friedlander, R.V. Sampogna, T.P. Martens, C. Liu, A. Efstratiadis, and Q. Al-Awqati, *Proliferation and migration of label-retaining cells of the kidney papilla.* Journal of the American Society of Nephrology : JASN, 2009. **20**(11): p. 2315-27.

97. Szotek, P.P., H.L. Chang, K. Brennand, A. Fujino, R. Pieretti-Vanmarcke, C. Lo Celso, D. Dombkowski, F. Preffer, K.S. Cohen, J. Teixeira, and P.K. Donahoe, *Normal ovarian surface*

epithelial label-retaining cells exhibit stem/progenitor cell characteristics. Proceedings of the National Academy of Sciences of the United States of America, 2008. **105**(34): p. 12469-73.

98.   Kiel, M.J., S. He, R. Ashkenazi, S.N. Gentry, M. Teta, J.A. Kushner, T.L. Jackson, and S.J. Morrison, *Haematopoietic stem cells do not asymmetrically segregate chromosomes or retain BrdU.* Nature, 2007. **449**(7159): p. 238-42.

99.   Foudi, A., K. Hochedlinger, D. Van Buren, J.W. Schindler, R. Jaenisch, V. Carey, and H. Hock, *Analysis of histone 2B-GFP retention reveals slowly cycling hematopoietic stem cells.* Nature biotechnology, 2009. **27**(1): p. 84-90.

100.   Kistner, A., M. Gossen, F. Zimmermann, J. Jerecic, C. Ullmer, H. Lubbert, and H. Bujard, *Doxycycline-mediated quantitative and tissue-specific control of gene expression in transgenic mice.* Proceedings of the National Academy of Sciences of the United States of America, 1996. **93**(20): p. 10933-8.

101.   Furth, P.A., L. St Onge, H. Boger, P. Gruss, M. Gossen, A. Kistner, H. Bujard, and L. Hennighausen, *Temporal control of gene expression in transgenic mice by a tetracycline-responsive promoter.* Proceedings of the National Academy of Sciences of the United States of America, 1994. **91**(20): p. 9302-6.

102.   Hochedlinger, K., Y. Yamada, C. Beard, and R. Jaenisch, *Ectopic expression of Oct-4 blocks progenitor-cell differentiation and causes dysplasia in epithelial tissues.* Cell, 2005. **121**(3): p. 465-77.

103.   Ip, M.M. and B.B. Asch, *Methods in mammary gland biology and breast cancer research*2000, New York: Kluwer Academic/Plenum Publishers. xvi, 329 p., 4 leaves of col. plates.

104.   Fazekas de St, G., *The evaluation of limiting dilution assays.* Journal of immunological methods, 1982. **49**(2): p. R11-23.

105.   Debnath, J., S.K. Muthuswamy, and J.S. Brugge, *Morphogenesis and oncogenesis of MCF-10A mammary epithelial acini grown in three-dimensional basement membrane cultures.* Methods, 2003. **30**(3): p. 256-68.

106.   Taupin, P., *BrdU immunohistochemistry for studying adult neurogenesis: paradigms, pitfalls, limitations, and validation.* Brain research reviews, 2007. **53**(1): p. 198-214.

107.   Hennighausen, L., R.J. Wall, U. Tillmann, M. Li, and P.A. Furth, *Conditional gene expression in secretory tissues and skin of transgenic mice using the MMTV-LTR and the tetracycline responsive system.* Journal of cellular biochemistry, 1995. **59**(4): p. 463-72.

108.   Cheng, L., P.R. Ziegelhoffer, and N.S. Yang, *In vivo promoter activity and transgene expression in mammalian somatic tissues evaluated by using particle bombardment.* Proceedings of the National Academy of Sciences of the United States of America, 1993. **90**(10): p. 4455-9.

109.   Wortge, S., L. Eshkind, N. Cabezas-Wallscheid, B. Lakaye, J. Kim, R. Heck, Y. Abassi, M. Diken, R. Sprengel, and E. Bockamp, *Tetracycline-controlled transgene activation using the ROSA26-iM2-GFP knock-in mouse strain permits GFP monitoring of DOX-regulated transgene-expression.* BMC developmental biology, 2010. **10**: p. 95.

110.   Gouon-Evans, V., M.E. Rothenberg, and J.W. Pollard, *Postnatal mammary gland development requires macrophages and eosinophils.* Development, 2000. **127**(11): p. 2269-82.

111.   Shultz, L.D., P.A. Schweitzer, S.W. Christianson, B. Gott, I.B. Schweitzer, B. Tennent, S. McKenna, L. Mobraaten, T.V. Rajan, D.L. Greiner, and et al., *Multiple defects in innate and adaptive immunologic function in NOD/LtSz-scid mice.* Journal of immunology, 1995. **154**(1): p. 180-91.

112.   Kuperwasser, C., T. Chavarria, M. Wu, G. Magrane, J.W. Gray, L. Carey, A. Richardson, and R.A. Weinberg, *Reconstruction of functionally normal and malignant human breast tissues in mice.* Proceedings of the National Academy of Sciences of the United States of America, 2004. **101**(14): p. 4966-71.

113.   Hilakivi-Clarke, L., A. Stoica, M. Raygada, and M.B. Martin, *Consumption of a high-fat diet alters estrogen receptor content, protein kinase C activity, and mammary gland morphology in virgin and pregnant mice and female offspring.* Cancer research, 1998. **58**(4): p. 654-60.

114. Olson, L.K., Y. Tan, Y. Zhao, M.D. Aupperlee, and S.Z. Haslam, *Pubertal exposure to high fat diet causes mouse strain-dependent alterations in mammary gland development and estrogen responsiveness.* International journal of obesity, 2010. **34**(9): p. 1415-26.

115. Cheshier, S.H., S.J. Morrison, X. Liao, and I.L. Weissman, *In vivo proliferation and cell cycle kinetics of long-term self-renewing hematopoietic stem cells.* Proceedings of the National Academy of Sciences of the United States of America, 1999. **96**(6): p. 3120-5.

116. Lim, E., D. Wu, B. Pal, T. Bouras, M.L. Asselin-Labat, F. Vaillant, H. Yagita, G.J. Lindeman, G.K. Smyth, and J.E. Visvader, *Transcriptome analyses of mouse and human mammary cell subpopulations reveal multiple conserved genes and pathways.* Breast cancer research : BCR, 2010. **12**(2): p. R21.

117. Ciarloni, L., S. Mallepell, and C. Brisken, *Amphiregulin is an essential mediator of estrogen receptor alpha function in mammary gland development.* Proceedings of the National Academy of Sciences of the United States of America, 2007. **104**(13): p. 5455-60.

118. Park, D.S., H. Lee, C. Riedel, J. Hulit, P.E. Scherer, R.G. Pestell, and M.P. Lisanti, *Prolactin negatively regulates caveolin-1 gene expression in the mammary gland during lactation, via a Ras-dependent mechanism.* The Journal of biological chemistry, 2001. **276**(51): p. 48389-97.

119. Brisken, C., S. Kaur, T.E. Chavarria, N. Binart, R.L. Sutherland, R.A. Weinberg, P.A. Kelly, and C.J. Ormandy, *Prolactin controls mammary gland development via direct and indirect mechanisms.* Developmental biology, 1999. **210**(1): p. 96-106.

120. Lu, P., A.J. Ewald, G.R. Martin, and Z. Werb, *Genetic mosaic analysis reveals FGF receptor 2 function in terminal end buds during mammary gland branching morphogenesis.* Developmental biology, 2008. **321**(1): p. 77-87.

121. Parsa, S., S.K. Ramasamy, S. De Langhe, V.V. Gupte, J.J. Haigh, D. Medina, and S. Bellusci, *Terminal end bud maintenance in mammary gland is dependent upon FGFR2b signaling.* Developmental biology, 2008. **317**(1): p. 121-31.

122. Daniel, C.W., K.B. Deome, J.T. Young, P.B. Blair, and L.J. Faulkin, Jr., *The in vivo life span of normal and preneoplastic mouse mammary glands: a serial transplantation study. 1968.* Journal of mammary gland biology and neoplasia, 2009. **14**(3): p. 355-62.

123. Yamaji, D., R. Na, Y. Feuermann, S. Pechhold, W. Chen, G.W. Robinson, and L. Hennighausen, *Development of mammary luminal progenitor cells is controlled by the transcription factor STAT5A.* Genes & development, 2009. **23**(20): p. 2382-7.

124. Sicinski, P. and R.A. Weinberg, *A specific role for cyclin D1 in mammary gland development.* Journal of mammary gland biology and neoplasia, 1997. **2**(4): p. 335-42.

125. Booth, B.W., C. Jhappan, G. Merlino, and G.H. Smith, *TGFbeta1 and TGFalpha contrarily affect alveolar survival and tumorigenesis in mouse mammary epithelium.* International journal of cancer. Journal international du cancer, 2007. **120**(3): p. 493-9.

126. Wagner, K.U., C.A. Boulanger, M.D. Henry, M. Sgagias, L. Hennighausen, and G.H. Smith, *An adjunct mammary epithelial cell population in parous females: its role in functional adaptation and tissue renewal.* Development, 2002. **129**(6): p. 1377-86.

127. Martin, R.M., H. Leonhardt, and M.C. Cardoso, *DNA labeling in living cells.* Cytometry. Part A : the journal of the International Society for Analytical Cytology, 2005. **67**(1): p. 45-52.

128. Jones, F.E. and D.F. Stern, *Expression of dominant-negative ErbB2 in the mammary gland of transgenic mice reveals a role in lobuloalveolar development and lactation.* Oncogene, 1999. **18**(23): p. 3481-90.

129. Ewan, K.B., H.A. Oketch-Rabah, S.A. Ravani, G. Shyamala, H.L. Moses, and M.H. Barcellos-Hoff, *Proliferation of estrogen receptor-alpha-positive mammary epithelial cells is restrained by transforming growth factor-beta1 in adult mice.* The American journal of pathology, 2005. **167**(2): p. 409-17.

130. Campbell, J.J., N. Davidenko, M.M. Caffarel, R.E. Cameron, and C.J. Watson, *A multifunctional 3D co-culture system for studies of mammary tissue morphogenesis and stem cell biology.* PloS one, 2011. **6**(9): p. e25661.

131. Soulier, S., M.G. Stinnakre, L. Lepourry, J.C. Mercier, and J.L. Vilotte, *Use of doxycycline-controlled gene expression to reversibly alter milk-protein composition in transgenic mice.* European journal of biochemistry / FEBS, 1999. **260**(2): p. 533-9.

132. Asselin-Labat, M.L., F. Vaillant, J.M. Sheridan, B. Pal, D. Wu, E.R. Simpson, H. Yasuda, G.K. Smyth, T.J. Martin, G.J. Lindeman, and J.E. Visvader, *Control of mammary stem cell function by steroid hormone signalling.* Nature, 2010. **465**(7299): p. 798-802.

133. Miermont, A.M., A.R. Parrish, and P.A. Furth, *Role of ERalpha in the differential response of Stat5a loss in susceptibility to mammary preneoplasia and DMBA-induced carcinogenesis.* Carcinogenesis, 2010. **31**(6): p. 1124-31.

134. Quintana, E., M. Shackleton, M.S. Sabel, D.R. Fullen, T.M. Johnson, and S.J. Morrison, *Efficient tumour formation by single human melanoma cells.* Nature, 2008. **456**(7222): p. 593-8.

135. Al-Hajj, M., M.S. Wicha, A. Benito-Hernandez, S.J. Morrison, and M.F. Clarke, *Prospective identification of tumorigenic breast cancer cells.* Proceedings of the National Academy of Sciences of the United States of America, 2003. **100**(7): p. 3983-8.

136. Vaillant, F., M.L. Asselin-Labat, M. Shackleton, N.C. Forrest, G.J. Lindeman, and J.E. Visvader, *The mammary progenitor marker CD61/beta3 integrin identifies cancer stem cells in mouse models of mammary tumorigenesis.* Cancer research, 2008. **68**(19): p. 7711-7.

137. Stingl, J., A. Raouf, J.T. Emerman, and C.J. Eaves, *Epithelial progenitors in the normal human mammary gland.* Journal of mammary gland biology and neoplasia, 2005. **10**(1): p. 49-59.

138. Engler, A.J., S. Sen, H.L. Sweeney, and D.E. Discher, *Matrix elasticity directs stem cell lineage specification.* Cell, 2006. **126**(4): p. 677-89.

139. Wall, R., A. Powell, E. Sohn, J. Foster-Frey, D. Bannerman, and M. Paape, *Enhanced host immune recognition of mastitis causing Escherchia coli in CD-14 transgenic mice.* Animal biotechnology, 2009. **20**(1): p. 1-14.

140. Stein, T., J.S. Morris, C.R. Davies, S.J. Weber-Hall, M.A. Duffy, V.J. Heath, A.K. Bell, R.K. Ferrier, G.P. Sandilands, and B.A. Gusterson, *Involution of the mouse mammary gland is associated with an immune cascade and an acute-phase response, involving LBP, CD14 and STAT3.* Breast cancer research : BCR, 2004. **6**(2): p. R75-91.

141. Moore, K.J., L.P. Andersson, R.R. Ingalls, B.G. Monks, R. Li, M.A. Arnaout, D.T. Golenbock, and M.W. Freeman, *Divergent response to LPS and bacteria in CD14-deficient murine macrophages.* Journal of immunology, 2000. **165**(8): p. 4272-80.